1998

M1 Strength Distributions in Deformed Nuclei.

Thomas Georg Beuschel
Louisiana State University and Agricultural & Mechanical College

INFORMATION TO USERS

This manuscript has been reproduced from the microfilm master. UMI films the text directly from the original or copy submitted. Thus, some thesis and dissertation copies are in typewriter face, while others may be from any type of computer printer.

The quality of this reproduction is dependent upon the quality of the copy submitted. Broken or indistinct print, colored or poor quality illustrations and photographs, print bleedthrough, substandard margins, and improper alignment can adversely affect reproduction.

In the unlikely event that the author did not send UMI a complete manuscript and there are missing pages, these will be noted. Also, if unauthorized copyright material had to be removed, a note will indicate the deletion.

Oversize materials (e.g., maps, drawings, charts) are reproduced by sectioning the original, beginning at the upper left-hand corner and continuing from left to right in equal sections with small overlaps. Each original is also photographed in one exposure and is included in reduced form at the back of the book.

Photographs included in the original manuscript have been reproduced xerographically in this copy. Higher quality 6" x 9" black and white photographic prints are available for any photographs or illustrations appearing in this copy for an additional charge. Contact UMI directly to order.

UMI

A Bell & Howell Information Company
300 North Zeeb Road, Ann Arbor MI 48106-1346 USA
313/761-4700 800/521-0600

M1 STRENGTH DISTRIBUTIONS IN DEFORMED NUCLEI

A Dissertation

Submitted to the Graduate Faculty of the
Louisiana State University and
Agricultural and Mechanical College
in partial fulfillment of the
requirements for the degree of
Doctor of Philosphy

in

The Department of Physics and Astronomy

by
Thomas Beuschel
Diplom, Universität Bonn, 1991
December 1998

To the memory of my father

Acknowlegements

Six years ago I had a difficult decision to make when I met my adviser Professor Jerry P. Draayer in Tübingen where he made the offer to work on a Ph. D. in his research group at Louisiana State University. At the end of my dissertation project I wish to express my sincere gratitude for this generous offer and also the expertise, guidance, and support he provided during my work here. Not only did he introduce me to an exciting area of physics, he also gave me the opportunity to learn about a different culture and to widen my horizons – as he had promised six years ago. An important part of this experience was the hospitality shown by him and his wife Lois Draayer, who invited students and visitors on many occasions to their home.

I also enjoyed and benefited from my work with Dirk Rompf from the University of Gießen, who was my collaborator on many parts of this dissertation project. I also would like to thank Professor Jorge Hirsch with whom I have worked here and in Mexico City. The discussions with him were an important part of my work and I also have to thank him and his family for their warm hospitality.

I also would like to thank Professors R. L. Imlay, A. R. P. Rau, E. F. Zganjar and Professor R. Pike Jr. from the Department of Chemical Engineering for serving on my dissertation committee.

Thanks also go to the recent and former graduate students in the Nuclear Theory group at Louisiana State University who contributed to the good working environment. Especially I would like to thank my office mates Jutta Escher and Gabriela Popa and also Chairul Bahri, Andrey Blokhin, Dirk Troltenier, Guergana Stoicheva, and Vesselin Guerguiev.

I also appreciate the support I received from friends outside the Nuclear Theory group. Especially I would like to thank Jennifer Maclean, Robert Sanford, Kenneth Bernstein, and his wife Ashley.

Finally I have to thank my mother, my grandmother, and my two brothers for their encouragement and support. This work is dedicated to the memory of my father whom we all lost much too early ten years ago. His kindness and positive attitude towards life, despite a long fight against cancer, will always be remembered.

Table of Contents

List of Tables

List of Figures

Abstract

The Elliott SU(3) Model, extended via pseudo-spin for heavy nuclei, is used to study low-lying magnetic dipole excitations in deformed nuclei which are known as "scissors" modes. Proton and neutron degrees of freedom are handled explicitly and a system Hamiltonian that preserves SU(3) symmetry and one that includes single particle energies as well as quadrupole-quadrupole and pairing two-body interactions are considered.

Starting from a basic nuclear Hamiltonian that preserves SU(3) symmetry, a microscopic interpretation of the "scissors" mode of the Two Rotor Model is realized through a linear mapping between invariants of the rotor group and SU(3). The model allows for a classification of SU(3) shell-model configurations in terms of collective degrees of freedom. Triaxiality of the parent proton and neutron distributions is shown to add a "twist" degree of freedom to the usual "scissors" mode picture. An analysis of the results for the M1 transition strength given in the SU(3) limit of the theory provides evidence for the underlying collective nature of the "scissors" mode.

The low-energy spectrum and M1 strength distribution are also calculated using a realistic Hamiltonian that includes the SU(3) symmetry breaking pairing and single particle terms. These additional terms generate the experimentally observed fragmentation, that is, the breakup of the M1 strength among several levels, thus providing a natural explanation for the complex structure of the M1 transition spectra. Results for the strongly-deformed even-even $^{156-160}$Gd and $^{156-160}$Dy isotopes are shown to be in good agreement with experiment. Further results for the γ-unstable (soft rotor) ^{196}Pt nucleus and the even-odd ^{163}Dy system are also discussed and found to compare favorably with the available experimental data.

Chapter 1

Introduction

A relatively new discovery in nuclear structure physics has attracted considerable theoretical and experimental attention over the last few years. Initially predicted in 1978 within the framework of a phenomenological two-rotor model (TRM) by Lo Iudic and Palumbo [79], the strongly enhanced M1 transitions in heavy deformed nuclei were detected experimentally six years later in an (e, e') scattering experiment on ^{156}Gd.

The early interpretation of this so-called scissors mode was that of rigid proton and neutron rotors with axial symmetric shapes performing rotational oscillations against each other. Numerous experiments, using electron-scattering and nuclear resonance fluorescence techniques that have been carried out in the rare-earth and actinide region [77] have shown, however, that this simple picture has to be modified. While the predominantly orbital character of this magnetic dipole excitation that was predicted by the two-rotor model was confirmed experimentally, other features can not be explained in a simple collective model. One of them is the so-called fragmentation, that is, the breakup of the M1 strength among several levels closely packed and clustered around a few strong transition peaks in the energy region between 2 and 4 MeV.

Very recent experiments have also established the scissors mode for the γ-soft nucleus ^{196}Pt an even-odd nuclei with an unpaired neutron. In these cases the structure of the M1 transition spectrum is very different from the one observed for well deformed even-even actinides and remains largely unexplained. As will be shown in this work. a nuclear model that is able to address all these issues is the pseudo SU(3) scheme.

Since its introduction in the late sixties [65, 101], the pseudo-spin concept has been applied to various properties of heavy deformed nuclei [71, 118, 24]. However, the nucleon-nucleon interaction used in these pseudo-SU(3) investigations is very schematic in nature because of technical difficulties related to the calculation of SU(3) matrix elements of more general interactions. Recently a code was released [6] that lifts these limitations and allows for the introduction of interactions like pairing, which are important for an adequate description of experimental results within the framework of pseudo-SU(3) model calculations [115].

The pseudo-SU(3) model is a many particle shell-model theory that takes full advantage of pseudo-spin symmetry [5, 17], which is manifest in the near degeneracy of the orbital pairs $[(l-1)_{j=l+1/2}, (l+1)_{j=l-1/2}]$, and also takes full account of the Pauli Exclusion Principle. As an algebraic shell-model theory the pseudo-SU(3) scheme exploits powerful group theoretical methods in the construction of the basis states and for the calculation of required matrix elements [24, 101].

As an introduction, the second chapter discusses some basic features of the SU(3) symmetry and a classification scheme for many particle states using SU(3) quantum numbers. An aspect that will be important for the later application is the coupling of proton and neutron many-particle states that are classified in a SU(3) scheme. As is already clear from the basic description of the scissors mode, the interaction of protons and neutrons and their possible couplings are essential for the description of this phenomenon.

The third chapter gives an outline of the SU(3) model and introduces the different operators that are needed for a realistic description of the scissors mode. These are either operators that conserve SU(3) symmetry and can be interpreted in terms of a collective model, or operators that break SU(3) symmetry and describe single particle effects. As will be shown, the interplay of these different operators is essential for a description of the complex structure of the scissors mode.

In chapter four we discuss the pseudo symmetry which allows one to describe heavy nuclei in the rare-earth and actinide region using relatively small configuration spaces. A question that is of interest for the application to the γ-soft nucleus ^{196}Pt is the goodness of the pseudo-spin for

triaxial deformations. Earlier studies had only investigated the goodness of this symmetry for axial deformations.

Chapter five gives a discussion of the scissors mode in the framework of the pseudo-SU(3) model. After the main experimental results are presented and a short review of other nuclear models is given, a generalization of the TRM model for the case of triaxial proton and neutron deformations will be discussed. This generalization makes use of the close relation between SU(3) and the rotor picture which allows one to find a relation between collective variables and SU(3) parameters. As will be discussed, with this generalization of the TRM model the underlying collective structure of the scissors mode can be described naturally in terms of the pseudo SU(3) model.

The results for a realistic nuclear pseudo SU(3) Hamiltonian that includes pairing and single particle terms will be discussed next. With this extension it becomes possible to explain the observed fragmentation and to describe the γ-soft and odd-even isotopes that are of experimental interest and for which so far no reasonable results have been found by other nuclear theories.

The final chapter six summarizes the findings and an appendix presents some of the group theoretical tools needed for the calculation.

Chapter 2

The SU(3) symmetry

Group theoretical methods allow for a mathematically elegant treatment of complex physical systems that have specific symmetry properties. A well-known example for the use of group theory in physics is the classification of hadrons into different families according to their quark structure. A total of six different quarks serve as building blocks and form either three quark or quark-antiquark systems. If a subset of only three quark families is considered, the symmetry group used is SU(3). If more quark families are taken into account, higher symmetry groups are employed to classify mesons and baryons. In high energy physics SU(3) is also realized as the color symmetry group for quarks and gluons [58, 61].

Another example is the use of the group SO(3) for rotationally invariant systems. This symmetry allows for the classification of eigenstates with angular momentum quantum numbers and the use of powerful group theoretical tools like coupling coefficients and the Wigner-Eckart theorem for the evaluation of matrix elements [121].

The symmetries in the above example are so called *exact symmetries*, meaning that the systems remain unchanged under the full set of transformations that generate the symmetry. But even in a more general setting where this strong requirement can not be met, the symmetry concept can still be useful. A second symmetry type is *dynamical symmetry*. In this case the system is not necessarily left invariant under the symmetry operations, but eigenstates can still be associated with an irreducible representation of the group.

This concepts of a *dynamical symmetry* can be illustrated by the Zeeman effect. In the presence of an uniform magnetic field the rotational invariance of the Hamiltonian is lifted and the corresponding degeneracy of eigenstates with the same angular momentum disappears. The additional interaction term $\vec{\mu}\cdot\vec{B}$ prefers certain orientations over others, but since the magnetic moment $\vec{\mu}$ is proportional to the angular momentum and thus does not mix different L values, one can still ascribe a good angular momentum quantum number to the eigenstates.

In nuclear physics group theoretical methods have evolved as an important tool because of the complex many particle nature of the nucleus. An important example is the Interacting Boson model (IBM) which in its earliest version assumes that the nucleus consists of bosonic proton and neutron pairs that are coupled to spin zero and angular momentum zero or two [2, 3]. The group corresponding to this system is U(6).

In the nuclear shell model, where the three dimensional isotropic harmonic oscillator is used as an approximation for the nuclear mean field SU(3), the symmetry group of the harmonic oscillator emerges as an important symmetry. SU(3) becomes a *dynamical symmetry* if a quadrupole-quadupole deformation term is added to the mean field. Due to the dominance of the quadrupole-quadrupole interaction in the mid-shell region, the SU(3) symmetry remains useful as an *approximate symmetry* even if small SU(3) symmetry breaking single particle or pairing terms are added to the nuclear Hamiltonian.

The features of this so called SU(3) or Elliott model will be discussed after an introduction to some basic concepts of group theory and the classification of many particle states using SU(3) quantum numbers.

2.1 Basic defintions

An important concept that is used in group theory is that of a Lie group. A continuous Lie group G has an infinite number of elements that are parameterized by n variables. A well-known example

Table 2.1: Rank and number of generators for different groups.

Group	number of generators	rank
SO($2N$)	$N(2N-1)$	N
SO($2N+1$)	$N(2N+1)$	N
U(N)	N^2	N
SU(N)	N^2-1	$N-1$

is SO(3), the group of rotations in three dimensions where the elements are parameterized by three angles.

The objects of interest, however, are not so much the group elements but the operators that generate infinitesimal group transformations. These operators X_α form the so-called Lie Algebra and are characterized by their commutation relation

$$[X_\alpha, X_\beta] = c^\gamma_{\alpha,\beta} X_\gamma \,, \tag{2.1}$$

where the structure constants, $c^\gamma_{\alpha,\beta}$, define most of the group properties. The finite group transformations are then given by the generators as:

$$U(\alpha_1, \alpha_2 \ldots \alpha_s) = \exp \sum_{i=1}^{s} \alpha_i X^i \,. \tag{2.2}$$

A Lie group has one or more invariant operators that can be built from inner products of its generators and that commute with all generators of the groups:

$$[C, X_\alpha] = 0, \quad \alpha = 1, 2, \ldots s \tag{2.3}$$

The maximum number of these so called Casimir operators possible in a group is given by its rank. For the different groups that will be discussed in this chapter, the rank and number of generators are listed in Table 2.1.

The generators of the rotational group SO(3), for example, are given by the three components of the angular momentum L_x, L_y and L_z and the Casimir operator is $L^2 = L_x^2 + L_y^2 + L_z^2$.

2.2 SU(3) and the harmonic oscillator

The group that is of special interest here and will be discussed in more detail is the symmetry group of the harmonic oscillator. Its special symmetry is reflected in the energy spectrum where within a shell not only the states with fixed angular momentum have the same energy – corresponding to the rotational invariance of the Hamiltonian – but all the states regardless of the L value.

The other well-known example for a higher symmetry than rotational invariance is the Hamiltonian of the hydrogen atom with a $1/r$ dependent Coloumb potential. Its energy spectrum also shows an extra degeneracy, reflecting the SO(4) symmetry of the Hamiltonian.

The underlying symmetry group of the harmonic oscillator Hamiltonian,

$$H_0 = \frac{\vec{p}^2}{2m} + \frac{1}{2} m \vec{r}^2 \,, \tag{2.4}$$

becomes visible if it is rewritten it in terms of boson creation and annihilation operators that are defined as:

$$b_i = \sqrt{\frac{m\omega}{2\hbar}}(x_i + i\frac{p_i}{m\omega}) \tag{2.5}$$

$$b_i^\dagger = \sqrt{\frac{m\omega}{2\hbar}}(x_i - i\frac{p_i}{m\omega}) \tag{2.6}$$

where b_i and the hermitian conjugated operator $b_i^\dagger$, respectively, reduces or increases the number of oscillator quanta in the i-th direction. With these two operators that satisfy the commutation relations

$$[b_i, b_j{}^\dagger] = \delta_{ij} \tag{2.7}$$

$$[b_i, b_j] = [b_i{}^\dagger, b_j{}^\dagger] = 0 \,. \tag{2.8}$$

the Hamiltonian for an harmonic oscillator (h. o.) can be written as

$$H_0 = \hbar\omega(\vec{b}^\dagger\vec{b} + \frac{3}{2}) \ . \tag{2.9}$$

In this notation the Hamiltonian has been expressed in terms of the U(3) generators,

$$A_{ij} = b_i^\dagger b_j \ , \tag{2.10}$$

that shift an oscillator quanta from the j-th to the i-th direction. The h. o. Hamiltonian thus clearly conserves the U(3) symmetry and basically counts the total number of quanta in the x, y and z direction.

The commutation relations for the U(3) generators introduced in Eq. (2.10) can easily be derived from the ones between the space and momentum coordinates ($[x_i, p_j] = \hbar\,\delta_{ij}$) and are:

$$[A_{ij}, A_{kl}] = \delta_{jk}A_{li} - \delta_{il}A_{kj} \tag{2.11}$$

The three Casimir operators that exist for U(3) (see Table 2.1) can be expressed by the shift operators as:

$$N = \sum_i A_{ii} \tag{2.12}$$

$$C_2 = \frac{3}{2}\sum_{i,j} A_{ij}A_{ji} \tag{2.13}$$

$$C_3 = \sum_{i,j,k} A_{ij}A_{jk}A_{ki} \ , \tag{2.14}$$

where the factor 3/2 for C_2 reflects a common convention. Using the commutation relation given in Eq. (2.11) it is easy to show that N, C_2 and C_3 commute with all generators as necessary.

The generators of the U(3) Lie algebra given in Eq. (2.10) can be modified to SU(3) generators by removing the trace. This amounts to subtracting the boson number operator,

$$A_{ij}{}' = A_{ij} - \frac{1}{3}\delta_{ij} \,, \tag{2.15}$$

which leaves the physics described in either the SU(3) or U(3) picture unchanged.

Since the total number of quanta is conserved, the SU(3) irreducible represenations [87] – the so-called irreps – only depend on the relative difference of quanta along the three axes and only two quantum numbers are necessary to classify these. Commonly these are given by the so-called highest weight state that is characterized by a maximum number of quanta along the z-axis and the maximum of the remainder along the x-axis as:

$$\lambda = n_z - n_x \tag{2.16}$$

$$\mu = n_x - n_y \tag{2.17}$$

For a single particle in the n-th shell the SU(3) irrep is thus given by $(\lambda, \mu) = (n, 0)$.

2.2.1 The $SU(3) \supset SO(3)$ group chain

Different options exist for a further classification of the SU(3) irreps (λ, μ) with the sublabels depending on the choice of subgroups.

An important example for the physical significance of the choice of group chains is the Interaction Boson Model (IBM). As was mentioned earlier, this model assumes that proton and neutron pairs are coupled to bosons with spin zero and angular momentum zero or two. From the number of different angular momentum states it follows that the symmetry group of such a system is U(6). The interesting feature of this model is the existence of three different group chains that each contain the rotational group SO(3) as a subgroup and correspond to a specific limit of the model: The U(5) chain is used for the description of vibrational nuclei (applicable near closed shells), the O(6) chain for the description of γ-unstable nuclei (transition region), and the SU(3) chain for the description of rotational nuclei (applicable in the mid-shell region).

For applications in the shell model which use the SU(3) symmetry it is convenient to make use of the rotational invariance of the system by selecting SO(3) as a subgroup. To do so, a set of SU(3) generators that transform as rotational tensors will be introduced. They can be expressed by the U(3) generators A_{ij} introduced in Eq. (2.10) that correspond to a cartesian scheme and shift oscillator quanta in the x, y or z direction, as:

$$L_{10} = i\,(A_{32} - A_{23})\,, \tag{2.18}$$

$$L_{1\pm1} = -\frac{1}{\sqrt{2}}\,(A_{12} - A_{21} \pm i(A_{31} - A_{13}))\,, \tag{2.19}$$

$$Q^a_{20} = 2A_{11} - A_{22} - A_{33}\,, \tag{2.20}$$

$$Q^a_{2\pm1} = \sqrt{\frac{3}{2}}\,(A_{12} + A_{21} \pm i(A_{13} + A_{31}))\,, \tag{2.21}$$

$$Q^a_{2\pm2} = \sqrt{\frac{3}{2}}\,(A_{22} - A_{33} \pm i(A_{23} + A_{32}))\,. \tag{2.22}$$

This set of SU(3) generators uses the three components of the angular momentum operator L_i and the five components of the algebraic quadrupole operator $Q^a_{2\mu}$. The algebraic quadrupole operator has angular momentum 2 and can be expressed in cartesian coordinates as:

$$Q^a_{2\mu} = \sqrt{\frac{4\pi}{5r_0^4}}\,\left(r^2 Y_{2\mu}(\vec{r}) + r_0^4 p^2 Y_{2\mu}(\vec{p})\right)\ ,\ \mu = -2,-1,0,1,2\,. \tag{2.23}$$

The commutation relation between these generators are:

$$\begin{aligned}
[L_{1\mu}, L_{1\nu}] &= -\sqrt{2}\langle 1\mu, 1\nu|1, \mu+\nu\rangle\, L_{1\mu+\nu}\,, \\
[L_{1\mu}, Q^a_{2\nu}] &= -\sqrt{6}\langle 1\mu, 2\nu|2, \mu+\nu\rangle\, Q^a_{2\mu+\nu}\,, \\
[Q^a_{2\mu}, Q^a_{2\nu}] &= 3\sqrt{10}\langle 2\mu, 2\nu|1, \mu+\nu\rangle\, L_{1\mu+\nu}\,.
\end{aligned} \tag{2.24}$$

where $\langle l_1 m_1, l_2 m_2|l_3 m_3\rangle$ is the usual notation for a Clebsch Gordan coefficient.

This choice of SU(3) generators, using the three components of the angular momentum, makes clear that SO(3) is a subgroup of SU(3). A classification scheme for the spatial part of harmonic oscillation states is thus given by the group chain

$$SU(3) \supset SO(3) \supset SO(2)\,, \tag{2.25}$$

where SO(2) is the group of rotations around one axis that gives the m projection quantum number.

As is known from the solutions of the harmonic oscillator, for the single particle case the allowed angular momenta within the n-th shell are given by:

$$l = n, n-2, \ldots 1 \text{ or } 0 \tag{2.26}$$

reflecting the fact that all states within a fixed shell have the same parity $P = (-1)^n$.

In the many particle case, where the SU(3) irrep (λ, μ) is not restricted to $(n, 0)$, the total angular momentum is given by a generalization of the rule above:

$$l = \lambda + \mu, \lambda + \mu - 2, \ldots, 1 \text{ or } 0 \tag{2.27}$$

for $k = 0$ and

$$l = k, k+1, k+2, \ldots, \lambda + \mu - k \tag{2.28}$$

for $k \neq 0$ where k is given by

$$k = \min(\lambda, \mu), \min(\lambda, \mu) - 2, \ldots, 1 \text{ or } 0\,. \tag{2.29}$$

The quantum number k reflects the fact that in this classification scheme multiple occurences of l are possible within a certain SU(3) irrep (λ, μ). This label also has a physical interpretation that will be discussed in a later section.

Alternatively, a multiplicity label κ can be introduced to distinguish between multiple occurrences of an angular momentum l. It runs from 0 to κ_{max} with the value of κ_{max} given by:

$$\kappa_{max} = \left[\frac{\lambda+\mu+2-L}{2}\right] - \left[\frac{\lambda+1-l}{2}\right] - \left[\frac{\mu+1-l}{2}\right] . \tag{2.30}$$

Here $[\cdots]$ is the notation for the greatest integer function.

A harmonic oscillator eigenstate can thus be labeled by the two SU(3) quantum numbers λ, μ plus the three additional sublabels l, m_l and κ.

2.2.2 The $SU(3) \supset SU(2) \times U(1)$ group chain

Another choice for SU(3) subgroups that is more natural from a mathematical point of view is a classification in terms of the group chain

$$SU(3) \supset SU(2) \times U(1) , \tag{2.31}$$

for which no extra multiplicity labels are needed. This classification scheme is usually choosen for applications in high energy physics, where the SU(3) appears as the group used to classify three quark systems or in context of the three "colors" that for the strong interaction are equivalent to the charge of the electromagentic interaction. This scheme can also be used to derive an elegant expression for the Casimir operators in terms of the SU(3) labels λ and μ which is the reason it is briefly discussed here.

Using the U(3) generators introduced in Eq. (2.10), the SU(2) generators Λ_i can be expressed by the subset of these operators, A_{xx}, A_{xy}, A_{yx} and A_{yy}, that is, as shift operators in the x-y plane:

$$\Lambda_0 = \frac{1}{2}(A_{xx} - A_{yy}) \tag{2.32}$$

$$\Lambda_+ = -\frac{1}{\sqrt{2}}A_{xy} \tag{2.33}$$

$$\Lambda_- = \frac{1}{\sqrt{2}}A_{yx} \tag{2.34}$$

The commutation relations between these generators can be derived from the ones between the U(3) generators given in Eq. (2.11) and are:

$$[\Lambda_+, \Lambda_-] = -\Lambda_0 , \quad [\Lambda_0, \Lambda_\pm] = \pm\Lambda_\pm . \tag{2.35}$$

These relations are equivalent to the ones of the three SO(3) generators, reflecting the fact that these two groups are isomorphic. This suggests how to choose the SU(2) quantum numbers corresponding to the SO(3) case. The eigenvalues of Λ_0 that can be associated with the magnetic quantum numbers are given by convention as $\nu/2$ which leads to:

$$-2\Lambda \leq \nu \leq 2\Lambda \tag{2.36}$$

for a fixed Λ. The SU(2) Casimir operator is Λ^2 and defined analogously to the angular momentum case as:

$$\Lambda^2 = {\Lambda_0}^2 + \Lambda_+\Lambda_- + \Lambda_-\Lambda_+ , \tag{2.37}$$

with its eigenvalues given by:

$$\langle\Lambda^2\rangle = \Lambda(\Lambda + 1) . \tag{2.38}$$

The U(1) generator is simply:

$$Q_0^a = 2A_{11} - A_{22} - A_{33} , \tag{2.39}$$

which commutes with SU(2) generators and has the eigenvalue ϵ that can take the values

$$\epsilon = 2\lambda + \mu, 2\lambda + \mu - 3, \cdots, -\lambda - 2\mu . \tag{2.40}$$

For a fixed ϵ, the values possible for Λ are given as:

$$\Lambda = \frac{1}{6}|2\lambda - 2\mu - \epsilon| , \frac{1}{6}|2\lambda - 2\mu - \epsilon| + 1, \cdots$$

$$\cdots, \min\left[\frac{1}{6}|2\lambda+4\mu-\epsilon|, \frac{1}{6}|4\lambda+2\mu+\epsilon|\right]. \tag{2.41}$$

A state classified according to the $SU(3) \supset SU(2) \times U(1)$ group is thus given by an eigenvector, $|(\lambda,\mu)\epsilon,\Lambda,\nu\rangle$, that satisfies the following relations:

$$Q_0\,|(\lambda,\mu)\epsilon,\Lambda,\nu\rangle = \epsilon|(\lambda,\mu)\epsilon,\Lambda,\nu\rangle\,, \tag{2.42}$$

$$\Lambda_0\,|(\lambda,\mu)\epsilon,\Lambda,\nu\rangle = \frac{\nu}{2}|(\lambda,\mu)\epsilon,\Lambda,\nu\rangle\,, \tag{2.43}$$

$$\Lambda^2\,|(\lambda,\mu)\epsilon,\Lambda,\nu\rangle = \Lambda(\Lambda+1)|(\lambda,\mu)\epsilon,\Lambda,\nu\rangle\,. \tag{2.44}$$

To determine the eigenvalue of the Casimir operator C_2, the fact that it depends only on the values of the SU(3) quantum numbers λ and μ can be used. Here it will be evaluated for the highest weight state $|(\lambda,\mu)\epsilon_{max},\Lambda,\nu_{max}\rangle$ for which the number of quanta are maximized first in the direction along the z-axis and then along the x-axis. For this state the shift operators A_{zx}, A_{zy} and A_{xy} give 0:

$$A_{zx}\,|(\lambda,\mu)\epsilon_{max},\Lambda,\nu_{max}\rangle = 0\,, \tag{2.45}$$

$$A_{zy}\,|(\lambda,\mu)\epsilon_{max},\Lambda,\nu_{max}\rangle = 0\,, \tag{2.46}$$

$$A_{xy}\,|(\lambda,\mu)\epsilon_{max},\Lambda,\nu_{max}\rangle = 0\,. \tag{2.47}$$

For the highest weight state ϵ has its maximum value, which implies:

$$\begin{aligned} \epsilon_{max} &= 2\lambda+\mu\,, \\ \Lambda &= \frac{\mu}{2}\,, \\ \nu &= \mu \end{aligned} \tag{2.48}$$

To apply these relations, the Casimir operator given in Eq. (2.13) in terms of U(3) generators has

to be rewritten in terms of SU(2) and U(1) generators as:

$$C_2 = 3\sum_{i<j} A_{ij}\,A_{ji} + \frac{1}{4}\left[Q_0(Q_0+6) + 6\Lambda_0(\Lambda_0+2)\right] . \tag{2.49}$$

Using the definitions given in Eqs. (2.42) and (2.43) it can now be shown that:

$$\begin{aligned} C_2|(\lambda,\mu)\epsilon_{max},\Lambda,\nu_{max}\rangle &= \\ &= \left(\lambda^2+\mu^2+\lambda\mu+3(\lambda+\mu)\right)|(\lambda,\mu)\epsilon_{max},\Lambda,\nu_{max}\rangle . \end{aligned} \tag{2.50}$$

Thus the eigenvalue for C_2 for any SU(3) irrep (λ,μ) is given. In a similar way it can be shown that the second SU(3) Casimir operator C_3 solves the following eigenvalue equation:

$$\begin{aligned} C_3\,|(\lambda,\mu)\epsilon_{max},\Lambda,\nu_{max}\rangle &= \\ &= \frac{1}{9}(\lambda-\mu)(\lambda+2\mu+3)(2\lambda+\mu+3)|(\lambda,\mu)\epsilon_{max},\Lambda,\nu_{max}\rangle , \end{aligned} \tag{2.51}$$

which provides the eigenvalues for the third order Casimir operator in terms of λ and μ.

To conclude this section on some basic properties of SU(3), the Casimir operators C_2 and C_3 in the spherical representation will be given. These representations can be derived from the expression for the Casimir operators given in terms of the shift operators:

$$C_2 = \frac{3}{2}\sum_{i,j} A_{ij}A_{ji} - \frac{N^2}{2} \tag{2.52}$$

$$C_3 = \sum_{i,j,k} A_{ij}A_{jk}A_{ki} - N^3 , \tag{2.53}$$

and using relations (2.19) to (2.22) to give:

$$C_2 = \frac{1}{4}\left[Q^a\cdot Q^a + 3L^2\right] \tag{2.54}$$

$$C_3 = -\frac{1}{36}\sqrt{\frac{35}{2}}\left[Q^a\times Q^a\times Q^a\right]^0 - \frac{1}{4}\sqrt{\frac{15}{2}}\left[L\times Q^a\times L\right]^0 \tag{2.55}$$

In the following applications the relation given in Eq. (2.54) that connects the Casimir operator C_2 of SU(3) with the scalar product $Q^a \cdot Q^a$ and the SO(3) Casimir L^2 will be useful. These results can be used to express the quadrupole-quadrupole interaction in terms of operators invariant under SU(3) and SO(3). The quadrupole-quadrupole interaction that describes the long-range part of the nuclear interaction is an important part of the shell model Hamiltonian and crucial for describing nuclei in the strongly deformed mid-shell region.

2.3 Classification of many particle wavefunction

An important feature of the SU(3) model is the classification of many particle states using SU(3) quantum numbers. As will be shown later, this choice of a symmetry adapted basis allows one to reduce dramatically the size of the configuration space and to use powerful group theoretical methods to evaluate matrix elements.

Without utilizing any special symmetry features of the Hamiltonian, an apparent choice for the basis state Φ of a k-particle system with n-levels is the product of single particle states ϕ_i:

$$\Phi = \phi_i(1)\, \phi_j(2) \ldots \phi_p(k) \tag{2.56}$$

with the subscripts denoting any of the single particle levels $\{1, 2, \ldots N\}$. The total total number of different product states that can be formed this way is N^k.

If U_{ij} denotes the elements of an (N x N) unitary matrix that transforms between one basis of single particle states ϕ_i (i = 1, 2, ... N) and another equally valid basis $\phi_j{}'$,

$$\phi_j{}' = \sum_{i=1}^{N} U_{ij} \phi_j \,, \tag{2.57}$$

then the unitary transformation between different sets of many particle basis states constructed according to Eq. (2.56) can be written as:

$$\Phi' = \sum_{i',j'\ldots p'} U_{ii'}U_{jj'}\ldots U_{pp'}\ \phi_i(1)\ \phi_j(2)\ldots\phi_p(k) \tag{2.58}$$

A many particle state can thus be classified according to its transformation behavior under $U(N)$, the group formed by the unitary matrices in N dimensions.

The irreducible representations of the group $U(N)$ can be labeled by a set of non-negative integers $[f_1\ f_2\ \ldots f_n]$ (often abbreviated as $[f]$) such that $f_1 \geq f_2 \geq \ldots f_n$.

2.3.1 Young diagrams

As can be shown, the above classification scheme is equivalent to the one given by the symmetric group S_k that describes the behavior under particle permutation. A useful tool for classifying the reducible representations of S_k are the so-called Young diagrams [30]. A k-particle wave function is represented by k squares that are arranged into s rows in such a way that the number of squares in row i is greater than or equal to the number in row $i+1$. A Young diagram can thus also be specified by a label $[f] = [f_1\ f_2 \ldots f_n]$ where f_i denotes the number of squares in the i-th row. A symmetric k-particle state corresponds to an one-rowed Young diagram. A totally antisymmetric state is labeled by an one-column diagram with k rows, $[1^k] = [1\ 1; \ldots 1]$. Other more complicated shapes correspond to mixed symmetry types. One important restriction on Young diagrams used to label the symmetries of a group $U(N)$ is that the number of rows can not exceed N since it is not possible to antisymmetrize more than N particles in a basis of N levels.

A Young diagram becomes a Young tableau when particle labels are inserted into the squares. For this labeling the numbers in each row have to increase from left to right and from top to bottom. The dimension of a representation, that is the numbers of Young tableaux possible for a specific Young diagram, is then given by

$$\dim(S_k, [f_1, f_2, \ldots f_s]) = \frac{k!}{\prod_{i=1}^{s}(f_i + s - i)} \prod_{i<j\leq s} (f_i - f_j + j - i) \tag{2.59}$$

with the totally symmetric and antisymmetric irreps having dimension one.

The dimension of a $U(N)$ irrep corresponding to a certain Young diagram is different from the one for the symmetry group,

$$\dim(U(N),[f_1,f_2,\dots f_s]) = \prod_{1\le i\le j\le N}(f_i - i - f_j + j) \tag{2.60}$$

The two dimension are related by the sum rule

$$N^k = \sum_\alpha \dim(U(N),[f]_\alpha)\cdot\dim(S_k,[f]_\alpha) \tag{2.61}$$

where the sum extends over all possible Young diagrams and N^k is the dimension of the basis of product states that was given in Eq. (2.56).

2.3.2 Coupling of Young diagrams

Young diagrams provide a framework to describe the coupling of two SU(3) representations. This problem is similar to the coupling of two angular momenta $\vec{l}_1$ and $\vec{l}_2$. In this case the possible values for the total angular momentum are given by the different ways to add the vectors $\vec{l}_1$ and $\vec{l}_2$ where the maximum total angular momentum given by $l_1 + l_2$ and the minimum is given by $|l_1 - l_2|$. The corresponding rules for the coupling of two Young diagrams have been derived by Littlewood [30] and can be summarized as:

1. Compose the Young diagrams for the two representations.
2. In the second diagram mark all the boxes in the first row with "a", the ones in the second one with "b" etc.
3. Add all the boxes marked with an "a" to the first diagram with the restrictions that
   (a) there are never more than two or more boxes marked with "a" in the same column
   (b) the diagram stays regular, i. e. no row contains less elements than the row beneath.
4. Follow the same procedure for the boxes marked with "b" with the additional restrictions that

(a) reading from right to left the number of boxes marked with "b" doesn't become larger than the ones marked with "a"

(b) Diagrams with more than N rows are prohibited for an $U(N)$ symmetry.

5. Repeat Step 4. for all additional rows of the second factor.

Following these rule, the tensor product $U(N) \otimes U(N)$ can be constructed from the factor Young diagrams.

As an example, the different possible couplings of two irreps corresponding to a single particle in the third shell will be given. This is equivalent to finding the different SU(3) irreps that can be constructed from two $(3,0)$ SU(3) irreps. Using the procedure given above, the first step requires the construction of the corresponding Young diagrams that are simply given by three boxes in a row. This simple structure allows one to then contract the irreps as given in Steps 2. and 3. with the resulting diagram giving the total SU(3) irreps $(6,0)$, $(4,1)$, $(2,2)$ and $(0,3)$.

This example can be generalized for the tensor product of two identical SU(3) irreps $(n,0)$:

$$(n,0) \otimes (n,0) = \bigoplus_{m=0}^{n} (2n-2m,\, m)\,, \tag{2.62}$$

where the quantum number m has been introduced to describe the construction rules given by the Littlewood rules.

In general the SU(3) components have quantum numbers (λ,μ) which are both different from zero so that the corresponding Young diagrams consist of two rows. The so-called leading representation that can be formed from two SU(3) irreps (λ_1,μ_1) is equivalent to the "stretched" coupling of two angular momenta $\vec{l}_1$ and $\vec{l}_2$ to a maximum value. It is given by the sum of the SU(3) quantum numbers:

$$(\lambda_1,\mu_1) \otimes (\lambda_2,\mu_2) \rightarrow (\lambda,\mu) = (\lambda_1+\lambda_2, \mu_1+\mu_2)\,. \tag{2.63}$$

The corresponding Young diagram has $\lambda_1+\lambda_2+\mu_1+\mu_2$ boxes in the first row and $\mu_1+\mu_2$ in the second one. Other allowed representation can be derived from this Young diagram by moving

a number of boxes from the first row to row number two and three. If m is the number of boxes moved from the first row and i the number of boxes added to the second row, then the resulting Young diagram has the following shape:

Row 1:	$\lambda_1 + \lambda_2 + \mu_1 + \mu_2 - m$	boxes ,
Row 2:	$\mu_1 + \mu_2 + i$	boxes ,
Row 3:	$m - i$	boxes .

which is equivalent to the representation

$$(\lambda, \mu) \;=\; (\lambda_1 + \lambda_2 - m - i,\, \mu_1 + \mu_2 + 2i - m)\,. \tag{2.64}$$

Moving an additional number of k boxes from the second row to the third row the Young diagram becomes:

Row 1:	$\lambda_1 + \lambda_2 + \mu_1 + \mu_2 - m$	boxes ,
Row 2:	$\mu_1 + \mu_2 + (i - k)$	boxes ,
Row 3:	$m - (i - k)$	boxes .

Every (λ, μ)-configuration that is constructed from the initial configurations (λ_1, μ_1) and (λ_2, μ_2) can thus be written as:

$$(\lambda, \mu) = (\lambda_1 + \lambda_2 - m - (i - k),\, \mu_1 + \mu_2 + 2(i - k) - m)\,, \tag{2.65}$$

where the quantum numbers i and k only appear as the difference $i - k$. The tensor product is therefore given by

$$\begin{aligned} (\lambda, \mu) &= (\lambda_1, \mu_1) \otimes (\lambda_2, \mu_2) \\ &= \bigoplus_{m,i,k} (\lambda_1 + \lambda_2 - m - (i - k), \mu_1 + \mu_2 + 2(i - k) - m)\,, \end{aligned} \tag{2.66}$$

with the limits for the summation over (m, i, k) restricted according to the Littlewood rules by

$$\begin{aligned} &i \geq 0\ ,\quad m-i \leq \mu_1\ ,\quad m+k-2i \leq \mu_1\ , \\ &k \geq 0\ ,\quad m-i \leq \lambda_2\ ,\quad i \leq \lambda_1\ , \\ &m \geq i\ ,\quad m-k \leq \lambda_2\ ,\quad k \leq \mu_2\ . \end{aligned} \tag{2.67}$$

Since only the difference $i-k$ enters in the above expression, a new parameter

$$l = m - i = k \tag{2.68}$$

can be introduced so that Eq. (2.66) can be rewritten in aform that is symmetric in the labels l and m:

$$(\lambda, \mu) = \bigoplus_{m,l,k} (\lambda_1 + \lambda_2 - 2m + l,\, \mu_1 + \mu_2 - 2l + m)\,. \tag{2.69}$$

This new set of parameters (m, l, k) is restricted by the following set of inequalities:

$$\begin{aligned} &k \geq 0\ ,\quad k \geq l-\mu_1\ ,\quad k \leq l\ , \\ &k \geq l-m\ ,\quad k \geq l-\lambda_2\ ,\quad k \leq \lambda_1+l-m\ , \\ &k \geq m-\lambda_2\ ,\quad k \geq 2l-m-\mu_1\ ,\quad k \leq \mu_2 \end{aligned} \tag{2.70}$$

In this notation the parameter k does not appear in the different terms of the tensor product but still remains a summation index restricted by the SU(3) quantum numbers λ_1, λ_2 μ_1, μ_2 and the other summation indices l and m. This reflects the fact that a particular SU(3) irrep (λ, μ) may appear multiple times in the tensor product of (λ_1, μ_1) and (λ_2, μ_2) and a multiplicity index ρ has to be introduced to distinguish multiple occurrences of a (λ, μ). This is an important difference from the coupling of vectors where the coupling is unique.

2.3.3 Further classification of states

More specifically, we are interested in classifying a k particle fermion state in a 2Ω dimensional space, where $\Omega = (n+1)(n+2)/2$ is the spatial dimension of the n-nth oscillator shell and the factor 2 reflects the dimension of the spin space for a spin $\frac{1}{2}$ particle. Because of the Pauli principle the k-particle state must transform as totally antisymmetric $[1^k]$ irrep of $U(2\Omega)$ which uniquely determines the SU(3) irrep for the many particle wavefunction.

To classify the state with additional quantum numbers, a relevant subgroup of U(N) has to be selected. The unitary groups admit a great variety of subgroups with the natural chain of subgroups being:

$$U(N) \supset U(N-1) \supset \ldots \supset U(1)\,. \tag{2.71}$$

In this case a set of N quantum numbers, $[h_{N1}h_{N2}\cdots h_{NN}]$, is necessary to classify the U(N) irrep followed by a set of $N-1$ quantum numbers for the U(N-1) irrep and the sets for the other unitary groups. Following this scheme a state in the U(3) case, for example, can be expressed in terms of the elegant Gel'fand-Zetlin notation [53] by:

$$\left| \begin{array}{ccc} h_{13} & h_{23} & h33 \\ & h_{12} \quad h_{22} & \\ & h_{11} & \end{array} \right\rangle . \tag{2.72}$$

For specific application however, it is sometimes more convenient to choose a different chain of subgroups. In the case of the nuclear wavefunction it is natural to separate the wavefunction into a spatial and spin part. The wavefunction is thus classified according to the group chain $U(2\Omega) \supset U(\Omega) \otimes U(2)$ and as can be shown [89], the wavefunctions for the space and spin part have to be labeled by so called conjugate Young patterns since the total wavefunction has to be antisymmetric. This means that the corresponding Young diagrams – $[f]$ for $U(\Omega)$ and $[f^c]$ for U(2) – are related to one another by row-column interchange where the patterns can be determined from another by reflecting across a downward sloping 45° diagonal through the first Young diagram.

Table 2.2: Group chain for k fermions in the n-th oscillator shell.

$U(2\Omega)$	$\supset$	$U(\Omega) \otimes U(2)$	$\supset$	$SU(3) \otimes SU(2)$	$\supset$	$SO(3) \otimes SU(2)$
$[1^k]$		$[f]$, $[f^*]$	α	(λ, μ), S	κ	L, S

As was discussed earlier, the maximum numbers of rows for a Young diagram representing a U(2) irrep is two which restricts the number of columns for the conjugate $U(\Omega)$ diagram to the same number. In the same way a restriction is given by the dimension Ω of the spatial part of the wavefunction. The number of boxes in the first and second row, f_1^c and f_2^c, of the U(2) irrep is thus given by the spin and particle number k – which determines the total number of boxes – as:

$$f_1^c = \frac{k}{2} + S \tag{2.73}$$

$$f_2^c = \frac{k}{2} - S\,. \tag{2.74}$$

To make use of the SU(3) symmetry of Hamiltonian, the spatial part of the wavefunction will be classified according to the group chain $U(N) \supset SU(3)$, assigning the SU(3) quantum numbers (λ, μ). In this classification scheme, which is motivated by the underlying physics and does not follow the mathematically natural chain of subgroups, a multiplicity label α has to be introduced that distinguishes between multiple occurrences of a SU(3) irrep (λ, μ) in a U(N) irrep $[f]$.

For a further classification of the spatial part, the $SU(3) \supset SO(3)$ subchain that was discussed earlier (2.1) will be used (see Table 2.2), so that the many particle wavefunction $|\phi)$ can be written as:

$$|N, [f], \alpha, (\lambda, \mu), \kappa, L, M_L, S, M_S)\,. \tag{2.75}$$

2.3.4 Proton-Neutron systems

So far the many particle wavefuction discussed does not account for the fact that the nucleus is a proton-neutron system. This can be done by introducing the isospin degree of freedom where protons and neutrons are interpreted as different states of an isospin 1/2 doublet. With spin, isospin and spatial degrees of freedom the total number of states within an oscillator shell is 4Ω with a factor two coming from the isospin part. As before $\Omega = (n+1)(n+2)/2$ gives the spatial dimension of the n-th oscillator shell.

The k-particle wavefunction has to transform like the totally antisymmetric representation $[f^k] = [1]^k$ of U(4Ω). For a further classification of the states it is natural to separate the spin and isopsin degrees of freedom, using the group chain $U(4\Omega) \supset U(\Omega) \otimes U(4)$ The spin-isospin part can then be classified according to its spin and isospin parts and the spatial part using the $U(N) \supset SU(3)$ group chain as discussed in the previous section.

This classification procedure with an isospin quantum number, however, is not used for heavy nuclei ($A \geq 150$) where protons and neutrons occupy different shells. Instead, the totally antisymmetric wavefunctions for protons, $|\pi\rangle$, and neutrons, $|\nu\rangle$, will be be coupled to a total wavefunction. $|\pi,\nu\rangle = |\pi\rangle \otimes |\nu\rangle$. The coupling of these two system is possible on different levels. For example

$$\begin{aligned}[\; & |N_\pi, [f_\pi], \alpha_\pi, (\lambda_\pi,\mu_\pi), \kappa_\pi, L_\pi, [f_\pi^c],\, S_\pi; J_\pi) \otimes \\ & |N_\nu, [f_\nu], \alpha_\nu, (\lambda_\nu,\mu_\nu), \kappa_\nu, L_\nu, [f_\nu^c],\, S_\nu; J_\nu\rangle \;\;]^{J\,M}\end{aligned} \tag{2.76}$$

in an SU(3) uncoupled (J_π-J_ν coupled) scheme or

$$\begin{aligned}[\; & |N_\pi, [f_\pi], \alpha_\pi, (\lambda_\pi,\mu_\pi),\rangle \otimes \\ & |N_\nu, [f_\nu], \alpha_\nu, (\lambda_\nu,\mu_\nu),\rangle \;\;]^{[\rho(\lambda\mu)\kappa L,(S_\pi\, S_\nu)S]J\,M}\end{aligned} \tag{2.77}$$

in an SU(3) coupled scheme.

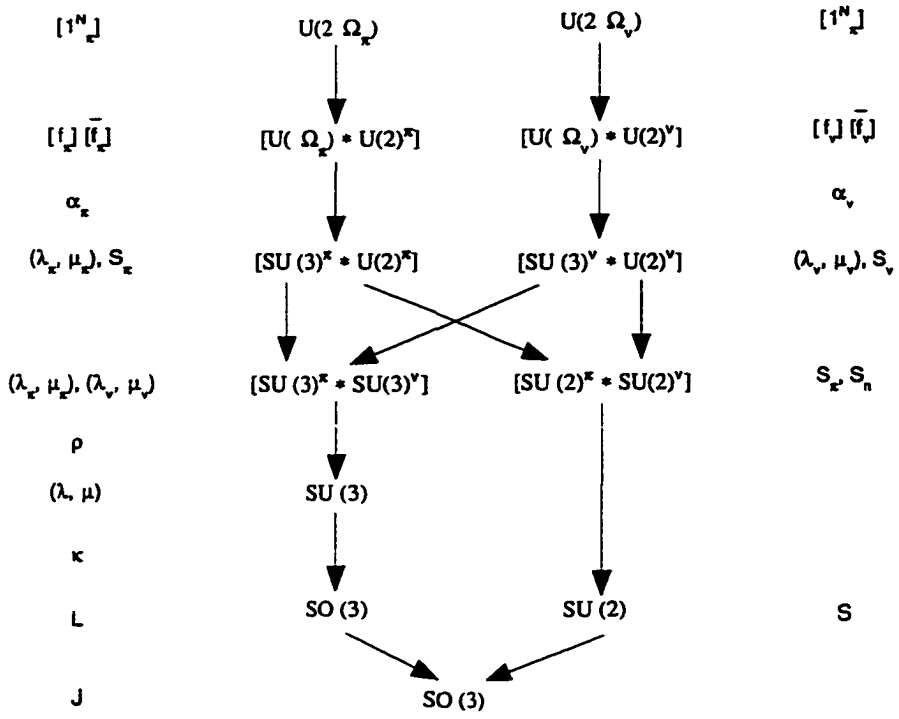

Figure 2.1: SU(3) coupling scheme for proton-neutron system.

Chapter 3

The SU(3) shell model

Having introduced basic SU(3) properties and a classification scheme for many particle states, the SU(3) shell model Hamiltonian will be discussed in this chapter.

As will be shown later in this chapter, a geometric interpretation of SU(3) eigenstates in terms of deformation parameters can be derived using the relation between the symmetry group of the triaxial rotor and SU(3). In a similar way, a correspondence between operators expressed in terms of SU(3) generators and the Hamiltonian of the triaxial rotor can be obtained. This allows us to introduce a SU(3) Hamiltonian that can be understood in terms of a collective picture.

Due to the underlying many particle nature of the theory, single particle and many particle terms that do not have a collective counterpart can be included in a SU(3) Hamiltonian. In particular, the addition of the pairing and spin-orbit interactions are important steps towards a more realistic nuclear Hamiltonian [7, 8, 46]. A formalism to evaluate these expressions in the framework of the SU(3) model will be introduced later in this chapter.

3.1 Collective vs. single particle shell model

In contrast with the case of atomic physics where electrons are moving in the strong coulomb potential generated by protons in the nucleus, it is not obvious that a mean field is also a good approximation for the averaged nuclear interaction acting on protons and neutrons inside the nucleus.

An experimental indication that a mean field approach is also valid for nuclear physics, lies in the shell closures at the so called magic numbers (2, 8, 20, 28, 40, 50, 82 and 126). These shell

closures are characterized among other effects by a vanishing quadrupole moment that corresponds to a spherical charge distribution and relatively large binding energies. Also, if an additional nucleon is added to a closed proton or neutron shell the binding energy of this extra nucleon is small, similar to the situation for alkali metals with a loosely bound single electron outside a full shell.

Motivated by these experimental results, the early version of the shell model was developed independently by Goepert Mayer [55, 56, 57] and Haxel, Jensen and Suess [62] in the late forties. To reproduce the magic numbers, a residual spin-orbit interaction, $\mathbf{l} \cdot \mathbf{s}$, that lowers the states with maximum j, had to be added to a harmonic oscillator potential. Thus, unlike atomic physics, shell closure in nuclei at the correct particle numbers can not be achieved by a mean field alone. With an additional l^2 term to make the oscillator potential similar to the more realistic square-well potential, a basic shell model Hamiltonian has the form:

$$H = H_{osc} + c\mathbf{l} \cdot \mathbf{s} + d\mathbf{l}^2 \ . \tag{3.1}$$

Besides reproducing the magic numbers, this model also allows one to predict successfully the ground state spin of odd nuclei if the pairing hypothesis is added, that is, pairs of nucleons are assumed to couple to zero total angular momentum. Building a nucleus by filling nucleons into single particle levels, the ground state spin is then determined by the last unpaired nucleon. Another single particle feature that can be described is the magnetic moment of odd-even nuclei which is also mainly determined by the unpaired valence nucleon.

On the other hand, the single particle picture is not able to account for the observed collective phenomena in nuclei, particularly enhanced E2 transition rates between members of identical bands. This failure of the simplest shell model scheme also spurred the development of the complementary collective model by Bohr and Mottelson [19] which describes nuclei in terms of shape variables rather than microscopic degrees of freedom.

In the collective model, the nucleus is pictured as a continuous object with vibrational and rotational degrees of freedom that can acquire a deformed equilibrium shape. For deviations from

sphericity that are small the nuclear surface is parameterized using an expansion in spherical harmonics:

$$R(\theta,\phi) = R_0[1 + \sum_{\lambda=0}^{\infty}\sum_{\mu=-\lambda}^{\lambda} a_{\lambda,\mu}Y^*_{\lambda\mu}(\theta,\phi) \qquad R_0 = 1.2\text{fm}A^{1/3} \tag{3.2}$$

where the first non-zero terms in this expansion are the ones for $\lambda = 2$. The term $\lambda = 0$ (monopole term) corresponds to a volume change that is only expected to play a role at much higher energies (so called breathing modes at 40-50 MeV) because nuclear matter seems to be relatively incompressible. The term with $\lambda = 1$ corresponds to a translation of the total nucleus and is therefore neglected. In first order the shape is thus defined by the five quadrupole moments $a_{2\lambda}$, three of which are independent since $a^*_{-\mu} = (-1)^\mu a_\mu$ for a real R_0. The Hamiltonian of the nuclear system is then constructed from these parameters and their time derivatives or conjugate momenta.

This model provides an intuitive picture and for many nuclei can reproduce the basic collective rotational and vibrational features it was constructed for. On the other hand, other nuclear features related to the underlying single particle structure of the nucleus lie outside the framework of this model.

3.2 Basic features of the SU(3) model

A theory that is able to describe collective phenomena and treats a nuclear system as a many particle fermionic system was developed by Elliott in the late fifties [39, 40, 41, 42]. The Elliott or SU(3) shell model uses the three dimensional isotropic oscillator as an approximation for the nuclear mean field and makes use of the associated symmetry group SU(3) for the classification of the many particle states and the construction of the Hamiltonian. A key feature of the SU(3) model that is also discussed in this section is its relation to the rotor picture. This allows for a geometric interpretation of the SU(3) eigenstates thus bridging the gap between collective theories and theories that include single particle aspects.

The price one has to pay for the microscopic description with fermion degrees of freedom, however, are the large dimensionalities of the many particle configuration space A basic assumption used that

greatly reduces the size of the model space, is that only particles in an open so-called valence shell have to be considered for the many particle wave function. The completely filled shells are treated as an inert spherical core with no direct effect on the nuclear properties, thus allowing one to truncate significantly the configuration space.

But even the configuration space restricted to one oscillator shell η for which $n = (\eta+1)(\eta+2)/2$ levels are available, remains large with a binomial growth of the dimension that for m fermions in n levels is approximately given by n^m. For many realistic applications this growth prohibits or severely slows down calculations even on today's computers.

An elegant solution for this dilemma is provided by group theoretical methods that make use of symmetry properties of the Hamiltonian. A crucial ingredient is the construction of a realistic nuclear Hamiltonian using the generators of a specific group. For a symmetry adapted basis no mixing between the basis vectors belonging to a fixed group irrep occurs if the Hamiltonian describes a system with exact or dynamical symmetry. A relevant subspace can then be selected which can lead to a drastic reduction of the configuration space.

For the Elliot model this is done by introducing a nuclear Hamiltonian with SU(3) symmetry, the symmetry group of the unitary transformations in an oscillator shell. As is already known from the single particle shell model, the harmonic oscillator can be used as an approximation for the nuclear mean field of a realistic Hamiltonian. However, additional terms are necessary that have to conserve the SU(3) symmetry.

A key feature of the SU(3) Hamiltonian introduced by Elliott is the use of the "algebraic" quadrupole operator

$$Q^a_{2\mu} = \sqrt{\frac{4\pi}{5b^2}}\left(\frac{r_s^2}{b^2}Y_{2\mu}(\vec{r}_s) + b^2 p_s^2 Y_{2\mu}(\vec{p}_s)\right) \quad (b = \sqrt{\hbar/m\omega}) \ , \tag{3.3}$$

in place of the usual "collective" quadrupole operator,

$$Q^c_{2\mu} = \sqrt{16\pi/5}\frac{r_s^2}{b^2}Y_{2\mu}(\vec{r}_s) \ . \tag{3.4}$$

As can be shown [43], the long range part of the nucleon-nucleon interaction is given by the quadrupole-quadrupole interaction and it is an important part of a realistic nuclear Hamiltonian. For the description of the well-deformed nuclei away from the magic numbers the quadruople-quadrupole term is essential.

Within a major oscillator shell the matrix elements of Q^c and Q^a are identical, but since Q^c couples states belonging to the η-th shell with those of the η'-th shell that differs by two quanta, $\eta'=\eta\pm2$, it introduces a mixing between these shells. For small and medium deformations however, the effect of both operators is comparable.

The advantage of using the algebraic quadrupole operator instead of the collective quadrupole operator lies in the fact that its five components together with the three components of the angular momentum are generators of SU(3), as was discussed in the previous chapter.

The rotationally invariant quadrupole-quadrupole operator $Q^a \cdot Q^a$ is thus diagonal in a SU(3) basis with its eigenvalues E_{qq} given by

$$E_{qq} = 4C_2 - 3L(L+1) \quad , \tag{3.5}$$

where L is the angular momentum and C_2 is the second degree Casimir operator of SU(3). As was shown earlier (2.54), the expectation value of C_2 is given by:

$$\langle(\lambda,\mu)|C_2|(\lambda,\mu)\rangle = (\lambda+\mu)(\lambda+\mu+3) - \lambda\mu. \tag{3.6}$$

The I^2 dependence of the $Q^a \cdot Q^a$ eigenvalue allows to reproduce a rotational spectrum with a SU(3) conserving Hamiltonian that is constructed using the harmonic oscillator potential plus the quadrupole-quadrupole interaction:

$$H_{SU(3)} = H_{osc} - \frac{\chi}{2} Q^a Q^a \quad , \tag{3.7}$$

Thus, the simplest version of the SU(3) model Hamiltonian is able to describe a collective feature that is not included in the single particle model.

Another important collective feature that can be successfully described using the simplest version of the SU(3) Hamiltonian are the enhanced E2 transitions between members of identical bands.

As was mentioned earlier, the large dimensionality of the configuration space for many particle wavefunctions makes an effective truncation scheme essential for practical applications. A natural choice for this truncation scheme is given by the structure of the $Q^a \cdot Q^a$ eigenvalue. Because of its C_2 dependence, the rotational band with lowest energy can be associated with the SU(3) irrep that has the largest C_2 value possible for a given particle configuration. This so called leading irrep with a few additional SU(3) irreps that come next in an ordering scheme according to the value of C_2 are sufficient to describe the low-energy spectrum of a well-deformed nucleus. This simple truncation scheme yields a dramatic reduction of the configuration space.

How the SU(3) states can be interpreted in terms of their deformation, thus providing a geometric picture for this truncation scheme, is discussed in the following section.

3.3 The rotor and SU(3)

An additional important property of the SU(3) model is its relation to the rotor model. Since the simple SU(3) Hamiltonian (3.7) with quadrupole-qadrupole interaction is able to reproduce a rotational spectrum where the ground state band is given by a unique SU(3) irrep, such a relation can already be anticipated from the results given so far. This relation then allows an interpretation of SU(3) irreps in terms of the shape variables β and γ that are commonly used as a measure for the axial and triaxial deformation thus bridging the gap between a microscopic and a macroscopic description of nuclei [78, 24]. This mapping between shape variables and SU(3) irreps will be discussed after a short introduction to some basic properties of the quantum rotor that are needed later.

3.3.1 The quantum rotor

The triaxial quantum rotor has been one of the first applications of quantum mechanics in the late 20s and 30s [75, 23] and its Hamiltonian has the form

$$H_{rot} = A_x I_x^2 + A_y I_y^2 + A_z I_z^2 \,, \tag{3.8}$$

where the I_α ($\alpha = x$, y and z) are the projections of the total angular momentum on the α-th body fixed symmetry axis and A_α are the corresponding inertia parameters. These inertia parameters are labeled according to the usual convention $A_y \leq A_x \leq A_z$.

The eigenvalues E_τ of H_{rot} are given by

$$E_\tau = \frac{1}{2}(A_y + A_z)I(I+1) + \frac{1}{2}(A_z - A_y)\mathcal{E}_\tau(\kappa) \,, \tag{3.9}$$

where $\mathcal{E}_\tau(\kappa)$ is a function that has been evaluated numerically by a number of authors. It depends on the label τ that is introduced to distinguish between multiple occurrences of I and on the asymmetry parameter κ which is defined as

$$\kappa = (2A_x - A_y - A_z)/(A_z - A_y) \,. \tag{3.10}$$

For the cases of a axial symmetry with $\kappa = -1$ (prolate, $A_y = A_x \leq A_z$) or $\kappa = +1$ (oblate, $A_y \leq A_x = A_z$) the Hamiltonian is diagonal with eigenvalues

$$\begin{aligned} E_{sym} &= A_y I(I+1) + (A_z - A_y)K^2 \quad \kappa = -1 \\ E_{sym} &= A_z I(I+1) + (A_z - A_x)K^2 \quad \kappa = +1 \end{aligned} \tag{3.11}$$

where K is the eigenvalue of the projection of the angular momentum on the intrinsic z axis. In the

limiting cases of a prolate or oblate top, the spectrum thus shows a rotational band with $I(I+1)$ spacing for each value of K.

A convenient choice for the eigenfunction in the axial symmetric case is

$$\Phi^{(\lambda\mu)KI}_{sym\ M} = \sqrt{\frac{2I+1}{16\pi^2(1+\delta_{K0})}}(D^{I*}_{MK} + (-1)^{\lambda+\mu+I} D^{I*}_{M-K}) \ . \tag{3.12}$$

Here $D^{I}_{MK}(\Omega)$ denotes a D function [87] and the Euler angles Ω specify the orientation of the lab frame with respect to the body-fixed coordinate system of the rotor.

In the general case of a triaxial deformation, K does not remain a good quantum number and the eigenfunctions $\Phi^{(\lambda,\mu)}_{asr}$ are a superposition of the symmetric solutions $\Phi^{(\lambda\mu)}_{sym}$

$$\Phi^{\lambda,\mu}_{asr} = \sum_{K}{}' C^{(\lambda\mu)} \Phi^{(\lambda\mu)KI}_{sym\ M} \ , \tag{3.13}$$

where the coefficients $C^{(\lambda\mu)}$ have to be determined numerically and the prime indicates the summation is over odd or even K only.

The quantum numbers λ and μ that appear in the phase factor in the symmetric solution, $\Phi^{(\lambda\mu)KI}_{sym\ M}$, reflect a special symmetry of the quantum rotor. The four different combinations of even and odd values for λ and μ distinguish states that transform different under π rotations about a principle axis. This is a special symmetry property of H_{rot} since the three corresponding rotation operators around the principal axes,

$$T_\alpha = \exp(-i\pi I_\alpha), \qquad \alpha = 1,2,3 \tag{3.14}$$

leave the rotor Hamiltonian invariant,

$$[H_{rot}, T_\alpha] = 0 \ . \tag{3.15}$$

Together with the identity, 1, the rotation operators T_α form the so called Vierergruppe, D_2, that allows one to order rotor eigenstates into four different subgroups, A and B_{1-3}. Each of these subgroups is defined by the transformation behavior of the eigenstates under the T_α (see Table 3.3.1)

Table 3.1: Irreducible representations of Vierergruppe D_2.

Symmetry	Transformation				Index		Dimension	
Type	1	T_1	T_2	T_3	λ	μ	I(even)	I(odd)
A	1	1	1	1	e	e	$(I+2)/2$	$(I-1)/2$
B_1	1	1	−1	−1	e	o	$I/2$	$(I+1)/2$
B_2	1	−1	1	−1	o	o	$I/2$	$(I+1)/2$
B_3	1	−1	−1	1	o	e	$I/2$	$(I+1)/2$

that can be derived from the properties of the Wigner D functions:

$$T_1\, D^{I*}_{M,K}(\Omega) = (-1)^{I+K}\, D^{I*}_{M,-K}(\Omega)\,, \tag{3.16}$$

$$T_2\, D^{I*}_{M,K}(\Omega) = (-1)^{I-K}\, D^{I*}_{M,-K}(\Omega)\,, \tag{3.17}$$

$$T_3\, D^{I*}_{M,K}(\Omega) = (-1)^{K}\, D^{I*}_{M,K}(\Omega)\,. \tag{3.18}$$

As a consequence, the Hamiltonian matrix can also be written in a block diagonal form.

3.3.2 SU(3) and $T_5 \wedge SO(3)$

To find a correspondence between the physics described by a quantum rotor and the SU(3) model, the relationship between their corresponding algebras can be used.

The rotor algebra $T_5 \wedge SO(3)$ is generated by the five moments of the *collective* quadrupole operator (Eq. (3.4)) which coincide with the moments of the corresponding inertia tensor and three components of the angular momentum. The commutation relation between these generators of the semi-direct product of T_5 and SO(3) are

$$[L_\mu, L_\nu] = -\sqrt{2}\langle 1\mu, 1\nu | 1\mu+\nu\rangle\, L_{\mu+\nu},$$

$$[L_\mu, Q^c_\nu] = -\sqrt{6}\langle 1\mu, 2\nu | 2\mu+\nu\rangle\, Q^c_{\mu+\nu}, \tag{3.19}$$

$$[Q^c_\mu, Q^c_\nu] = 0\,, \tag{3.20}$$

reflecting the structure of the semi-direct product group with two sets of generators, each separately

closed under commutation ($[T_5, T_5] \rightarrow T_5, [SO(3), SO(3)] \rightarrow SO(3)$) but with the commutator of an element of one group with an element of the other yielding an element of only one of the sets ($[T_5, SO(3)] \rightarrow T_5$).

These commutator relations are similar to the ones between the *algebraic* quadrupole operator, Q^a_μ and the angular momentum, L, that are generators of SU(3):

$$\begin{aligned} [L_\mu, L_\nu] &= -\sqrt{2}\langle 1\mu, 1\nu | 1\mu+\nu \rangle \, L_{\mu+\nu}, \\ [L_\mu, Q^a_\nu] &= -\sqrt{6}\langle 1\mu, 2\nu | 2\mu+\nu \rangle \, Q^a_{\mu+\nu}, \\ [Q^a_\mu, Q^a_\nu] &= 3\sqrt{10}\langle 2\mu, 2\nu | 1\mu+\nu \rangle L_{\mu+\nu}, \ , \end{aligned} \tag{3.21}$$

where only the last commutation relation for the quadrupole operators are different, giving zero in the rotor case and non-zero in the SU(3) case.

When L is small compared to $\sqrt{C_2}$ the SU(3) algebra contracts to the $T_5 \wedge SO(3)$ algebra, which can be seen by rescaling Q^a as $Q^a/\sqrt{C_2}$. The rescaling leaves the first two commutation relations unchanged but implies $[Q^a_\mu, Q^a_\nu] \approx 0$ for $C_2 \gg L$ in the SU(3) case. This is equivalent to the statement that the SU(3) model describes rotational states very well as long as

$$L \ll \max[(2\lambda+\mu), (\lambda+2\mu)] \, . \tag{3.22}$$

This is related to the fact that SU(3) is a compact algebra with a maximum value for the angular momentum, L, whereas the rotor algebra is non-compact with unbound L.

Since both the rotor and SU(3) theory are describing the same physical phenomena – e. g. a rotational spectrum – and their algebras are closely related it is natural to require a correspondence between the invariants of both groups.

Because SU(3) is a rank two group it has two invariants C_2 and C_3 that can be expressed by the SU(3) labels (λ, μ) as:

$$C_2 = (\lambda+\mu)(\lambda+\mu+3) - \lambda\mu \quad \text{and}$$

$$C_3 = \frac{1}{9}(\lambda-\mu)(\lambda+2\mu+3)(2\lambda+\mu+3)\,. \tag{3.23}$$

The symmetry group of the rotor, $T_5 \wedge SO(3)$, also has two invariants, the traces of the square and cube of the collective quadrupole matrix:

$$\begin{aligned} Tr[(Q^c)^2] &= \lambda_1^2+\lambda_2^2+\lambda_3^2 \quad \text{and} \\ Tr[(Q^c)^3] &= \lambda_1\,\lambda_2\,\lambda_3\,. \end{aligned} \tag{3.24}$$

Here the λ_α are the expectation values of the quadrupole matrix in its body-fixed principal axis frame ($Q^c_{\alpha\beta}=\lambda_\alpha\delta_{\alpha\beta}$) that can be parameterized by the shape variables (β,γ) as:

$$\lambda_\alpha = \sqrt{\frac{5}{\pi}}\frac{Ar_0^2}{3}\cos(\gamma-2\pi\alpha/3) \qquad \alpha=1,2,3 \tag{3.25}$$

where A denotes the number of nucleons and r_0 the root-mean-square radius.

Requiring a correspondence between the invariants of the two groups, i. e. $C_2 \sim Tr[(Q^c)^2]$ and $C_3 \sim Tr[(Q^c)^3]$, leads to the following relation between the SU(3) labels (λ,μ) and the λ_i:

$$\begin{aligned} \lambda_1 &= -\frac{1}{3}(\lambda-\mu) \\ \lambda_2 &= -\frac{1}{3}(\lambda+2\mu+3) \\ \lambda_3 &= \frac{1}{3}(2\lambda+\mu+3) \end{aligned} \tag{3.26}$$

Using Eq. (3.25) this set of equations can be rewritten into a relation between the shape variables (β,γ) and the SU(3) irreps (λ,μ):

$$\beta^2 = \frac{4\pi}{5}\frac{1}{(Ar_0^2)^2}\left(\lambda^2+\lambda\mu+\mu^2+3(\lambda+\mu+1)\right) \tag{3.27}$$

$$\tan\gamma = \frac{\sqrt{3}(\mu+1)}{2\lambda+\mu+3}\,. \tag{3.28}$$

Alternatively, this relation can be interpreted as a mapping between labels (λ, μ) and spherical coordinates $(k\beta, \gamma) \leftrightarrow (r, \gamma)$

$$k\beta\cos(\gamma) = k\beta_x = (2\lambda + \mu + 3)/3 \tag{3.29}$$

$$k\beta\sin(\gamma) = k\beta_y = (\mu + 1)/\sqrt{3} \tag{3.30}$$

where the abbreviation $k = \sqrt{4/9\pi}Ar_0$ has been used.

According to this scheme, each irrep (λ, μ) corresponds to an unique shape parameterized by (β, γ). For example, Eq. (3.28) implies that for $\mu = 0$ the deformation parameter γ is close to zero. A SU(3) irrep with $\mu = 0$ thus corresponds to a prolate – cigar-like – shape. For the case $\lambda = \mu$ the SU(3) irrep describes an particle distribution with maximum triaxiality, $\gamma = 30°$ A SU(3) irrep with $\lambda = 0$ corresponds to an oblate – pancake-like – shape with $\gamma = 60°$.

Whereas every SU(3) irrep (λ, μ) can be mapped onto a particular shape (β, γ), the reverse mapping is not possible for every set (β, γ) . In sharp contrast with the collective model where β and γ can vary continuously, the group structure $U(\Omega) \supset SU(3)$ dictates a limited set of allowed (λ, μ) values depending on the number of particles in a shell. This reflects the fermionic nature of the nucleons, a feature that is not included in the collective model.

3.4 K_L-Band splitting in the SU(3) model

Since the quadrupole-quadrupole term, $Q^aQ^a = 4C_2 - 3L^2$, term can not distinguish between multiple occurrences of L in a SU(3) irrep (λ, μ), the simple SU(3) Hamiltonian with a harmonic oscillator potential plus quadrupole-quadrupole interaction given in Eq. (3.7) has an energy spectrum with only one rotational band for each irrep.

The experimental results for most deformed even-even nuclei [24, 91] however, show different types of rotational bands: The ground state band starts with a 0^+ state and contains only even angular momenta (resulting in a sequence $0^+, 2^+, 4^+ \ldots$). A so-called K-band has a 2^+ state as

its band head and the angular momentum increases in steps of $\Delta L = 1$ (resulting in a sequence $2^+, 3^+ \ldots$ with a L(L+1) spacing)

As was mentioned earlier, a K-band appears naturally within the framework of the rotor model where the operator $K^2 = I_3^2$ (I_3 is the projection of the total angular momentum on the third body-fixed axis) generates K-bands that are shifted in energy relative to the 0^+ ground state band, have a 2^+ state as band head, and an increase in angular momentum in steps of one, $\Delta L = 1$, is experimentally observed.

To derive the SU(3) model equivalent of the K^2 operator which is necessary for a realistic description of the rotational structure, the relation between the SU(3) algebra and the rotor algebra is used again. Ideally, in addition to being a rotational invariant such a SU(3) model equivalent of K^2 should conserve the SU(3) symmetry of the system. This can be achieved by employing a special minimal set of SO(3) scalars the so-called SU(3) $\rightarrow$ SO(3) integrity basis, which has been shown [74] to contain five operators that give rise to real symmetric matrix forms. They can be chosen to be the Casimir invariants L^2, C_2 and C_3, and two non-SU(3) invariant SO(3) scalars labeled X_3^a and X_4^a, which are of degree three and four, receptively, in the SU(3) generators:

$$\begin{aligned} X_3^a &= \sum_{i,j} L_i Q_{ij}^a L_j \\ X_4^a &= \sum_{i,j,k} L_i Q_{ij}^a Q_{jk}^a L_k \ . \end{aligned} \tag{3.31}$$

Since only the operators X_3^a and X_4^a are able to couple and mix multiple occurrences of a given SO(3) irrep in SU(3), they have to be part of a SU(3) Hamiltonian that is able to reproduce a more complex rotational spectrum. In the most general case, this Hamiltonian has the form

$$H_{SU(3)} = a_1 C_2 + a_2 C_3 + a_3 L^2 + a_4 X_3^a + a_5 X_4^a \ . \tag{3.32}$$

In order to extract the shell-model equivalent of the K^2 operator from this Hamilonian, the collective version of the three terms in $H_{SU(3)}$ with an angular momentum dependence have been

rewritten, replacing the algebraic quadrupole operator with its collective counterpart that is diagonal in the body-fixed principle axis frame: ($Q^c_{\alpha\beta} = \lambda_\alpha \, \delta_{\alpha\beta}$):

$$\begin{aligned} L^2 &= \sum_i L_i L_i = \sum_i I_i^2 \\ X_3^c &= \sum_{i,j} L_i Q^c_{ij} L_j = \sum_i \lambda_i I_i^2 \\ X_4^c &= \sum_{i,j,k} L_i Q^c_{ij} Q^c_{jk} L_k = \sum_i \lambda_i^2 I_i^2 \end{aligned} \tag{3.33}$$

As before, the notation I and L is used for the angular momentum in the body-fixed and lab-frame respectively. This set of equations can be inverted [91] to yield the following expression for the I_i^2 in terms of L^2 and X^{c}'s:

$$I_i^2 = [(\lambda_1\lambda_2\lambda_2)L^2 + (\lambda_i^2)X_3^c + (\lambda_i)X_4^c]/D_i \, , \quad D_i \equiv 2\lambda_i^3 + \lambda_1\lambda_2\lambda_3 \, . \tag{3.34}$$

Substituting these expressions into the Hamiltonian for an asymmetric Rotor,

$$H_{rot} = A_x I_x^2 + A_y I_y^2 + A_z I_z^2 \, , \tag{3.35}$$

gives a frame independent expression for H_{rot}

$$H_{rot} = aL^2 + bX_3^c + cX_4^c \tag{3.36}$$

where the parameters a, b and c are given as

$$\begin{aligned} a &= \sum_i \lambda_1\lambda_2\lambda_3 A_i/D_i \\ b &= \sum_i \lambda_i^2 A_i/D_i \\ c &= \sum_i \lambda_i A_i/D_i \, . \end{aligned} \tag{3.37}$$

To derive a SU(3) shell model image of $K^2 = I_3^2$ from this Hamiltonian, the operators X_3^c and X_4^c that couple shells differing by two quanta have to be changed back to their algebraic counterparts that were introduced in Eq. (3.31). As was shown by Leschber [78], this substitution does indeed yield a shell model Hamiltonian that is able to reproduce the rotor results and observed rotational phenomena in nuclei. The algebraic equivalent of H_{rot} in Eq. (3.36) for the special case $A_1 = A_2 = 0$ and $A_3 = 1$ is thus a natural definition for a shell model operator K^2

$$K^2 = (\lambda_1\lambda_2 L^2 + \lambda_3 X_3^a + X_4^a)/(2\lambda_3^2 + \lambda_1\lambda_2) \ . \tag{3.38}$$

Because of the correspondence between the invariants of the rotor group $T_5 \wedge SO(3)$ and SU(3) the parameters λ_i are given as a function of the SU(3) labels λ and μ as:

$$\lambda_1 = -\frac{1}{3}(\lambda - \mu) \quad \lambda_2 = -\frac{1}{3}(\lambda + 2\mu + 3) \quad \lambda_3 = \frac{1}{3}(2\lambda + \mu + 3) \ , \tag{3.39}$$

so that K^2 can be determined for a given SU(3) eigenfunction $|(\lambda, \mu)\rangle$.

Since the $SU(3)$ irreps are related to the shape of nuclear distribution, this can be seen as a generalization of the rotor Hamiltonian given in Eq. (3.11) where the coefficients are determined by the moments of intertia.

Like in the case of rotational spectra generated by the quadrupole-quadrupole operator, the correspondence between the K operator in the SU(3) and rotor picture is best for small values of L. This reflects the fact that SU(3) is a compact group with finite-dimensional irreps, while the symmetry group of the rotor is non-compact with infinite-dimensional representations.

3.5 Shell-model operator for K_J-band splitting

For the description of odd-A nuclei where the spin degree of freedom has to be taken into account, a generalization of the shell model operator, (3.38), that generates the K_L band splitting in even-A nuclei with total spin S = 0 has to be introduced. This operator has to be able to reproduce the

observed K_J band splitting in the spectra of odd-A nuclei, where $K_J = K_L + K_S$ is the projection of the total angular momentum, $\mathbf{J} = \mathbf{L} + \mathbf{S}$, on the principal symmetry axis of the system. This K_J^2 operator is also the appropriate form for $\mathbf{S} \neq 0$ states in even-A nuclei and has to reduce to the previous defined algebraic equivalent of K_L^2 for $\mathbf{S} = 0$.

The simplest starting point is the Hamiltonian of a generalized triaxial rotor,

$$H_{rot} = \sum_{i=1}^{3} A_I I_i^2 \,, \tag{3.40}$$

where $\mathbf{I}$ is now the total angular momentum that can be either half-integral or integral. Analogous to the $\mathbf{S} = 0$ case, this Hamiltonian can be rewritten in a frame-independent representation by introducing the three rotational scalars in the ls-coupled space

$$\begin{aligned} J^2 &= \sum_i J_i J_i = \sum_i I_i^2 \\ X_3^c &= \sum_{i,j} J_i Q_{ij}^c J_j = \sum_i \lambda_i I_i^2 \\ X_4^c &= \sum_{i,j,k} J_i Q_{ij}^c Q_{jk}^c J_k = \sum_i \lambda_i^2 I_i^2 \,. \end{aligned} \tag{3.41}$$

Like in the $\mathbf{S} = 0$ case, Eq. (3.41) can be solved for the I_i's to obtain a frame-independent rotor Hamiltonian that in turn gives a frame-independent expression for K_J^2 with the intertia parameters $A_1 = A_2 = 0$ and $A_3 = 1$:

$$K_J^2 = (\lambda_1 \lambda_2 J^2 + \lambda_3 X_3^c + X_4^c)/(2\lambda_3^2 + \lambda_1 \lambda_2) \,. \tag{3.42}$$

Replacing X_3^c and X_4^c with their algebraic counterparts – for which the collective quadrupole operator $Q_{\alpha\beta}^c$ is used instead of its algebraic version – is then a natural definition for a SU(3) shell model image of K_J^2.

For the evaluation of the matrix elements of the X_3^c and X_4^c operators and therefore of K^2 in the spin-coupled basis of the SU(3) scheme [24],

$$|\gamma(\lambda,\mu)\kappa LSJM_J\rangle \quad \text{with } \gamma = N[f]\alpha[\bar{f}]\beta \,, \tag{3.43}$$

it is usefull express these operators in a tensor notation,

$$X_3^a = \sum_{\alpha\beta} J_\alpha Q_{\alpha\beta} J_\beta = \frac{1}{6}\sqrt{30}\left[[J \otimes Q]^1 \otimes J\right]^0 \tag{3.44}$$

and

$$X_4^a = \sum_{\alpha\beta\gamma} J_\alpha Q_{\alpha\beta} Q_{\beta\gamma} J_\gamma = -\frac{5}{18}\sqrt{3}\left[[J \otimes Q]^1 \otimes [J \otimes Q]^1\right]^0 . \tag{3.45}$$

Since the reduced matrix elements of the SU(3) generator Q^a are known, the reduced matrix elements for X_3^a and X_4^a can also be evaluated and are given by

$$\begin{aligned} &\langle \gamma(\lambda,\mu)\kappa LSJ||X_3^a||\gamma(\lambda,\mu)\kappa' L'SJ\rangle \\ &= \sqrt{\frac{5}{6}} J(J+1)\sqrt{(2J+1)}W(J1J1;J2) \\ &\quad \times < (\lambda,\mu)\kappa LSJ\ ||Q^a||\ (\lambda,\mu)\kappa' L'SJ > \end{aligned} \tag{3.46}$$

and

$$\begin{aligned} &\langle \gamma(\lambda,\mu)\kappa LSJ||X_4^a||\gamma(\lambda,\mu)\kappa' L'SJ\rangle \\ &= \frac{5}{6} J(J+1)\sqrt{(2J+1)} \sum_{\kappa'' L'' J''} (-1)^{J-J''} W(J1J1;J2)^2 \\ &\quad \times < (\lambda,\mu)\kappa LSJ\ ||Q^a||\ (\lambda,\mu)\kappa'' L''SJ > \\ &\quad < (\lambda,\mu)\kappa'' L''SJ\ ||Q^a||\ (\lambda,\mu)\kappa' L'SJ > \end{aligned} \tag{3.47}$$

where the reduced matrix element for Q^A that has the SU(3) tensor character $(\lambda_0,\mu_0)\kappa_0 L_0 = (1,1)12$ is given by

$$\begin{aligned} &< (\lambda,\mu)\kappa LSJ\ ||Q^a||\ (\lambda,\mu)\kappa' L'SJ' > \\ &= (-1)^\phi 2\sqrt{C_2(\lambda,\mu)(2J'+1)(2J+1)}W(SJ'L2;L'J) \\ &\quad \times < (\lambda,\mu)\kappa' L';(1,1)12||(\lambda,\mu)\kappa L >_{\rho=1} . \end{aligned} \tag{3.48}$$

Here the Ws are SU(2) Racah coefficients and the $< (\lambda,\mu)\kappa' L';(1,1)12||(\lambda,\mu)\kappa L >_{\rho=1}$ denote SU(3) $\supset$ SO(3) coupling coefficients. The phase factor, $(-1)^\phi = -1$ if $\mu \neq 0$ and $+1$ if $\mu = 0$, is required

for consistency with the definition of SU(3) coupling coefficients [1, 36] In the $\mathbf{S = 0}$ configuration the matrix elements for K_J^2 reduce to those of the previously defined and simpler K_L^2 operator.

To explore the potential usefulness of the K_J^2 operator in the shell model, a comparison of results for the odd-A nucleus ^{24}Mg and ^{159}Dy and ^{165}Er were found to be in good agreement with the corresponding collective model values. [92].

3.6 One and two-body interactions

So far it was shown how collective aspects of the nuclear interaction can be described naturally within the framework of SU(3) model. To summarize, the close relation between the rotor and the SU(3) algebras translates into the ability of a SU(3) symmetry preserving Hamiltonian to describe the rotational spectrum of well-deformed nuclei and also allows one to map SU(3) eigenstates $|(\lambda, \mu)\rangle$ onto shapes parameterized by the deformation parameters β and γ.

Another strength of the SU(3) model is its ability to account for single particle degrees of freedom since it is a many particle theory that fully accounts for the fermionic structure of the nucleus. As can be seen for example by the importance of the spin-orbit and orbit-orbit terms in the single particle shell model, these additional degrees of freedom are an important ingredient for a realistic nuclear model.

The assumption that the last unpaired nucleon determines the spin of the nucleon – i. e. that proton or neutron pairs with opposing spin and the same $|m_l|$ value but otherwise identical quantum numbers couple to $\mathbf{S = L = 0}$ pairs, which is used in the single particle shell model, reflects the existence of the pairing interaction which lowers the energy of nucleon pairs coupled to total angular momentum zero. Indeed, the pairing-plus-quadrupole model [9] has been used to simulate both few particle non-collective and many particle collective features of nuclei [12]. The addition of this two-body interaction is thus an important step towards a more realistic Hamiltonian.

As this interaction is most effective between $(\mathbf{J = 0})$-coupled pairs, pairing correlations are normally attributed to the short-range part of the nucleon-nucleon interaction. Since the spatial

overlap of two nucleon densities is at its maximum if the nucleons have the same l and $|m|$ value and rotational invariance further requires J = 0, this is the configuration energetically favored by a short-range attractive interaction.

In the spectrum of even-even nuclei that are just a few nucleons away from a closed shell, the effect of the pairing interactions can be seen in the energy gap of about 1 MeV that occurs between the $J^\pi = 0^+$ and a set of nearly degenerate states ($J^+ = 2^+, 4^+, 6^+ \ldots$). This so-called "pairing gap" corresponds to the energy necessary to break up a nucleon pair and recouple it with S = 1 and thus gives an estimate for the strength of the pairing interaction.

To evaluate the one-body spin-orbit and orbit-orbit interaction and the two-body pairing interaction within the framework of the SU(3) model, they have to be expressed in a form compatible with the SU(3) eigenstate basis for the many particle wavefunction. This can be done by employing the so-called second-quantization formalism in which particle creation and annihilation operators are introduced. Since the fermion creation operator and the annihilation operators multiplied by a phase factor have good SU(3) transformation behavior, they can be coupled to SU(3) tensors, thus allowing one to rewrite any n-body operator as a sum of these basic unit-tensors. A generalization of the Wigner-Eckart theorem for the SU(3) case then provides an elegant way for the evaluation of matrix elements.

An additional advantage of this formalism is its ability to describe naturally operators in pickup or decay reactions, where the number of particles in the initial and final state are different [26, 71].

More specifically, a fermion creation operator $a^\dagger_\gamma$ is defined by its action on a vacuum state $|0\rangle$ which gives the single particle state $|\gamma\rangle$:

$$a^\dagger_\gamma|0\rangle = |\gamma\rangle \; . \tag{3.49}$$

Here the label γ has been introduced as an abbreviation for all the quantum numbers necessary to classify a single particle state. In the case of the SU(3) model these are spin quantum numbers and the SU(3) irrep and intra-irrep labels for the spatial part. An additional index distinguishes protons

and neutrons. This can be done by either the m-projection of the isospin or by using the labels π or ν respectively . For a proton in the η-th shell for example the abbreviation $|\gamma\rangle$ corresponds to the state $|(\eta,0)\ l, m_l, \frac{1}{2}m_s, \pi\rangle$ if the SU(3) $\supset$ SO(3) group chain is used and angular momentum and spin are not coupled.

The conjugate operator a_γ acts as a particle annihilation operator. Applied on the single particle state $|\gamma\rangle$ it gives the vacuum state $|0\rangle$:

$$a_\gamma|\gamma\rangle = |0\rangle\ . \tag{3.50}$$

Any annihilation operator acting on the vacuum state gives 0,

$$a_\gamma|0\rangle = 0\,, \tag{3.51}$$

which in turn can be used as a definition of the abstract vacuum state $|0\rangle$. In the context of the shell model, the vacuum state corresponds to an empty shell.

The fundamental symmetry properties that distinguish fermions from bosons and require a many particle fermionic wavefunction to be totally antisymmetric, are reflected in a set of anti-commutation relations for the fermion creation and annihilation operators:

$$\begin{aligned} \{a^\dagger_\gamma,\, a_{\gamma'}\} = a^\dagger_\gamma a_{\gamma'} + a_{\gamma'} a^\dagger_\gamma &= \delta_{\gamma,\gamma'} \\ \{a^\dagger_\gamma,\, a^\dagger_{\gamma'},\} = \{a_\gamma,\, a_{\gamma'}\} &= 0\,. \end{aligned} \tag{3.52}$$

Different from the creation operator, the annihilation operator introduced above is not a SU(3) tensor and an operator $\tilde{a}_\gamma$ with good SU(3) transformation behavior under SU(3) that differs from a_γ by a phase is more convenient for the following discussion:

$$\tilde{a}_\gamma = \tilde{a}_{(0,\eta)\ l, m_l, \frac{1}{2}m_s} \equiv (-1)^{\eta+l+m+\frac{1}{2}+m_s} a_{(\eta,0)\ l,-m_l,\frac{1}{2}-m_s} \tag{3.53}$$

With these defintions in place, a one-body unit tensor, ${}^{1,1}\mathcal{F}^{(\lambda\mu)\kappa LM_L SM_S}_{(\eta',0)(0,\eta)\frac{1}{2}\frac{1}{2}}$, can be introduced as

$$
\begin{aligned}
{}^{(1,1)}\mathcal{F}^{(\lambda\mu)\kappa LM_L SM_S}_{(\eta',0)(0,\eta)\frac{1}{2}\frac{1}{2}} &\equiv \left[a^{\dagger}_{(\eta',0)\frac{1}{2}} \otimes \tilde{a}_{(\eta,0)\frac{1}{2}}\right]^{(\lambda\mu)\kappa LM_L SM_s} \\
&= \sum_{ll'} \langle (\eta,0)l', (0,\eta)l || (\lambda,\mu)\kappa L\rangle \sum_{m_s m_s'} \langle \frac{1}{2}m_s', \frac{1}{2}m_s | SM_S\rangle \qquad (3.54) \\
&\quad \times \sum_{m'm} \langle l'm', lm | LM_L\rangle \; a^{\dagger}_{(\eta 0)l'm'\frac{1}{2}m_s'} \tilde{a}_{(0\eta)lm\frac{1}{2}m_s} \; , \qquad (3.55)
\end{aligned}
$$

where the coupling coefficients used are the SO(3) Clebsch Gordan coefficients, $\langle \cdots | \cdot \rangle$, and their SU(3) equivalent for which a notation with double bars, $\langle \cdots || \cdot \rangle$, has been introduced (see App. A.1).

For the expansion of one-body operators that have to be rotational invariant it is useful to also introduce a one-body unit tensor in the l-s coupled basis with J = 0 :

$$
\begin{aligned}
u^{(\lambda\lambda)LS}_{\eta\eta'} &\equiv \left[a^{\dagger}_{(\eta',0)\frac{1}{2}} \otimes \tilde{a}_{(\eta,0)\frac{1}{2}}\right]^{(\lambda\mu)\kappa LSJ=M_J=0} \\
&= \sum_{M_L M_S} < LM_L SM_S | 00 > {}^{(1,1)}\mathcal{U}^{(\lambda\mu)\kappa LM_L SM_S 0}_{(\eta',0)(0,\eta)\frac{1}{2}} \qquad (3.56)
\end{aligned}
$$

With their good SU(3) transformation behavior these unit tensors serve as an operator basis in which a general one-body operator, F, that acts symmetrically on a system of N identical particles,

$$
F = \sum_{i=1}^{N} f(x_i \sigma_i) \; , \qquad (3.57)
$$

can be expanded in a form compatible with the SU(3) basis used for the many particle states [101]. The second quantization formalism allows one to express the one-body operator in terms of fermion creation and annihilation operators

$$
F = \sum_{\beta,\gamma} < \beta | f | \gamma > a^{\dagger}_{\beta} a_{\gamma} \qquad (3.58)
$$

and thus introduces the basic operators that can be coupled to form the unit-tensor operators defined above (3.56).

Examples that will be used later, are the tensor expansions for the single particle spin-orbit and orbit-orbit interactions:

$$\sum_i l_i s_i = \sum_{(\lambda,\lambda)l} [a^\dagger_{(\eta,0)l\frac{1}{2}} \tilde{a}_{(0,\eta)l\frac{1}{2}}]_0^{(\lambda,\lambda)0,0,0} \langle((\eta,0)l,(0,\eta)l\|(\lambda,\lambda)0\rangle \times(-)^\eta [\frac{1}{2}l(l+1)(2l+1)]^{\frac{1}{2}} \tag{3.59}$$

and

$$\sum_i l_i^2 = \sum_{(\lambda,\lambda)l} [a^\dagger_{(\eta,0)l\frac{1}{2}} \tilde{a}_{(0,\eta)l\frac{1}{2}}]_0^{(\lambda,\lambda)1,1,0} \langle((\eta,0)l,(0,\eta)l\|(\lambda,\lambda)1\rangle \times(-)^\eta [l(l+1)[2(2l+1)]^{\frac{1}{2}} \tag{3.60}$$

In a completely analogous manner, it is possible to define a two-body SU(3) unit tensor, ${}^{(2,2)}\mathcal{F}$, as a product of a unit tensor ${}^{(2,0)}\mathcal{F}$ that creates a pair of particles and one ${}^{(0,2)}\mathcal{F}$ that annihilates a particle pair,

$${}^{(2,2)}\mathcal{F}^{\rho(\lambda,\mu)\kappa LM_L SM_S}_{(\lambda_1,\mu_1)(\lambda_2,\mu_2)S_1S_2} \equiv \left[{}^{(2,0)}\mathcal{F}^{(\lambda_1,\mu_1)S_1}_{(\eta_1',0)(\eta_1,0)\frac{1}{2}\frac{1}{2}} \times {}^{0,2}\mathcal{F}^{(\lambda_2,\mu_2)S_2}_{(0,\eta_2')(0,\eta_2)\frac{1}{2}\frac{1}{2}} \right]^{\rho(\lambda,\mu)\kappa LM_L SM_S}, \tag{3.61}$$

where the pair creation and annihilation unit tensors are defined as:

$$\begin{aligned} {}^{(2,0)}\mathcal{F}^{(\lambda,\mu)\kappa LM_L SM_S}_{(\eta',0)(\eta,0)\frac{1}{2}\frac{1}{2}} &\equiv \left[a^\dagger_{(\eta',0)\frac{1}{2}} \otimes a^\dagger_{(\eta,0)\frac{1}{2}}\right]^{(\lambda,\mu)\kappa LM_L SM_S} \\ {}^{(0,2)}\mathcal{F}^{(\mu,\lambda)\kappa LM_L SM_S}_{(0,\eta')(0,\eta)\frac{1}{2}\frac{1}{2}} &\equiv \left[\tilde{a}_{(0,\eta')\frac{1}{2}} \otimes \tilde{a}_{(0,\eta)\frac{1}{2}}\right]^{(\mu,\lambda)\kappa LM_L SM_S} . \end{aligned} \tag{3.62}$$

A general two-body operator,

$$G = \sum_{i<j=1}^{N} g(x_i\,\sigma_i, x_j\,\sigma_j)\,, \tag{3.63}$$

that acts on the single particle spin and space coordinates, can be expressed in second quantization as

$$G = \frac{1}{4} \sum_{\beta,\gamma,\delta,\epsilon} \langle \beta\gamma \,|\, f \,|\delta\epsilon\rangle a^\dagger_\beta a^\dagger_\gamma a_\delta a_\epsilon \,, \tag{3.64}$$

where $\langle \beta\gamma|$ and $|\delta\epsilon\rangle$ are normalized antisymmetric two-particle states.

Specifically, we are interested in the operator for the pairing interaction that can be written in second quantization as

$$V_p = -\frac{1}{4} G \sum_{\gamma,\gamma'} a^\dagger_\gamma a^\dagger_{\tilde{\gamma}} a_{\gamma'} a_{\tilde{\gamma}'} \,, \tag{3.65}$$

where $\tilde{\gamma}$ and $\tilde{\gamma}'$ denote the time reversed partners of the single particle states γ and γ' respectively, and G is the strength of the pairing interaction. It can be expressed in terms of second quantization as

$$V_p = \frac{G}{2} \sum_{(\lambda_1,\mu_1)(\lambda_2,\mu_2)} \sum_{\eta\eta'} P_{\eta\eta'}((\lambda_1,\mu_1)(\lambda_2,\mu_2)\rho_0(\lambda_0\mu_0)) \tag{3.66}$$

$$\left[[a^\dagger_\eta \otimes a^\dagger_\eta]^{\lambda_1\mu_1} \otimes [\tilde{a}_{\eta'} \otimes \tilde{a}_{\eta'}]^{\lambda_2\mu_2}\right]^{\rho_0\lambda_0\mu_0\kappa_0=1l_0=s_0=0} \,, \tag{3.67}$$

where the coefficient $P_{\eta\eta'}(\ldots)$ involves a sum over the product of three SU(3) reduced coupling coefficients

$$\begin{aligned} & P_{\eta\eta'}((\lambda_1,\mu_1)(\lambda_2,\mu_2)\rho_0(\lambda_0\mu_0)) \\ &= (-1)^{l-l'}\sqrt{(2l+1)(2l'+1)} < (\eta 0)l;(\eta 0)l||(\lambda_1\mu_1)10 > \\ &\quad \times < (\eta' 0)l;(\eta' 0)l||(\lambda_2\mu_2)10 >< (\lambda_1\mu_1)l;(\lambda_2\mu_2)l||(\lambda_0\mu_0)10 >_{\rho_0} \,. \end{aligned} \tag{3.68}$$

A problem with adding the one-body spin-orbit and orbit-orbit and the two-body pairing interaction to a SU(3) Hamiltonian lies is the fact that the corresponding operators break SU(3) symmetry. If a dominating quadrupole-quadrupole interaction is assumed however, SU(3) still remains extremely useful as an approximate symmetry. Specifically, this allows one to restrict the

configuration space to SU(3) irreps with a large C_2 value and the use of group theoretical tools for the evaluation.

For a systems with only a few particles, however, it is still possible to do shell model calculations in the complete many particle space. These toy models have been used to investigate the influence of different interactions on the nuclear shape [4, 7, 8]. From the structure of the quadrupole-quadrupole interaction it is obvious that it drives the nuclear shape towards strongly deformed shapes. For the pairing interaction it was assumed traditionally that it would favor a spherical shape. A detailed SU(3) model analysis however, showed that the pairing favors triaxially deformed many particle configurations where the deformation is generally rather soft.

In addition, the single particle spin-orbit interaction has been taken into account [46], so that the complete Hamiltonian investigated had the form:

$$H_{SU(3)} = \frac{\chi}{2} Q \cdot Q + G_\pi V_P^\pi + V_\nu H_P^\nu + aK_J + bJ^2 \,. \tag{3.69}$$

The $\mathbf{l} \cdot \mathbf{s}$ interaction breaks both the SU(3) symmetry and by mixing different spins the U(3) symmetry. A weak spin-orbit force pushes the system towards a more spherical shape i. e. towards smaller $k\beta$ values while leaving the triaxial deformation that is parameterized by γ unaffected. For a strong spin-orbit interaction mixing becomes so strong that the shape is no longer defined.

Although symmetry breaking effects of the single particle spin-orbit interaction are strong, they do not preclude the use of the SU(3) scheme, since for nuclei with $A \leq 100$ with a strong spin-orbit force the pseudo-spin concept can be applied which then leads to a pseudo-realization of SU(3). In this representation the spin-orbit interaction is weak enough to yield good pseudo-SU(3) quantum numbers.

The details of the pseudo-SU(3) concept that is crucial for the treatment of heavy nuclei, is the topic of the next chapter.

Chapter 4

Pseudo-spin symmetry

The pseudo-spin concept that was introduced first by Hecht and Adler in the late sixties [65, 101] can be described most naturally within the framework of the single particle shell model that was discussed in the previous chapter. As was described there, the shell model Hamiltonian h_0 uses the three-dimensional isotropic harmonic oscillator, h_{osc}, as a central potential, augmented with one-body spin-orbit ($\mathbf{l}\cdot\mathbf{s}$) and the orbit-orbit ($\mathbf{l}^2$) terms,

$$h_0 = h_{osc} + C\,\mathbf{l}\cdot\mathbf{s} + D\,(\mathbf{l}^2 - \langle\mathbf{l}^2\rangle_{shell})\,, \tag{4.1}$$

where here the mean value of $\mathbf{l}^2$ over a given spherical shell, $\langle\mathbf{l}^2\rangle_{shell} = n(n+3)/2$, has been subtracted. This ensures that the average single-nucleon energy is fixed by its harmonic oscillator value [59], a feature that will be important in the later discussion.

Unfortunately, for all but light ($A \leq 28$) nuclei, the splitting generated by the $\mathbf{l}\cdot\mathbf{s}$ term is so large that it destroys the underlying SU(3) symmetry of the isotropic oscillator. A consequence is that SU(3), which has been shown to be extremely useful for shell-model calculations in light nuclei, has little apparent value in heavier systems, especially those with ($A \geq 100$). In this mass region, however, another symmetry emerges.

The introduction of this so called pseudo symmetry is motivated by the observation that for heavy nuclei certain combinations of normal parity spherical orbitals (l_j-$(l+2)_{j+1}$) form subshell doublets (for example, $s_{\frac{1}{2}} - d_{\frac{3}{2}}$ and $d_{\frac{5}{2}} - g_{\frac{7}{2}}$ for $n = 4$, or $p_{\frac{3}{2}} - f_{\frac{5}{2}}$ and $f_{\frac{7}{2}} - h_{\frac{9}{2}}$ for $n = 5$) which can be treated

as (almost) degenerate levels with the same pseudo-angular momentum, $\tilde{l} = l_j + 1 = (l+2)_{j+1} - 1$, and (almost) decoupled pseudo-spin, $\tilde{s}$.

The degeneracy of states with the same pseudo-angular momentum can be reproduced by a Hamiltonian with pseudo $\mathbf{l} \cdot \mathbf{s}$ and $\mathbf{l}^2$ terms where the pseudo $\mathbf{l} \cdot \mathbf{s}$ is relatively small. A unitary transformation that effects this change carries h_{osc} into its pseudo equivalent, $\tilde{h}_{osc}$, which is simply the isotropic harmonic oscillator Hamiltonian for a system with one less quanta, transforming the total shell model Hamiltonian, h_0 as follows [5]:

$$\begin{aligned} & h_{osc} + C\,\mathbf{l} \cdot \mathbf{s} + D(\mathbf{l}^2 - \langle \mathbf{l}^2 \rangle_{shell}) \\ & \longrightarrow \tilde{h}_{osc} + (4D - C)\,\tilde{\mathbf{l}} \cdot \tilde{\mathbf{s}} + D(\tilde{\mathbf{l}}^2 - \langle \tilde{\mathbf{l}}^2 \rangle_{shell}) + (\hbar\omega + 2D - C)\,. \end{aligned} \tag{4.2}$$

The significance of this result comes from the fact that for heavy nuclei

$$4D - C \approx 0\,, \tag{4.3}$$

which means that the pseudo-spin symmetry breaking in h_0, generated by the $\tilde{\mathbf{l}} \cdot \tilde{\mathbf{s}}$ term, is small. More specifically, empirical results for medium and heavy mass nuclei give the parameter $\mu = \frac{2D}{C}$ as $\mu_\pi \approx 0.4$ and $\mu_\nu \approx 0.6$ for protons and neutrons respectively [106, 20]. This places the average of μ for protons and neutrons parameters exactly on the symmetry limit. As a result, the large $\mathbf{l} \cdot \mathbf{s}$ splitting found in heavy nuclei therefore gives way to a small pseudo $\tilde{\mathbf{l}} \cdot \tilde{\mathbf{s}}$ term upon application of the pseudo space-spin transformation.

The crucial relation Eq. (4.3) can not only be obtained empirically from experimental data but also from relativistic mean-field results, which suggest a microscopic origin for the symmetry, as will briefly discussed next.

4.1 Microscopic origin

To investigate the goodness of pseudo-spin symmetry from relativistic mean field results, estimates for the strength of the spin-orbit and orbit-orbit interactions have been derived [5], that these show that the parameter $\mu = \frac{2D}{C}$ indeed has a value close to the exact symmetry limit 0.5.

Using the usual Dirac equation as a starting point (with only the time component of the scalar and vector potentials taken into account) and using a nonrelativistic reduction of the relativistic mean-field theory, the spin-orbit interaction potential can be expressed as

$$V_{ls} = \frac{\hbar^2}{2M}\frac{2}{r}\frac{d}{dr}\left[\frac{1}{1 - B\rho/\rho_0}\right] \mathbf{l}\cdot\mathbf{s}\,, \tag{4.4}$$

where the parameters ρ and ρ_0 are respectively the nucleon density at radius r and the nuclear matter density. In the simplest version of the theory, the dimensionless quantity $B = \frac{1}{2}(B_s + B_v)$ is just the average of the scalar and vector coupling constants of the corresponding mesons. Using the fact that dr/r vanishes everywhere except near the surface, the spin-orbit strength, C, can be obtained by averaging V_{ls} over the region inside the nucleon radius R as

$$C = \frac{-\hbar^2}{2MR}\frac{1 - B}{3B}\,. \tag{4.5}$$

To find an estimate for the strength of the orbit-orbit interaction, one can use the fact that the origin of the $\mathbf{l}^2$ term lies in the flatness of the mean field in the interior region as compared with the quadratic oscillator form used in the shell model Hamiltonian. In the large mass limit a more realistic potential is that of a spherical well with finite depth. If this potential is replaced with one of infinite depth, the single particle energies are given by

$$E_{nl} = \frac{\hbar^2}{2MR^2}x_{nl}^2\,, \tag{4.6}$$

where M is the nucleon mass, R the radius of the well, and the x_{nl} are the zeros of spherical Bessel functions that are approximately given by $x_{nl}^2 \approx [(\frac{1}{2}n + 1)\pi]^2 - l(l+1)$. The energy splitting thus follows an $l(l+1)$ rule and the orbit-orbit strength, D, is given by

$$D = -\frac{\hbar^2}{2MR^2}\,. \tag{4.7}$$

Using these estimates for C and D, μ can be approximated by the ratio

$$\mu = \frac{2D}{C} = \frac{1-B}{3B}, \tag{4.8}$$

which is independent of the mass number.

Using estimates for B derived in the Nambu Jona-Lasinio model [90] which starts with massless quarks and generates the hadron masses by spontaneous symmetry breaking, gives $\mu = 0.686$. Also, results derived from other microscopic models like the Walecka model [111] and a derivative coupling model due to Zimany and Moszkowski [127], that give $\mu = 0.447$ and $\mu = 0.635$ respectively, are consistent with the pseudo-spin picture. The pseudo-spin symmetry thus appears to be a feature of the nuclear interaction that can also be seen on a more fundamental level.

4.2 The pseudo-spin transformation

For practical purposes, and to gain a deeper understanding of the pseudo-spin symmetry, the structure of the unitary pseudo-spin transformation U that transforms a shell model Hamiltonian according to Eq. (4.2) has been investigated extensively in the last few years [27, 15, 17].

For single particle basis states this unitary transformation U from the normal space to the pseudo space can be expressed as

$$U_{njm\,\tilde{n}\tilde{j}\tilde{m}}|n\,(l,s)\,j,m\rangle = |\tilde{n}\,(\tilde{l},\tilde{s})\,\tilde{j},\tilde{m}\rangle, \tag{4.9}$$

where the spherical shell model quantum numbers j, n and s, for total angular momentum, oscillator shell and spin respectively, transform as:

$$\tilde{j} = j,\ \tilde{n} = n-1,\ \tilde{s} = s \tag{4.10}$$

and the transformation for the angular momentum l depends on the value of the corresponding j:

$$\tilde{l} = l \pm 1 \quad \text{according to whether } j = l \pm \frac{1}{2}. \tag{4.11}$$

Thus, the pseudo transformation amounts to a simple relabeling of the spherical basis states, mapping levels of the n-th oscillator shell onto the $\tilde{n} = n - 1$ shell of a pseudo oscillator. Disregarded in this mapping are the oscillator states with maximum total angular momentum, j, that is, the ones with $j = n + \frac{1}{2}$. Because the spin-orbit interaction is so strong for heavy nuclei, these levels are pushed down among the levels of the $(n-1)$-th shell. These states are called "defectors" when they become part of the core and "intruders" when they penetrate down into the valence space from above. In both cases they are "unique parity" states because they have an opposite parity than their "normal parity" partners.

More specifically, a *normal* $\rightarrow$ *pseudo* single particle transformation operator U can be introduced as:

$$U(\mathbf{r}, \mathbf{p}, \sigma) = (d \cdot d^{\dagger})^{-1/2} d, \qquad \text{with} \quad d = \mathbf{b} \cdot \sigma, \tag{4.12}$$

where σ is the Pauli spin matrix and $\mathbf{b}$ the bosonic annihilation operator, $b_i = \sqrt{m\omega/(2\hbar)} r_i + i\sqrt{1/(2\hbar m\omega)} p_i$. Its presence can be understood by the fact that the pseudo-spin transformation lowers the n-quantum number by one. For a system of A nucleons in the spherical oscillator representation the *normal* $\rightarrow$ *pseudo* transformation can then be written in a multiplicative form:

$$U_{\text{total}} = \prod_{i=1}^{A} U(\mathbf{r_i}, \mathbf{p_i}, \sigma_i) \, . \tag{4.13}$$

As can be shown [27], the action of d on a h. o. eigenstate, $|n(l,s)j,m\rangle$, is given by:

$$d|n\,(l,1/2)\,l+1/2,m\rangle \;=\; (n-l)^{1/2}|n-1\,(l+1,1/2)\,l+1/2,m\rangle\,, \tag{4.14}$$

$$d|n\,(l,1/2)\,l-1/2,m\rangle \;=\; (n+l+1)^{1/2}|n-1\,(l-1,1/2)\,l-1/2,m\rangle\,. \tag{4.15}$$

so that U indeed has the form required in Eq. (4.9). However, since the intruder levels with $j = l + \frac{1}{2}$ have no counterpart in the pseudo space and are being destroyed by d, see Eq. (4.14), U is only unitary within the subshell with $j < j_{max} = n + \frac{1}{2}$.

For an analysis of a variety of nuclear Hamiltonians, it is also necessary to know the pseudo-spin structure of different operators. Results for the operator that counts the number of oscillator quanta,

$$UnU^{\dagger} = n + 1 \ , \tag{4.16}$$

the operator used to generate spin orbit splitting,

$$U\mathbf{l}\cdot\mathbf{s}U^{\dagger} = -\mathbf{l}\cdot\mathbf{s} - 2 \ , \tag{4.17}$$

and the orbit-orbit interaction,

$$U\mathbf{l}^2U^{\dagger} = \mathbf{l}^2 + 2\mathbf{l}\cdot\sigma + 2 \ . \tag{4.18}$$

have been derived by Blokhin [16, 17] and show that the operator U given in (4.12) indeed transforms the shell model Hamiltonian in the way required in Eq. (4.2).

The transformation for other operators is more challenging and the more complex expressions for the transformation of the Pauli spin matrix and the Elliott quadrupole operator are given for example in [16].

The transformation operator described above, however, is not the only one possible. In the most general form, the pseudo-spin transformation, U, is a function of the position, $\mathbf{r}$, the momentum, $\mathbf{p}$, and the Pauli spin matrix, σ, of an individual nucleon and in order to give the correct pseudo Hamiltonian given in Eq. (4.2) with a small spin-orbit interaction it has to transform $\mathbf{l}^2$ according to:

$$U\mathbf{l}^2U^{-1} = \mathbf{l}^2 + 2\mathbf{l}\cdot\sigma + 2 = 2\mathbf{j}^2 - \mathbf{l}^2 + \frac{1}{2} \ . \tag{4.19}$$

The structure of $U(\mathbf{r},\mathbf{p},\sigma)$ can further be fixed by the following general constraints

$$[U,\mathbf{j}] = 0 \quad \text{rotational invariance} \tag{4.20}$$

$$[U,\mathcal{P}] = 0 \quad \text{parity conservation} \tag{4.21}$$

$$[U, T] = 0 \quad \text{time reversal symmetry} \tag{4.22}$$

$$UU^\dagger = U^\dagger U = 1 \quad \text{unitarity} \tag{4.23}$$

As was shown by Blokhin [16], three distinguishable choices for U remain with these restrictions. These have the general structure

$$U = (d \cdot d^\dagger)^{-1/2} d, \qquad d = (\cos\theta r_0 \mathbf{p} + i \sin\theta \mathbf{r}/r_0) \cdot \sigma \tag{4.24}$$

where due to the option of rescaling the characteristic length r_0 the values of θ can be fixed at $\pm\frac{\pi}{4}$, 0 or $\frac{\pi}{2}$. The first choice, $\theta = +\frac{\pi}{4}$, yields the boson creation operator $b_i^\dagger$,

$$b_i^\dagger = \sqrt{\frac{m\omega}{2\hbar}} r_i - i \frac{1}{\sqrt{2\hbar m\omega}} p_i \tag{4.25}$$

so that U corresponds to the transformation discussed above (4.12), while $\theta = -\frac{\pi}{4}$ yields the annihilation operator b_i:

$$b_i = \sqrt{\frac{m\omega}{2\hbar}} r_i + i \frac{1}{\sqrt{2\hbar m\omega}} p_i \,. \tag{4.26}$$

However, these operators that have also been discussed by Castaños et al. [27] are unitary only within a subspace of normal parity while their action is undefined in the unique parity subspace.

Two choices remain if global symmetry is required. The case $\frac{\pi}{2}$ corresponds to the so called r-helicity [18] $U_r = i\sigma \cdot \mathbf{r}/r$ which, however, is not compatible with translational invariance

$$[U, \mathbf{p}] = 0 \ . \tag{4.27}$$

A transformation that is invariant under translations is the so-called p-helicity $U_p = \sigma \cdot \mathbf{p}/p$

This transformation has been used to analyze the transformation behavior of a shell-model wave-function in a spherical representation:

$$\psi_{nljm_j}(\mathbf{r}, \sigma) = i^l R_{nl}(r)(\mathbf{Y}_l(\Omega) \otimes \chi)_{jm_j} \ , \tag{4.28}$$

where as usual n is the number of quanta, l, j and m denote orbital momentum, total angular momentum and its projection, respectively, $\mathbf{Y}_l(\Omega)$ is a spherical harmonic and χ a Pauli spin matrix. As was shown [17], ψ_{nljm_j} transforms under the p-helicity as:

$$U\psi_{nljm_j} = i^{\tilde{l}}\mathcal{R}_{\tilde{n},\tilde{l}q}(r)(\mathbf{Y}_{\tilde{l}}(\Omega)\otimes\chi)_{jm_j} \ , \tag{4.29}$$

where

$$q = 2(l-j), \qquad \tilde{l} = l - q, \qquad \tilde{n} = n - q \ , \tag{4.30}$$

and analytical expressions for the radial functions $\mathcal{R}_{n,l,+1}(r)$ and $\mathcal{R}_{n,l,+1}(r)$ are given in [17] as a sum over hypergeometric functions. These transformed radial functions behave in the bulk practically like the closest oscillator function, either slightly compressed ($q = 1$) or dilated ($q = -1$). Since the behavior of more realistic single particle functions (for instance, for the Woods-Saxon potential) is very similar to the one of their oscillator counterparts, the above remains valid for realistic mean-field models. The helicity transformation for the basis functions in the spherical limit is thus model independent to a good extent and can be accomplished by replacing the transformed functions by the closest oscillator functions as described in Eq. (4.9).

An even stronger argument for pseudo-spin as a more fundamental nuclear symmetry has been derived from the transformation behavior of a general shell model Hamiltonian that is consistent with relativistic theories (see Eq. (4.4)) and includes a r dependent spin-orbit strength, [15, 116]

$$H = \frac{p^2}{2M} + V(r) + W(r)\,\mathbf{l}\cdot\mathbf{s} \ . \tag{4.31}$$

The transformation of this general Hamiltonian yields

$$U\,H\,U^{+} = \frac{p^2}{2M} + \bar{V}(r) + \bar{W}(r)\,\mathbf{l}\cdot\mathbf{s} \ , \tag{4.32}$$

and is complicated by the fact that the helicity transformation is highly non-local in nature. To get

a localized estimated for $\bar{V}(r)$ and $\tilde{W}(r)$ these transformed potentials were calculated in first order perturbation theory. Results of this work, in which a microscopic one-boson-exchange potential [83] was considered, show that the minimum in the spin-orbit potential, $\tilde{W}(r)$, which is located in the surface region in the normal representation gets shifted deeper into the bulk. From this it follows that the magnitude of the spin-orbit interaction in the region with larger radius which is primarily responsible for the interaction strength shows a strong decrease.

Consistent with the work by Bahri [5, 4], the small spin-orbit strength present in a pseudo shell-model Hamiltonian can thus be derived from a microscopic theory that includes relativistic features. The pseudo-spin symmetry thus seems to be a fundamental feature of the nuclear interaction.

4.3 Pseudo-spin for axial deformed nuclei

In the discussion of the pseudo-spin symmetry so far a spherical symmetric Hamiltonian has been assumed. For more realistic applications and to further probe the nature of this symmetry, the case of a shell-model Hamiltonian with axial deformation terms will be covered in this section.

Because the spherical quantum numbers l, j, and m are not conserved for a non-spherical Hamiltonian, the relabeling scheme (4.10) does not any longer relate a single particle particle wavefunction in the real space to a unique pseudo counterpart. Also, since the pseudo-transformation of non-scalar deformation terms is problematic, the goodness of the pseudo-spin concept for deformed nuclei can not be investigated using the pseudo transformations introduced for the spherical case. How these problems can be addressed will be discussed after a short introduction to the single particle Hamiltonian used to describe axial deformed nuclei and the related asymptotic quantum numbers.

The so-called Nilsson Hamilonian [96] is an extension to the single particle Hamiltonian given in Eq. (4.1),

$$h_{nil} = h_{osc} + C\,\mathbf{l}\cdot\mathbf{s} + D\,\mathbf{l}^2 + h_\beta\,, \tag{4.33}$$

where the deformed quadrupole field added is given by

$$h_\beta = -m\omega^2 r^2 \beta Y_{20}(\theta, \phi) \, . \tag{4.34}$$

In order to guarantee volume conservation, the oscillator frequency is deformation dependent, with $\omega(\beta)$ given as

$$\omega(\beta) = \omega(0) \left(1 + \frac{15}{4\pi}\beta^2 - \frac{16}{27}\beta^3 \right)^{1/6} \, . \tag{4.35}$$

The deformation part of the Hamiltonian mixes the spherical basis states so that l and j no longer remain good quantum numbers. As was demonstrated by Nilsson in the limit of very large quadrupole transformations, the physical states can be classified by means of asymptotic quantum numbers $[Nn_z l_z j_z]$, where N is the total number of oscillator quanta, n_z is the number of quanta along the body-fixed symmetry axis (z-axis), l_z is the projection of the single particle orbital angular momentum on the z-axis, while $j_z = l_z \pm 1/2$ is the third component of the total spin. Since for an axial average field $[h_{nil}, j_z] = 0$, j_z is a constant of motion. However, neither n_z nor l_z nor the z component of the particle spin, $\Sigma = \pm 1/2$, are good quantum numbers especially at small and moderate deformations.

A first indication for the goodness of the pseudo-spin concept for axial deformations can be found in the so called Nilsson diagrams that show single particle energies plotted as a function of the axial deformation parameter β. A prominent feature of these Nilsson diagrams are pairs of energy levels that stay close together independent of deformation and which for the spherical case, $\beta = 0$, correspond to the pseudo-spin doublets, $(l_j\text{-}(l+2)_{j+1})$. The asymptotic quantum numbers of these doublets are N, n_z, l_z with $j_z = l_z + \frac{1}{2}$ and N, n_z, $l_z + 2$ with $j_z = (l_z + 2) - \frac{1}{2}$.

Guided by this observation and the relabeling scheme used for a spherical basis [101], the deformed normal parity Nilsson states can be classified by pseudo-asymptotic quantum numbers

$\tilde{N}, \tilde{n}_z, \tilde{l}_z, \tilde{s}_z$ and $\tilde{j}_z$ where

$$\tilde{N} = N - 1, \quad \tilde{n}_z = n_z, \quad \tilde{l}_z = l_z + s_z, \quad \tilde{s}_z = -s_z, \quad \tilde{j}_z = j_z \,. \tag{4.36}$$

This relabeling scheme is equivalent to the action of a pseudospin transformation U_∞ in the asymptotic region that acts on the cylindrical basis states $|N, n_z, l_z, j_z\rangle$ as:

$$U_\infty \, |N, n_z, l_z, l_z \pm \frac{1}{2}\rangle = |N-1, n_z, l_z \pm 1, l_z \pm \frac{1}{2}\rangle \,. \tag{4.37}$$

As was shown by Castoños et al. [28], this pseudo-spin transformation in the asymptotic region has the form

$$U_\infty = (d_\infty d_\infty^+)^{-1/2} d_\infty \,, \tag{4.38}$$

where d_∞ is given as

$$d_\infty = b'_x \, \sigma_x + b'_y \, \sigma_y \tag{4.39}$$

and the b'_i $(i = x, y)$ are deformed boson annihilation operators with β dependent frequencies ω',

$$b'_s = \sqrt{\frac{m\omega'}{2\hbar}} x_s + i \frac{1}{\sqrt{2\hbar m\omega'}} p_s \quad \text{where} \quad \omega' = \omega \frac{(1 + \sqrt{\frac{5}{4\pi}}\beta)^{1/6}}{(1 - \sqrt{\frac{5}{\pi}}\beta)^{-1/6}} \,. \tag{4.40}$$

Using this transformation for the cylindrical deformed limit, it can be shown that a Nilsson type Hamiltonian, (4.33), can be approximated by its pseudo-spin counterpart

$$\tilde{h} = \tilde{h}_{osc} + C \, \tilde{l} \cdot \tilde{s} + D \, \tilde{l}^2 + \tilde{h}_\beta \,, \tag{4.41}$$

which is characterized by a much weaker spin-orbit splitting and slightly higher oscillator frequencies but that essentially keeps its original structure.

To analyze the goodness of the pseudo-spin picture not only for the limiting case of extreme deformations for which U_∞ is valid but also for continuous deformations from oblate to prolate,

Troltenier [118] made a detailed comparison of the single particle energies and the wavefunctions given by the deformed pseudo Nilsson Hamiltonian and a more realistic deformed Woods-Saxon potential [93, 10] defined as:

$$V(\mathbf{r},\beta) = \frac{V_0}{1+\exp(\mathrm{dis}_\Sigma(\mathbf{r},\beta)/a)] } \tag{4.42}$$

with $\mathrm{dis}_\Sigma(\mathbf{r},\beta_2)$ being the distance between the nuclear surface Σ and the space point $\mathbf{r}$ at a given deformation β_2. The nuclear surface is defined by the usual quadrupole expansion:

$$R(\Omega) = c(\beta) = r_0(1+\beta Y_{20}(\Omega)) \; . \tag{4.43}$$

In contrast to the pseudo Nilsson Hamiltonian where the symmetry limit of zero pseudo spin-orbit interaction strength was used, the spin-orbit splitting was not neglected in the Woods-Saxon calculation. Also the $\Delta = 2, 4, \ldots$ couplings were taken into account correctly and the coupling to the abnormal parity subshell (intruder) with $j = N + \frac{1}{2}$ was included in the more complex Woods-Saxon calculation.

The remarkable agreement that was found for single particle energies and wavefunctions confirms the presence of the pseudo-spin symmetry in the realistic average potential for any oblate and prolate deformations. In addition, this comparison between the two models shows how the existence of the pseudo-spin symmetry allows one to use a much simpler Hamiltionian and a significant reduction of space necessary to describe a nuclear shell. The last point is an advantage that will be especially useful for many particle calculations for which the dimensionality grows almost exponentially with particle number.

Based on these investigations that show the validity of the pseudo-spin picture also for axial deformations, a variety of features of heavy deformed nuclei have been studied using pseudo-SU(3) model calculations. In turn, the success of these calculations can be used as an additional argument for goodness of the pseudo-spin symmetry.

One example for these calculations are magnetic moments of odd-A nuclei that were evaluated [118] using the single particle wavefunctions given by the pseudo-Nilsson Hamiltonian (4.41) and

for which a rather close agreement with experimental values was found. Other applications are rotational spectra, transition strengths and double beta decay [117, 14, 70].

4.4 Pseudo-spin for triaxial deformations

Whereas most deformed nuclei are thought to have an axial deformation, the existence of triaxial shapes in transitional nuclei has also been established in the last few years [63].

Even though static transformations are in the strict sense not physical observables, many investigations predict a rather flat energy surface in the triaxiality parameter γ for these nuclei. The non-symmetric shape of these so-called gamma-soft nuclei is reflected among other things by a low-energy spectrum that does not show rotor-like characteristics. The investigation of triaxial nuclei using the pseudo SU(3) model thus allows one to probe the limits of the SU(3) model that is closely related to the rotor picture. In comparison, axially deformed nuclei usually show a well pronounced minimum in the parameter β and a rotational spectrum with $L(L+1)$ characteristics.

As was discussed in the previous chapter, the close relation between SU(3) and rotor algebras translates into a one-to-one correspondence between the nuclear shape parameterized in terms for the collective variables β, γ and the SU(3) labels (λ, μ). Thus, SU(3) model calculations for gamma-soft nuclei with their not well-deformed shape requires the mixing of different SU(3) irreps. An investigation of gamma-soft nuclei within the framework of the pseudo SU(3) model, however, poses the question of the goodness of the pseudo-spin picture in the general case of non-axial deformations.

The positive answer to this question – which will be discussed later in this chapter – justifies the application of the pseudo-SU(3) model to gamma soft nuclei that is presented later in this work and is one of the important results of this thesis.

Before the goodness of the pseudo-spin for deformed nuclei is analyzed, a short introduction to some properties of the deformed harmonic oscillator potential and to the notation used is given next.

4.4.1 The triaxial deformed oscillator

In the single particle picture, a triaxial nucleus can be described by an extension of the Nilsson Hamiltonian for axial deformation given in Eq. (4.33). This generalized Nilsson Hamiltonian includes a triaxial deformation term $(Y_2^2 + Y_{-2}^2)$ parameterized by γ,

$$h_{nil} = h_0 - m\,\omega^2\,r^2\,\beta\,[\cos(\gamma)Y_0^2 + \frac{\sin\gamma}{\sqrt{2}}(Y_2^2 + Y_{-2}^2)]\,. \tag{4.44}$$

Here, h_0 is the (rotational invariant) Nilsson Hamiltonian defined in Eq. (4.1). To guarantee volume conservation the oscillator frequency ω is a function of β and γ given by:

$$\omega(\beta,\gamma) = \omega_0(1 + \frac{15}{4\pi}\beta^2 - \frac{1}{4}(\frac{5}{\pi})^{\frac{3}{2}}\cos^3 3\gamma)^{-\frac{1}{6}}\,. \tag{4.45}$$

The deformation terms, $r^2Y_{2\mu}$, introduce mixing that couples different shells with $\Delta n = \pm 2$ where the matrix elements are given in a spherical basis, $|nl,\Lambda\Sigma\rangle$, as:

$$\langle n'l'\Lambda'\Sigma'|r^2Y_{2\mu}|nl\Lambda\Sigma\rangle = \langle n'l'|r^2|nl\rangle\langle l'\Lambda|Y_{2\mu}|l\Lambda l\rangle\delta_{\Sigma'\Sigma}\,. \tag{4.46}$$

The radial part of this matrix element is [38],

$$\begin{aligned}
\langle n'l'|r^2|nl\rangle \;=\; & \delta_{n'n-2}\frac{1}{2}\Big[\sqrt{(n+l+1)(n+l-1)}\,\delta_{l'l-2} \\
& + \sqrt{(n-l)(n+l+1)}\,\delta_{l'l} + \sqrt{(n-l)(n-l-2)}\,\delta_{l'l+2}\Big] \\
& + \delta_{n'n}\Big[\sqrt{(n-l+2)(n+l+1)}\delta_{l'l-2} \\
& + (n+\frac{3}{2})\delta_{l'l} + \sqrt{(n-l)(n+l+3)}\delta_{l'l+2}\Big] \\
& + \delta_{n'n+2}\Big[\frac{1}{2}\sqrt{(n+l+1)(n+l+3)}\delta_{l'l-2} \\
& \frac{1}{2}\sqrt{(n-l+2)(n+l+3)}\delta_{l'l}\frac{1}{2}\sqrt{(n-l)(n-l+2)}\delta_{l'l+2}\Big]\,,
\end{aligned} \tag{4.47}$$

and the angular integral is given as:

$$\langle l'\Lambda'|Y_{20}|l\lambda\rangle = (-1)^{l'-\lambda'} \cdot \begin{pmatrix} l' & 2 & l \\ \Lambda' & \mu & \Lambda \end{pmatrix} \sqrt{(2l'+1)(2l+1)} \tag{4.48}$$

Even for moderate deformations ($\beta \approx 0.3$) this shell mixing is relatively large, making it difficult to assign certain single particle states to a particular oscillator shell.

The deformation can also be expressed by oscillator frequencies that are different in the x, y or z directions. An alternative form for the generalized Nilsson Hamiltonian, Eq. (4.44), that is more suitable for a cartesian basis is thus:

$$H = \frac{\mathbf{p}^2}{2m} + \frac{1}{2}m\left[\omega_x^2 x^2 + \omega_y^2 y^2 + \omega_z^2 z^2\right] + C\mathbf{l}\cdot\mathbf{s} + D\mathbf{l}^2 \tag{4.49}$$

where the frequencies, ω_i, are given as:

$$\omega_i = \epsilon_i \omega_0 \,. \tag{4.50}$$

For the different direction $i = x, y, z$ the parameter ϵ_i is defined as:

$$\begin{aligned} \epsilon_z &= \epsilon_0 \left(1 - \sqrt{\frac{5}{\pi}}\beta\cos\gamma\right)^{1/2} \\ \epsilon_x &= \epsilon_0 \left(1 + \sqrt{\frac{5}{\pi}}\beta\cos(\gamma + \frac{\pi}{3})\right)^{1/2} \\ \epsilon_y &= \epsilon_0 \left(1 + \sqrt{\frac{5}{\pi}}\beta\cos(\gamma - \frac{\pi}{3})\right)^{1/2} \end{aligned} \tag{4.51}$$

and ϵ_0 is as a deformation dependent normalization factor that ensures volume conservation:

$$\epsilon_z\,\epsilon_x\,\epsilon_y = 1\,. \tag{4.52}$$

For the following application it is also convenient to introduce deformed cartesian coordinates that are defined as:

$$x_i' = \sqrt{\epsilon_s}\, x_s \tag{4.53}$$

$$p'_i = \sqrt{1/\epsilon_s}\, p_s \,. \tag{4.54}$$

These cordinates allow one to express the oscillator with different frequencies in x, y and z direction in terms of deformed boson operators:

$$b'_s = \sqrt{\frac{m\omega}{2\hbar}} x'_s + i\frac{1}{\sqrt{2\hbar m\omega}} p'_s \,, \qquad b'^{+}_s = \sqrt{\frac{m\omega}{2\hbar}} x'_s - i\frac{1}{\sqrt{2\hbar m\omega}} p'_s \tag{4.55}$$

so that the generalized Nilsson Hamiltonian, Eq. (4.44), can also be written as:

$$\begin{aligned} h_{nils} &= (\sum_i \epsilon_i (b'^{+}_s b'_s + \frac{1}{2}) - C\,\mathbf{l}\cdot\mathbf{s} + D\,\mathbf{l}^2 \\ &= h'_{osc} - C\,\mathbf{l}\cdot\mathbf{s} + D\,\mathbf{l}^2 \,. \end{aligned} \tag{4.56}$$

In the deformed basis, x'_i, the deformed harmonic oscillator potential, h'_{osc}, is diagonal, whereas the spin-orbit ($\mathbf{l}\cdot\mathbf{s}$) and orbit-orbit ($\mathbf{l}^2$) terms create shell mixing. Thus, the shell mixing coming from the deformation terms disappears but is replaced by the a smaller mixing coming from the physical orbital momentum $\mathbf{l} = i\mathbf{b}\times\mathbf{b}^{+}$ where the spherical boson operators are given in terms of deformed coordinates as:

$$\begin{aligned} b_s &= (\epsilon_s)^{-1/2}\sqrt{\frac{m\omega}{2\hbar}}\, x'_s + i(\epsilon_s)^{1/2}\frac{1}{\sqrt{2\hbar m\omega}}\, p'_s \qquad (4.57)\\ &= \frac{1}{2}(\epsilon_s{}^{-1/2} + \epsilon_s{}^{1/2})\, b'_s + \frac{1}{2}(\epsilon_s{}^{-1/2} - \epsilon_s{}^{1/2})\, b'^{+}_s \\ b^{+}_s &= (\epsilon_s)^{-1/2}\sqrt{\frac{m\omega}{2\hbar}}\, x'_s - i(\epsilon_s)^{-1/2}\frac{1}{\sqrt{2\hbar m\omega}}\, p'_s \qquad (4.58)\\ &= \frac{1}{2}(\epsilon_s{}^{-1/2} - \epsilon_s{}^{1/2})\, b'_s + \frac{1}{2}(\epsilon_s{}^{-1/2} + \epsilon_s{}^{1/2})\, b'^{+}_s \end{aligned}$$

For reasonable deformations of about $|\beta| \leq 0.5$, however, this mixing is much smaller than the one present in a spherical basis which will be crucial for the following discussion.

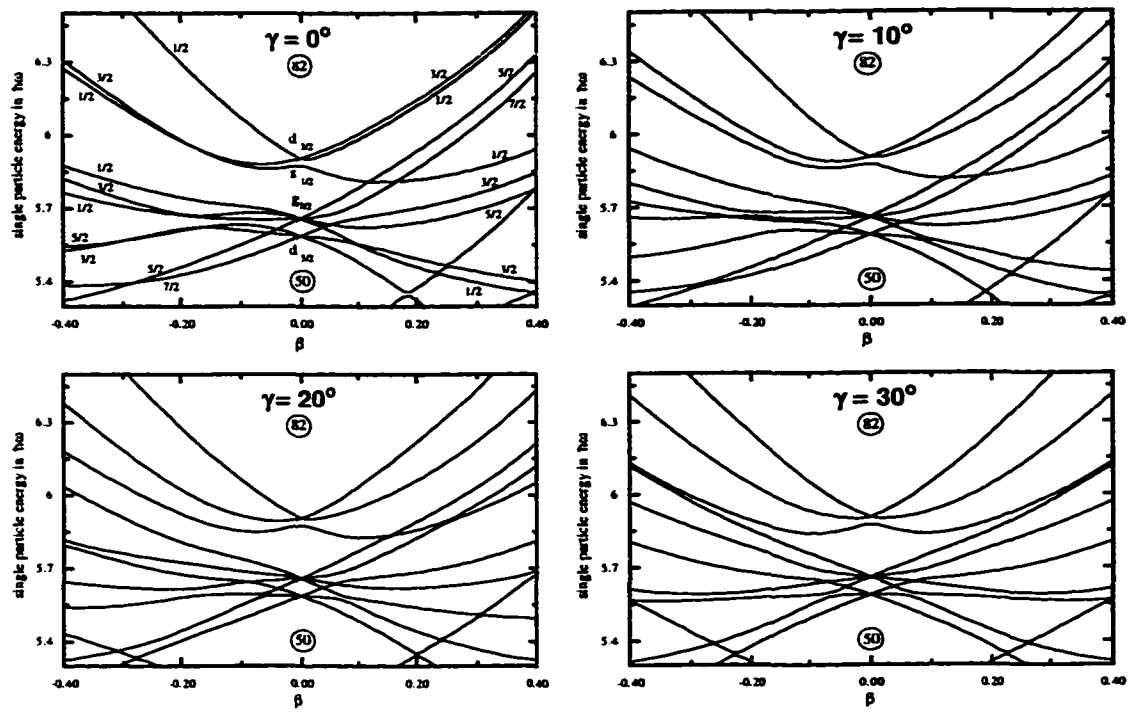

Figure 4.1: Single particle energies for triaxial deformations. The neutron single particle energies are plotted for the $n = 4$ normal parity subspace as a function of β for different triaxial deformations γ. For $\gamma = 0$ the asymptotic states are labeled by $j_z = l_z + s_z$ ($\Omega = \Lambda + \Sigma$)

4.4.2 Correlation coefficients

The fact that the pseudo-spin doublets seen in a Nilsson diagram with only axial deformations stay together (see Fig. 4.1 for $\gamma = 0$) even for strong deformation ($-0.4 \leq \beta \leq 0.4$) has been used as an argument that the pseudo scheme is also valid for axial deformations, that is, that the strength of the pseudo $\mathbf{l} \cdot \mathbf{s}$ term remains small for $\beta \neq 0$ and $\gamma = 0$.

The situation is quite different for triaxial deformations [38]. The generalized Nilsson diagrams, shown in Fig. 4.1 for the $n = 4$ shell (without defector states) and $\gamma = 0°, 10°, 20°$, and $30°$ illustrate that the characteristic pseudo-spin degeneracy of the prolate ($\gamma = 0°$) case is lost as the system approaches maximum triaxiality ($\gamma = 30°$). Because positive values of β with $30° \leq \gamma \leq 60°$

correspond to negative β values with $30° \geq \gamma \geq 0°$, respectively, these results also show the re-appearance of the symmetry as the system approaches the oblate axial limit ($\gamma = 60°$).

This disappearance of the pseudo spin-orbit doublets with increasing triaxiality could be simply a result of the loss of the axial symmetry since the z-component of the total spin, $j_z = l_z \pm \frac{1}{2}$, is no longer a good quantum number. As a consequence the degeneracy of the pseudo-spin levels with $\bar{\Lambda} \pm \frac{1}{2}$ disappears as well, so that even if the pseudo-symmetry is still valid it doesn't manifest itself in the almost degenerate energy levels. On the other hand, it is possible that the additional triaxial deformation terms actually destroy the pseudo-spin symmetry.

To determine whether pseudo-spin symmetry is a valid concept for non-axial systems requires a non-spectral measure because the near level degeneracies that signal its importance in axial cases disappear as γ increases. A logical choice for this measure is the correlation coefficient [29] between the generalized Nilsson Hamiltonian and the pseudo spin-orbit interaction, $\bar{\mathbf{l}}\cdot\tilde{\mathbf{s}}$, in the physical space of states. This relatively simple statistical measure gives a good indication for the relative significance of a particular interaction in h_{nil} thus allowing one, for example, to compare the smallness of the symmetry breaking in the triaxial case with the one for axial deformations where peudo-spin symmetry as a dynamical symmetry is well established [118, 45, 24]. A further advantage of this measure is that it can be applied without knowing exact analytic forms for the general ($\gamma \neq 0$) pseudo-spin transformation.

The correlation coefficient ζ is a statistical measure that is global in nature and depends only on traces of operators over model spaces. It is also a normalized measure, $-1 \leq \zeta \leq +1$, one that is often given in terms of a corresponding angular measure, $\zeta = \cos\theta$, where θ ranges from $-90°$ ($\zeta = -1$, anti-parallel) through $0°$ ($\zeta = 0$, perpendicular), to $+90°$ ($\zeta = +1$, parallel). Specifically, the correlation coefficient ζ for two physical operators h and k is defined by

$$\begin{aligned} \zeta_{h,k} &= \frac{\langle\langle(h-\bar{h})(k-\bar{k})\rangle\rangle}{\sqrt{\langle\langle(h-\bar{h})^2\rangle\rangle\langle\langle(k-\bar{k})^2\rangle\rangle}} \\ &= \frac{\langle\langle hk\rangle\rangle - \bar{h}\bar{k}}{\sqrt{\langle\langle(h-\bar{h})^2\rangle\rangle\langle\langle(k-\bar{k})^2\rangle\rangle}}, \end{aligned} \tag{4.59}$$

where the double bracket $\langle\langle\rangle\rangle$ denotes the trace over the model space. The bar over an operator is a shorthand notation for its average which is simply its trace divided by the dimension, d, of the model space: $\bar{k} = \langle k \rangle = \langle\langle k \rangle\rangle/d$.

Clearly, if $k = \pm h$, $\zeta_{h,k} = \pm 1$ and the operators are parallel (+) and anti-parallel (−), respectively. And if $\zeta_{h,k} = 0$ the two are perpendicular, meaning that the product of their matrix elements summed over the subspace vanishes. In statistical terms, the latter means they are uncorrelated within the subspace. However, in spaces with large dimensions even $|\zeta| \approx 0.5$ ($\theta \approx 60°$) is a strong correlation. In this context, a statement that the pseudo-spin scheme is valid for triaxially deformed nuclei means that the correlation coefficient between h and $k = \tilde{\mathrm{l}} \cdot \tilde{\mathrm{s}}$ is small, ideally 0, reflecting the fact that the pseudo-$SU(3)$ symmetry breaking term $\tilde{\mathrm{l}} \cdot \tilde{\mathrm{s}}$ is relatively unimportant. It is also important to note that $\zeta_{h,k} = 0$ does *not* imply that $[h, k] = 0$, which is the stringent condition required for an *exact* symmetry. Instead, the correlation coefficient is a statistical measure of the similarity (or dissimilarity) of two operators. Nonetheless, even though the correlation coefficient is a soft (non-stringent) measure, it is a valid one or determining the goodness of a symmetry.

The trace introduced in Eq. (4.59) is defined with respect to a specific model space. For the correlation coefficient to be a physically meaningful measure, this space should be decoupled, at least approximately, from neighboring spaces. The mixing between shells with $\Delta = \pm 2$ introduced by the deformation terms, however, makes it problematic to use an oscillator shell as such a space.

In the present case, a more natural choice for the summation in Eq. (4.59) is the set of states belonging to a major shell n of the deformed oscillator that was introduced above. In a deformed basis the shell mixing originates from the relatively small spin-orbit ($\mathrm{l} \cdot \mathrm{s}$) and orbit-orbit ($\mathrm{l}^2$) terms, whereas the deformation generating part of the generalized Nilsson Hamiltonian, Eq. (4.44), preserves n. For example, the deviation of the expectation value of the deformation parameter in the deformed basis, $<\hat{n}>$, from the integer n is less than 0.5 % even for relatively large deformations like $\beta = 0.4$. Only for extreme deformations such as $\beta = 0.6$ is more than 20 % found. This increase in mixing of n values with increasing deformation occurs as a result of two complementary features; namely,

a real growth with deformation in the strength of the $\delta n = 2$ to the $\delta n = 0$ parts of the spin-orbit $(\mathbf{l} \cdot \mathbf{s})$ and orbit-orbit $(\mathbf{l}^2)$ interactions and an increase in the number and frequency of level crossings at high deformations.

For reasonable deformations of about $|\beta| \leq 0.5$ this mixing is much smaller than the one present in a spherical basis and the expectation value for the number operator in the deformed basis $\langle n' \rangle = \langle n'_x \rangle + \langle n'_y \rangle + \langle n'_z \rangle$ lies close to the value n thus allowing one to unambiguously identify the $(n+1)(n+2)/2$ eigenstates within a deformed oscillator shell. This identification of an appropriate subspace is crucial to evaluate the correlation coefficient ζ defined in Eq. (4.59).

Once all the eigenstates within a deformed oscillator shell are identified, the generalized Nilsson Hamiltonian, Eq. (4.44), was diagonalized in the spherical basis [38] so that the eigenstates $|\,i\rangle$ in Eq. (4.59) are also given as an expansion

$$|\,i\rangle = \sum c_{njm_j} \psi_{njm_j} \ , \tag{4.60}$$

where the ψ_{njm_j} are the eigenfunctions of the isotropic oscillator with the mixing to higher shells explicitly included. Since the energy of an eigenstate does not depend on the particular represenation one chooses, an eigenstate given in a deformed basis can easily be mapped on the corresponding states given in a spherical basis.

The advantage of having the eigenstates in a spherical as well as a deformed representation, lies in the fact that it is much easier to evaluate the pseudo spin-orbit operator $(\tilde{\mathbf{l}} \cdot \tilde{\mathbf{s}})$ within a spherical basis, since the pseudo-spin transformation can be achieved by simply relabeling the spherical quantum numbers according to Eq. (4.10).

Specifically, we are interested in evaluating the trace

$$\langle\langle\, k \,\rangle\rangle = \sum_{i \in n} \langle i|\, k \,|i\rangle \tag{4.61}$$

where the sum is over the $(n+1)(n+2)/2$ eigenstates of the generalized Nilsson Hamiltonian that

have expectation values of the deformed oscillator number operator, $\langle\hat{n}\rangle = \langle\hat{n}_x\rangle + \langle\hat{n}_y\rangle + \langle\hat{n}_z\rangle$, lying closest to the value n.

If the trace is evaluated for the pseudo spin-orbit operator $k = \tilde{\mathbf{l}} \cdot \tilde{\mathbf{s}}$,

$$\langle\langle\, \tilde{\mathbf{l}} \cdot \tilde{\mathbf{s}}\,\rangle\rangle = \langle\langle(U^{\dagger}\mathbf{l} \cdot \mathbf{s}U)\rangle\rangle = \sum_{i\in n} \left(\langle i|U^{\dagger}\right)\mathbf{l} \cdot \mathbf{s}\left(U|i\rangle\right) , \tag{4.62}$$

we can use the fact that the pseudo transformation $U|i\rangle$ is given by a simple relabeling scheme, Eq. (4.10), if the eigenstate is given in a spherical basis.

4.4.3 Results

To evaluate the correlation coefficients, ζ, for the pseudo spin-orbit interaction, and thus to find a measure for the relative importance of this interaction for a realistic nuclear Hamiltonian, the values for the spin-orbit and orbit-orbit strengths, C and D in Eq. (4.44), that were used in the calculations are typical numbers for actinide nuclei [59], namely, $C = 0.1274$ and $D = 0.0382$ or $D = 0.0267$ for protons or neutrons, respectively. To have a scale for comparison, the correlation coefficients of the generalized Nilsson Hamiltonian, Eq.(4.44), with the pseudo $(\tilde{\mathbf{l}} \cdot \tilde{\mathbf{s}})$ as well as the normal $(\mathbf{l} \cdot \mathbf{s})$ spin-orbit operators were calculated. The results are shown in Figs. 4.2 and 4.3.

The value of ζ for $4D = C$, which corresponds to exact pseudo-spin symmetry in the spherical limit, is itself very interesting because it provides an independent measure of the breaking of pseudo-spin symmetry by the deformation. For $\beta = \gamma = 0$, the $\tilde{\mathbf{l}} \cdot \tilde{\mathbf{s}}$ term drops out $(4D = C)$ of the Hamiltonian, Eq.(4.2). This yields a correlation coefficient $\zeta = 0$ corresponding to pseudo-spin as an exact symmetry for this case. Therefore, for non-zero deformation a ζ close to 0 is also expected if the breaking of the symmetry by the deformation term is small and pseudo-spin remains a good dynamical symmetry. The calculated results are shown in Fig. 4.2 for prolate $(\beta \geq 0)$ and oblate $(\beta < 0)$ axial deformations. As expected, ζ for $\tilde{\mathbf{l}} \cdot \tilde{\mathbf{s}}$ (pseudo case) is much smaller (by about a factor of ten) then ζ for $\mathbf{l} \cdot \mathbf{s}$ (normal case).

An interesting feature for all Fig. 4.2 curves is the similar behavior of the correlation coefficients in the $n = 4, 5$, and 6 shells if realistic values for C and D are used. In this case the ζs for the

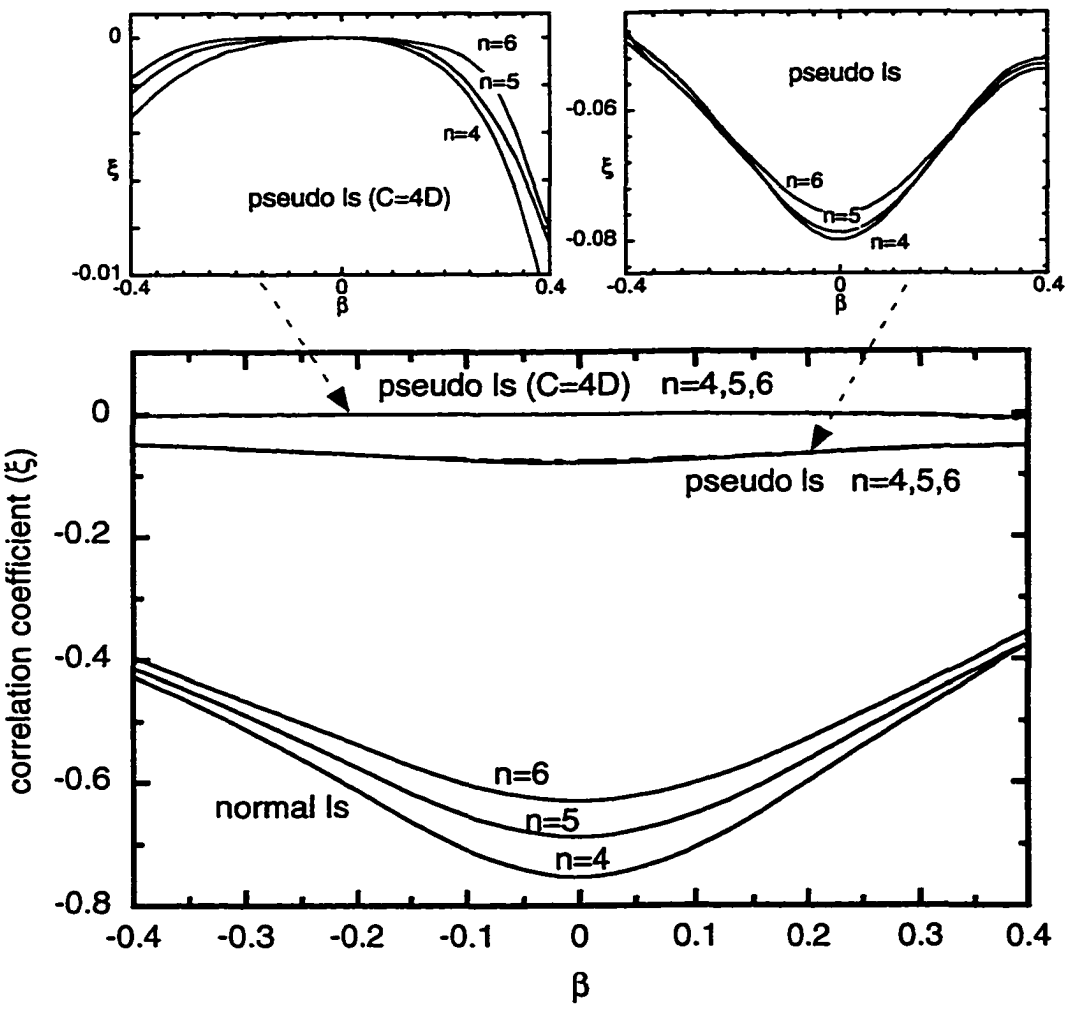

Figure 4.2: Correlation coefficients for axial deformations. For the $n = 4, 5$ and 6 proton shells the correlation coefficient ζ is plotted for $-0.4 \leq \beta \leq 0.4$ and $\gamma = 0$ To document small differences, the pseudo-spin cases are shown with an expanded y-axis above the main figure.

normal and the pseudo $\mathbf{l} \cdot \mathbf{s}$ have their maximum values for $\beta = 0$. This behavior reflects the fact that with increasing deformation other (non-deformation related) features of the Hamiltonian like the spin-orbit interaction become less important.

Note that in the pseudo-limit, $C = 4D$, the correlation coefficient ζ for $k = \tilde{\mathbf{l}} \cdot \tilde{\mathbf{s}}$ remains very close to 0 for all non-zero axial deformations ($\beta \neq 0$). Thus, the contribution to $\tilde{\mathbf{l}} \cdot \tilde{\mathbf{s}}$ generated by the Y_0^2 distortion transformed into the pseudo-spin space – which is the only possible source – is small.

In summary, these results support the already well-established goodness of the pseudo-spin concept for axially deformed systems previously discussed. Beyond this, the results also suggest that the correlation coefficient measure is a reliable indicator for the goodness of pseudo-spin symmetry, one that can be applied with confidence to the case of triaxial deformations.

The behavior of the correlation coefficients for the case of triaxial deformation, $0° \leq \gamma < 60°$ with β fixed at 0.2, is shown in Fig. 4.3. The results again show the smallness of the correlation coefficients for $\tilde{\mathbf{l}} \cdot \tilde{\mathbf{s}}$ for any deformation. As before, it is about a factor of ten smaller than the correlation coefficient of $\mathbf{l} \cdot \mathbf{s}$. Standing in contrast with the the axial case, however, is the fact that the correlation measure remains nearly constant as γ ranges from 0° to 60°. In short, the correlation coefficients of the normal ($\mathbf{l} \cdot \mathbf{s}$) as well as the pseudo ($\tilde{\mathbf{l}} \cdot \tilde{\mathbf{s}}$) spin-orbit operators are almost independent of the γ degree of freedom.

Thus, these results suggests that pseudo-spin symmetry is at least as good for nonaxial systems ($0° \leq \gamma \leq 60°$) as it is for the corresponding (same β) axial case. This conclusion is also supported by the results of the "pure" symmetry limit ($C = 4D$) where the correlation coefficient is extremely small with its absolute value slightly less for oblate than for prolate deformations. So even though pseudo-spin doublets are no longer observed in the single particle spectra of the generalized Nilsson scheme, it is still justified to use the pseudo-spin symmetry for triaxial deformations.

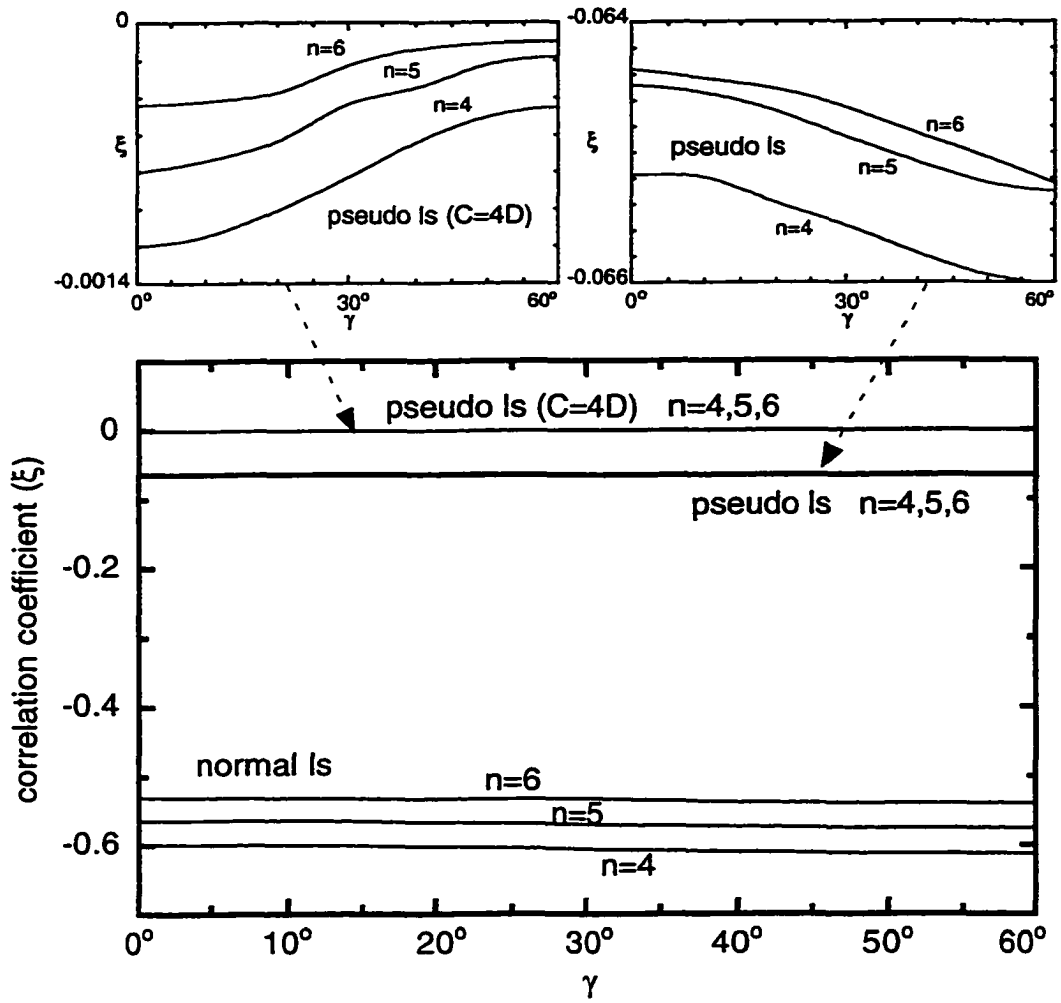

Figure 4.3: Correlation coefficients for triaxial deformations. For the $n = 4, 5$ and 6 proton shells the correlation coefficient ζ is plotted for $0° \leq \gamma \leq 60°$ and a fixed axial deformation of $\beta = 0.2$ To document small differences, the pseudo-spin cases are shown with an expanded y-axis above the main figure.

4.4.4 General pseudo-spin transformation

With this statistical argument as background, it is also useful to introduce a general pseudo-spin transformation for the triaxial case where $\gamma \neq 0$ [17]. Using the results of the axial deformation as a starting point it is natural to assume that a general transformation is of the form

$$U = d\,(d^{+}d)^{-1/2} = (dd^{+})^{-1/2}d\,, \tag{4.63}$$

defining the structural blocks d as

$$d = \sum_{s} \sqrt{\epsilon_s}\, b'_s\, \sigma_s\,, \tag{4.64}$$

where the b' and $b^{\dagger}$ are the deformation dependent boson annihilation and creation operators operators introduced in Eq. (4.55) and the parmeters ϵ_j have been defined in Eq. (4.51). For $\gamma = 0$ and $\beta = 0$ or $\beta \neq 0$ this transformation corresponds to the known spherical case and axial deformation, respectively.

Different from these earlier cases, however, the permutation relations for d and d^{+} are not closed expressions and as a consequence the transformed Nilsson Hamiltonian for the general case of a non-zero triaxial transformation can not be written in a closed form and no simple expression which is useful for practical purposes can be given. For the spherical and axial deformed case, in contrast, the bilinear combinations of d and d^{+} form a closed set under both commutation and anticommuatation, resulting in a deformed Hamiltonian that is almost as simple as the original one as was discussed in the previous sections

An approximate transformation that is based on a power-valued operator expansion can be used [17] to show that the strength of the pseudo spin-orbit interaction is drastically reduced for any axial and triaxial deformation and that the usual prescription of transforming a general Nilsson Hamiltonian is still valid.

Chapter 5

The scissors mode in the pseudo SU(3) model

After having introduced and discussed general features of the SU(3) model and its pseudo extension for the region of heavy deformed nuclei in the previous chapter, our focus will now be on the application of this theory. In spite of many successful applications of the pseudo SU(3) model, the Hamiltonian that was used in most cases was highly schematic due to the technical problems associated with the evaluation of matrix elements that break SU(3) symmetry. This situation changed only recently, when a general code was released [6] that allows for the evaluation of matrix elements of general one-body and two-body operators and thus removes the earlier limitations on pseudo SU(3) model calculations. So far however, this code has been used mainly for general studies of pairing and single particle terms as part of a nuclear Hamiltonian [4, 7, 115, 46].

A relatively new discovery in nuclear structure physics appears to be an ideal candidate for an investigation using the pseudo SU(3) model. This so-called scissors mode has been observed in well-deformed heavy nuclei which the pseudo-SU(3) is expected to describe well. The mainly collective character with additional single particle features also agrees with the underlying assumptions made in the pseudo-SU(3) model.

That the pseudo SU(3) model is in fact well suited for a description of the scissors mode will be shown after a short introduction to the experimental situation and the results of other theories.

5.1 Experimental situation

In 1983 a new rather collective isovector magnetic dipole excitation at an energy of $\approx$ 3 MeV was discovered in the strongly deformed rare earth nucleus ^{156}Gd. Immediately after the first report [102] of this discovery in a high resolution electron scattering experiment, the strong M1 excitations in ^{156}Gd and the neighboring isotopes ^{158,160}Gd were confirmed in a nuclear resonance fluorescence (NRF) experiment using γ scattering [11]. Since then considerable experimental and theoretical efforts have been focussed on this new class of states with collective properties [123, 77].

The existence of a low-lying collective $J^\pi = 1^+$ state in heavy deformed nuclei had been predicted five years earlier by Lo Iudice and Palumbo [79] within their Two-Rotor-Model (TRM). In this model neutrons and protons are assumed to act as rigid, axial deformed bodies that might rotate against each other around a common axis perpendicular to the symmetry axes. An appropriate restoring force then leads to a scissors-like oscillation. Because of this geometrical, macroscopic picture of the mode, it is usually referred to as "scissors mode" and the model already implies the predominantly orbital character of this magnetic dipole excitation.

Now, the scissors mode seems to be a rather general phenomenon in deformed nuclei that is observed in the energy region between 2 and 4 MeV. Experimentally it has been established by numerous electron and photon scattering experiments not only in the rare earth region – for which the majority of experimental studies were performed (see e. g. [21, 105, 76]) – but it has been observed in actinide isotopes [66, 82] and medium-light fp-shell nuclei as well [35, 32, 103, 104].

Until now, measurements for the island of well-deformed nuclei in the actinide region [66] have been restricted to just a few Thorium and Uranium isotopes (^{232}Th, ^{236,238}U). The high atomic numbers Z produce a high background of nonresonantly scattered photons in the NRF measurements and increased radiative tails in the electron scattering spectra. Other experimental challenges come from the increased γ background due to the radioactive decay of the actinide targets and their impurities.

Evidence for the scissors mode is not only restricted to well-deformed nuclei but also found for the γ-soft nuclei ^{134}Ba [86] and ^{196}Pt [22]. Experiments in this mass region had been proposed a decade ago [73], but since the transition strength is about a factor five smaller than in the mid-shell region, they have become possible only recently with the advent of continuous wave electron beams combined with a highly efficient and high-resolution γ-ray setup.

Common signatures and characteristics of these interesting low-lying M1 excitations can be summarized as follows:

- a mean excitation energy of about 3 MeV in deformed rare earth nuclei,
- a total strength of $\sum B(M1)$ on the order of 3 μ_N^2 for mid-shell rare earth nuclei,
- a predominantly orbital character,

where the orbital character has been confirmed using proton scattering experiments [122].

The systematic study of a larger number of even-even isotopes in the rare earth region ($50 \leq Z \leq 82$) has shown a large variation of the total M1 transition strength. A maximum of about 3 μ_N^2 exists in the mid-shell region for ^{168}Er and ^{164}Dy and a minimum of about 0.6 μ_N^2 for the γ-soft nuclei ^{134}Ba and ^{196}Pt with almost empty and almost full proton and neutron shells, respectively. This behavior can be interpreted as a quadratic dependence of the total M1 strength on the axial deformation parameter β and seems to be valid in the actinide region as well [84]. A more model independent description of this feature is the linear relation [97] between the total M1 strength and the B(E2) transition strength from the 0^+ ground state to the first 2^+ state divided by Z^2,

$$\sum_i B(M1; 0_1^+ \rightarrow 1_i^+) \text{ [s. p. u.] } = 11 \frac{B(E2; 0_1^+ \rightarrow 2_1^+) \text{ [s. p. u.]}}{Z^2} \tag{5.1}$$

that has been derived empirically by fitting the experimental data. This close relation between the $M1$ strength and $B(E2; 0_1^+ \rightarrow 2_1^+)$ is an additional argument for the underlying collective nature of the scissors mode.

Another generally observed feature of this mode is its fragmentation, that is, the breakup of the strength among several excited levels that are closely packed and clustered around a few strong

transition peaks. As an illustration, a typical experimental spectrum [77] is shown in Fig. 5.1, where the M1 transition strength distribution for ^{156}Gd is given. The spectrum is dominated by a strong M1 transition at 3.070 MeV and also shows additional transitions with smaller strength close to it – corresponding to the fragmentation of this main state.

A comparison of different transition spectra (see Fig. 5.1) shows a variation in the degree of fragmentation for different isotopes. For example, only relatively few M1 transitions have been measured for ^{160}Dy as compared to the spectrum of ^{158}Gd.

To have a quantitative description for the degree of fragmentation, the following measure has been suggested by Pietrella [98]:

$$F_1 = \sum_i \frac{|E_i - E_{sc}|}{E_{sc}} \frac{B(M1)_i}{\sum_i B(M1)_i} \tag{5.2}$$

where E_i and $B(M1)_i$ are the energy and M1 transition strength of a particular state and E_{sc} is the weighted energy average:

$$E_{sc} = \frac{\sum_i E_i B(M1)_i}{\sum_i B(M1)_i} . \tag{5.3}$$

The dimensionless measure F_1 disappears for a single state and increases with the number of states or the size of the energy interval in which the states lie and thus has the properties one intuitively expects for this quantity.

Using F_1 for an analysis of fragmentation in even-even rare earth nuclei shows that even within an isotope chain the degree of fragmentation varies strongly. However, an even larger variation exists for different elements, which points to a dependence on the proton number: For actinides the fragmentation increases initially for larger Z and then decreases slightly for Os and Pt which are close to a full shell. Within an isotope chain, in contrast, an increase in neutrons seems to lower the degree of fragmentation.

Whereas the earliest interpretation of the scissors mode was one of a collective state, describing rotational oscillations of protons against neutrons, the fragmentation seems to be an additional

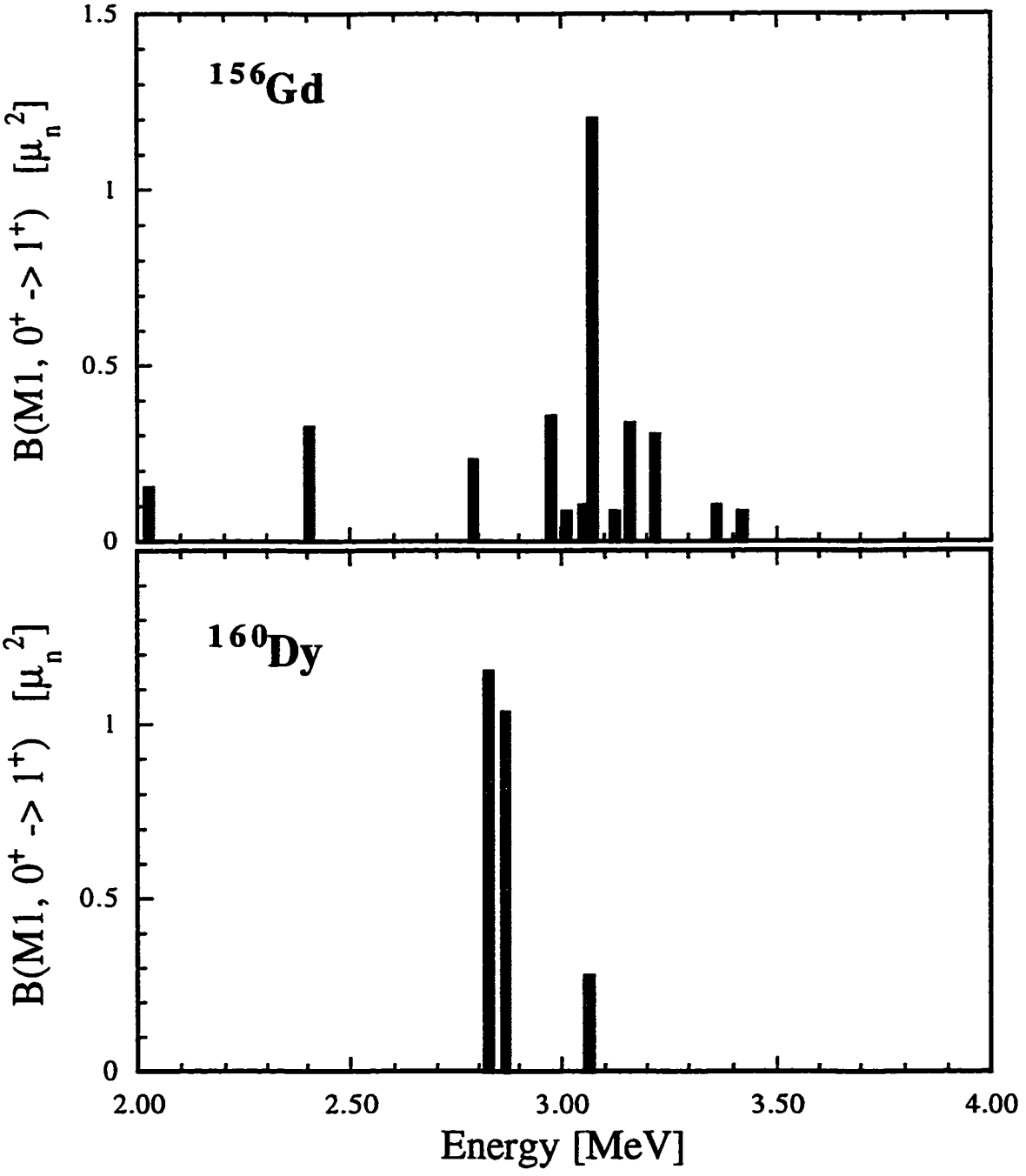

Figure 5.1: M1 transition spectrum for ^{156}Gd and ^{160}Dy. These experimental results illustrate the possible difference in fragmentation for two isotopes that differ only by a proton and neutron pair.

non-collective feature [31, 104] and the detailed exploration of this interplay between collective and non-collective aspects of the nuclear interaction is one of the main topics of this work.

Despite some inherent difficulties, progress in experimental techniques has also made the investigation of odd-A nuclei possible. Due to the half integer spin of the ground and excited state, the angular distributions become nearly isotropic and unambiguous spin assignments are almost impossible. Also, the half-integer spins cause the transitions to become nearly unpolarized and thus one cannot extract parities from NRF measurements.

An additional problem is related to the strong fragmentation of the M1 strength which results in much smaller peaks for excitations in odd-A nuclei as compared to even-even nuclei.

Some of the few odd-A isotopes that have been investigated experimentally [85] are ^{161}Dy and ^{163}Dy for which the spectrum of the neighboring even-even Dy isotopes is well known. A comparison shows the much reduced transition strength for odd-A isotopes mentioned earlier but also that the strong transition peaks of the even-even nuclei seem to have counterparts in the spectrum of even-odd isotopes which, however, are smaller and much more fragmented. (see Fig. 5.2)

This picture observed in the Dy isotopic chain changes dramatically when going to the Gd isotopes for which the M1 transition spectra are also well known in the even-even case. For ^{157}Gd, no concentration of dipole strength could be detected in the region of the scissors mode [85]. Instead, the excitations are spread over the entire range and a total of 90 ground state transitions were observed in the energy interval 1.9 - 4 MeV. Since the sensitivity of the measurements in ^{161,163}Dy and ^{157}Gd were comparable, an experimental reason for this difference can be ruled out.

To shed some light on this Gd-Dy problem, measurements on ^{159}Tb have also been performed [110]. This odd-proton nucleus links the Gd and Dy chains, and differs from ^{157}Gd and ^{161}Dy by one neutron-proton pair. Surprisingly features of both spectra were found in ^{159}Tb, that is, a few relatively large transitions and a background of almost evenly distributed smaller ones. Thus, the question persists, on weather the different fragmentation pattern in neighboring Gd and Dy isotopes and if a concentration of strength or an extreme fragmentation the common feature in the deformed

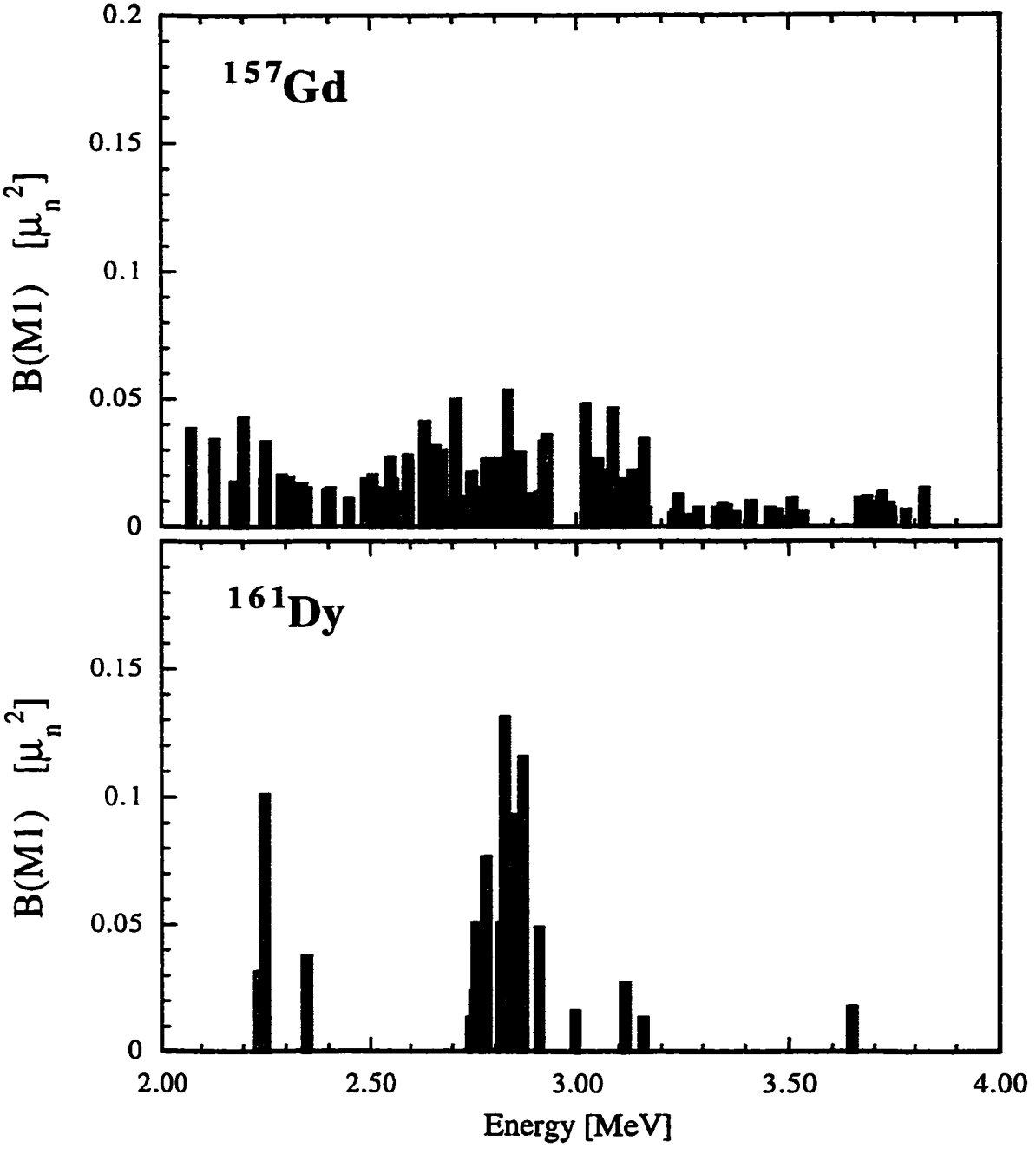

Figure 5.2: M1 transition spectrum for ^{157}Gd and ^{161}Dy. These experimental results illustrate how different the fragmentation is for odd-even nuclei as compared to the one observed for their even-even neighbors. For ^{157}Gd, no concentration of dipole strength could be detected in the region of the scissors mode. Note the different scale used for the y-axis as compared to the previous plot for the even-even case.

odd-A nuclei. To help answer the later question, more data is needed on the deformed nuclei with an unpaired nucleon. A discussion based on SU(3) model calculations will follow later in this chapter.

5.2 Theoretical situation

Different theoretical models have been used to analyze the scissors mode and to explain the different features observed. Starting not long after the first predictions for the scissors mode given by the Two Rotor Model (TRM) [79, 80, 81], many calculations in the neutron-proton interacting boson model (IBM-2) have been performed to study the strength systematics and the form factor behavior of the scissors mode excitations [34, 67, 120]. Efforts to explain the underlying microscopic structure have been made by several groups using different random phase approximation (RPA) calculations, with the most active groups in this field from Tübingen [48, 49, 94], Gent [31, 67, 68, 69] and Jülich [114, 125, 126].

None of the models mentioned above, however, is able to give a comprehensive description of all the different aspects that characterize the scissors mode excitation. The collective TRM model provides an intuitive picture but predicts only one transition state and is unable to reproduce a more complex spectrum that also includes fragmentation. The IBM-2 model is also not able to describe the single particle aspects of the scissors mode. In addition, macroscopic models can not be applied to the odd-even case.

Early results from microscopic random-phase approximation (RPA) calculations with realistic single particle Hamiltonians [60] did not produce significant collective states. Also, subsequent calculations could not increase the collectivity much, so that the B(M1) strengths of single particle states stay well within the range of single particle estimates [114, 124]. The RPA calculations, however, were able to reproduce the general structure of the fragmentation.

This brief comparison of different theoretical models already indicates that a theory which at the same time can describe non-collective features and the underlying collective nature of the scissors mode is necessary for a realistic description. As was discussed in the previous chapter, the ability

to account for these two complementary features of the nuclear interaction is one of the strengths of the pseudo SU(3) model which makes it well-suited for an investigation of the M1 spectrum.

As one of its advantages, the pseudo SU(3) model gives an elegant background for a generalization of the geometrical picture associated with the Two Rotor Model (TRM) by allowing one to lift the restriction to axial deformations. The consequences of this generalization will be discussed in the next section.

After this discussion of the SU(3) equivalent of a coupled rotor Hamiltonian, this Hamiltonian will be extended by adding single particle terms and pairing, thus introducing the fragmentation of the M1 transition strength.

5.3 Relation between pseudo SU(3) and Two Rotor Model

5.3.1 Geometric interpretation of the SU(3) Hamiltonian

As has be shown by Rompf [108, 109], the geometric picture associated with the scissors mode can be generalized if the restriction to axial shapes for proton and neutron distributions is lifted and triaxial shapes are considered as well. In this case, rotations of proton and neutron distributions around their z-axis emerge as an additional degree of freedom and an additional "twist" mode is possible. Both the "scissors" and "twist" mode can be described as excitations in a two-dimensional, oscillator-like potential which for small angles is equivalent to a general nuclear SU(3) Hamiltonian as will be shown in this section. It also allows for a classification of states with definite $SU(3)$ symmetry in terms of the relative orientation of two rotors and thus can explain naturally the general structure of the M1 transition spectrum.

The starting point for a geometric interpretation of the SU(3) Hamiltonian is the well-known relation of the $SU(3)$ symmetry group to the symmetry group of the triaxial rotor, $T_5 \wedge SO(3)$, [119, 25]. A similar relation holds in the case of two coupled quantum rotors and is based on a linear relation between the eigenvalues of the Casimir operators of the rotor group and $SU(3)$. Specifically, the irrep labels of total $SU(3)$ can be mapped onto collective variables of the joint rotor system.

In order to examine the nature of the scissors mode within the framework of the pseudo $SU(3)$ model, first a general SU(3) preserving nuclear Hamiltonian will be rewritten in terms of the angles that describe the relative motion of the proton and neutron distributions. In the mid-shell region the dominant term in this Hamiltonian,

$$H = c_1 Q\cdot Q + c_2\vec{L}^2 + c_3 K_L^2 + c_4\, L_\pi^2 + c_5\, L_\nu^2\,, \tag{5.4}$$

is the quadrupole deformation $Q\cdot Q = 4C_2 - 3\vec{L}^2$ which allows one to restrict the model space to the $SU(3)$ irreps with maximum C_2. In addition, $\vec{L}$ is the total angular momentum and K_L its projection on the intrinsic body-fixed axis, generating rotational bands and K-band splitting. Guided by the notion used in the TRM [79] that the Hamiltonian can be composed of a rotational part and a part that describes the intrinsic motion of the protons (index π) and neutrons (index ν), this Hamiltonian can be rewritten as

$$H = H_{rot} + H_{int}\,, \tag{5.5}$$

with the rotational part given by

$$H_{rot} = a\vec{L}^2 + bK_L^2\,, \tag{5.6}$$

and the intrinsic part by

$$H_{int} = c\vec{l}^2 - dC_2\,. \tag{5.7}$$

For the derivation of H_{rot} and H_{int} the identities

$$Q\cdot Q = 4C_2 - 3\vec{L}^2 \tag{5.8}$$

$$\vec{L} = \vec{L}_\pi + \vec{L}_\nu \tag{5.9}$$

$$\vec{l} = \vec{L}_\pi - \vec{L}_\nu\,, \tag{5.10}$$

have been used, thus defining the relative orbital momentum, $\vec{l}$, that appears as a dynamical variable in the Hamiltonian that describes the proton-neutron interaction.

Assuming that protons and neutrons have similar moments of inertia, the relative angular momentum $\vec{l}$ can be related to the angle θ between the main axis of the proton and neutron distribution according to the Two Rotor Model [108]

$$\vec{l} = \sin(\theta)\, l_+ \vec{e}_x + \cos(\theta)\, l_- \vec{e}_y + l_\theta \vec{e}_z \,. \tag{5.11}$$

where an intrinsic coordinate frame has been introduced following Lo Iudice et al. [79] as

$$\vec{e}_x = \frac{\vec{x}_\pi + \vec{x}_\nu}{2\sin(\theta)} \tag{5.12}$$

$$\vec{e}_y = \frac{\vec{x}_\pi - \vec{x}_\nu}{2\cos(\theta)} \tag{5.13}$$

$$\vec{e}_z = \frac{\vec{x}_\pi \times \vec{x}_\nu}{\sin(2\theta)} \,, \tag{5.14}$$

and the abreviations

$$\begin{aligned} l_+ &= L_{x_\pi} + L_{x_\nu} \\ l_- &= L_{x_\pi} - L_{x_\nu} \\ l_\theta &= L_{z_\pi} + L_{z_\nu} \,, \end{aligned}$$

have been used, so that the kinetic part of the intrinsic Hamiltonian (5.7) can be written as

$$\vec{l}^2 = \sin^2(\theta/2)\, l_+^2 + \cos^2(\theta/2)\, l_-^2 + l_\theta^2 \,. \tag{5.15}$$

To simpify this expression where the different degrees of freedom are strongly coupled, a restriction to small angles is used, taking into account only terms up to second order in angular variables,

$$\vec{l}^2 = l_-^2 + l_\theta^2 - \theta^2 (l_+^2 - l_-^2) \,. \tag{5.16}$$

Assuming further, that in the low-energy region of the nuclear spectrum it is justified to consider

that rotations around either $\vec{x}_\pi$ or $\vec{x}_\pi$ are slow, which means $\langle I_-^2 \rangle \approx \langle I_-^2 \rangle$, simplifies the expression for $\vec{I}^2$ simplifies further to:

$$\vec{I}^2 = I_-^2 + I_\theta^2 \,. \tag{5.17}$$

The next step is to express the potential part of the intrinsic Hamiltonian given in Eq. (5.7) - which is the Casimir invariant C_2 of $SU(3)$ - in terms of the rotation angles θ, ϕ_π and ϕ_ν, where ϕ_π and ϕ_ν have been introduced to parameterize the rotation around the z-axis of the proton or neutron distributions. This way it can been shown that C_2 can be regarded as a restoring potential that gives H_{int} the desired oscillator structure.

The starting point are the invariants of the rotor group $Rot(3) = T_5 \wedge SO(3)$. As for $SU(3)$, it has two Casimir invariants, traces of the square $Tr((Q^c)^2)$ and cube $Tr((Q^c)^3)$ of the collective quadrupole matrix. The quadrupole matrix of a nucleus composed of protons and neutrons is calculated as the sum of the quadrupole matrices of the separate sub-systems, with the protons rotated relative to the neutrons.

Under the assumption that both rotors are initially described in their body-fixed principal axes frame, the transformation to a joint coordinate frame can be carried out by rotating the proton and neutron systems first about the body-fixed z-axis by an angle ϕ_π and ϕ_ν, respectively, so that the rotated y' axes and the unrotated y axes point in the same direction for the proton and neutron system. In the second step, a rotation about this joint axis is performed where the rotation angle is given by $\pm\theta/2$ for the proton and neutron distributions, respectively.

The quadrupole operator of the joint rotor system in its cartesian representation can thus be related to those of each initial distribution according to

$$\begin{aligned} Q^c &= \mathcal{R}(\theta/2) \cdot \mathcal{R}_{z_\nu}(\phi_\nu) \cdot Q_\nu^C \cdot \mathcal{R}_{z_\nu}^{-1}(\phi_\nu) \cdot \mathcal{R}^{-1}(\theta/2) \\ &\quad + \mathcal{R}^{-1}(\theta/2) \cdot \mathcal{R}_{z_\pi}(\phi_\pi) \cdot Q_\pi^C \cdot \mathcal{R}_{z_\pi}^{-1}(\phi_\pi) \cdot \mathcal{R}(\theta/2) \,. \end{aligned} \tag{5.18}$$

In this expression, $\mathcal{R}(\theta/2)$ and $\mathcal{R}_{z_i}(\phi_i)$ $(i = \pi, \nu)$ are rotational matrices

$$\mathcal{R}(\theta/2) = \begin{pmatrix} \cos\theta/2 & 0 & -\sin\theta/2 \\ 0 & 1 & 0 \\ \sin\theta/2 & 0 & \cos\theta \end{pmatrix},$$

$$\mathcal{R}_{z_i}(\phi_i) = \begin{pmatrix} \cos\phi_i & -\sin\phi_i & 0 \\ \sin\phi_i & \cos\phi_i & 0 \\ 0 & 0 & 1 \end{pmatrix},$$

and Q^c_i denotes a quadrupole matrix in its principal axes frame,

$$Q^c_{i\,\alpha\beta} = \lambda^i_\alpha \delta_{\alpha\beta} \quad ; i = \pi, \nu\,. \tag{5.19}$$

Hence, the joint quadrupole tensor and the Casimir operators of $Rot(3)$ become explicitly dependent on the relative orientation of the proton and neutron distributions,

$$\begin{aligned} Tr((Q^c)^2) = & \\ & Tr((Q^c_\pi)^2) + Tr((Q^c_\nu)^2) \\ & +2Tr\left(\mathcal{R}(\theta)\mathcal{R}_{z_\nu}(\phi_\nu)Q^C_\nu\mathcal{R}^{-1}_{z_\nu}(\phi_\nu)\mathcal{R}^{-1}(\theta)\mathcal{R}_{z_\pi}(\phi_\pi)Q^C_\pi\mathcal{R}^{-1}_{z_\pi}(\phi_\pi)\right)\,, \end{aligned} \tag{5.20}$$

$$\begin{aligned} Tr((Q^c)^3) = & \\ & Tr((Q^c_\pi)^3) + Tr((Q^c_\nu)^3) \\ & +3Tr\left(\mathcal{R}(\theta)\mathcal{R}_{z_\nu}(\phi_\nu)(Q^C_\nu)^2\mathcal{R}^{-1}_{z_\nu}(\phi_\nu)\mathcal{R}^{-1}(\theta)\mathcal{R}_{z_\pi}(\phi_\pi)Q^C_\pi\mathcal{R}^{-1}_{z_\pi}(\phi_\pi)\right) \\ & +3Tr\left(\mathcal{R}(\theta)\mathcal{R}_{z_\nu}(\phi_\nu)Q^C_\nu\mathcal{R}^{-1}_{z_\nu}(\phi_\nu)\mathcal{R}^{-1}(\theta)\mathcal{R}_{z_\pi}(\phi_\pi)(Q^C_\pi)^2\mathcal{R}^{-1}_{z_\pi}(\phi_\pi)\right)\Big)\,. \end{aligned} \tag{5.21}$$

The first and second term in the above equations are simply given by the interia parameters of the

quadrupole matrices as

$$Tr((Q_i^c)^2) = \lambda_1^{(i)^2} + \lambda_2^{(i)^2} + \lambda_3^{(i)^2} \tag{5.22}$$

$$Tr((Q_i^c)^3) = 3\lambda_1^{(i)}\lambda_2^{(i)}\lambda_3^{(i)} \tag{5.23}$$

where the λ_i can be replaced by the SU(3) labels (λ_i, μ_i) by using the linear correspondence between the invariant measures of $SU(3)$ and the rotor group (see Eq. (3.28)). The other terms in Eqs. (5.20) and (5.21) are of more complicated nature and include the rotational angles but can be evaluated in a lengthy but straightforward calculation [108]. Since it turns out that the angles ϕ_π and ϕ_ν always appear as their difference, the expressions can be simplified by introducing the angle ϕ_- which describes the relative difference between the rotations around the proton and neutron z-axis,

$$\phi_- = \frac{1}{2}(\phi_\pi - \phi_\nu)\,, \tag{5.24}$$

and is a measure for the "twist" degree of freedom. This extra degree of freedom does not exist in the TRM model and appears if at least one of the nucleon distributions is triaxial.

In the limit of small angles, neglecting terms of the order three and higher – which is consistent with the analysis for the kinetic energy – the invariants of the rotor group can be represented by the following expressions that depend on the SU(3) parameters (λ_i, μ_i) of protons and neutrons respectively and the angles θ and ϕ_- that describe their relative orientation:

$$\begin{aligned} Tr((Q^c(\theta,\phi_-))^2) &= \frac{2}{3}C_2 + 2 \\ &= -2(\lambda_\pi+1)(\lambda_\nu+1)\,\theta^2 - 2(\mu_\pi+1)(\mu_\nu+1)\,\phi_-^2 \\ &\quad + \frac{2}{3}\left[(\lambda_\pi+\lambda_\nu+2)^2 + (\mu_\pi+\mu_\nu+2)(\lambda_\pi+\lambda_\nu+2) + (\mu_\pi+\mu_\nu+2)^2\right]\,, \end{aligned} \tag{5.25}$$

and

$$
\begin{aligned}
Tr((Q^c(\theta,\phi_-))^3) &= \frac{3}{4}\langle C_3\rangle \\
&= -(\lambda_\pi+1)(\lambda_\nu+1)(\lambda_\pi+\lambda_\nu+2(\mu_\pi+\mu_\nu)+6)\,\theta^2 \\
&\quad +(\mu_\pi+1)(\mu_\nu+1)(2(\lambda_\pi+\lambda_\nu)+\mu_\pi+\mu_\nu+6)\,\phi_-^2 \\
&\quad -\frac{1}{9}((\lambda_\pi+\lambda_\nu)-(\mu_\pi+\mu_\nu)) \\
&\quad \times(2(\mu_\pi+\mu_\nu)+\lambda_\pi+\lambda_\nu+6)(2(\lambda_\pi+\lambda_\nu)+\mu_\pi+\mu_\nu+6)\,. \qquad (5.26)
\end{aligned}
$$

Using Eq. (5.25) to express C_2 in terms of the variables θ and ϕ_-, one can rewrite the Hamiltonian for the intrinsic motion, Eq. (5.7), as a two-dimensional harmonic, anisotropic oscillator with a scissors and twist degree of freedom,

$$
\begin{aligned}
H_{int} &= \qquad (5.27) \\
&= (cl_\theta^2+3d\,(\lambda_\pi+1)(\lambda_\nu+1)\,\theta^2) \\
&+ (cl_-^2+3d\,(\mu_\pi+1)(\mu_\nu+1)\,\phi_-^2\,)+E_0' \\
&= \hbar\omega_\theta\left(n_\theta+\frac{1}{2}\right)+\hbar\omega_-\left(n_-+\frac{1}{2}\right)+E_0'\,, \qquad (5.28)
\end{aligned}
$$

where the constant E_0' depends on the proton and neutron SU(3) quantum numbers,

$$
\begin{aligned}
E_0' &= -d\left[(\lambda_\pi+\lambda_\nu+2)^2+\right. \\
&\quad \left.+(\mu_\pi+\mu_\nu+2)(\lambda_\pi+\lambda_\nu+2)\,(\mu_\pi+\mu_\nu+2)^2-3\right]\,, \qquad (5.29)
\end{aligned}
$$

and the oscillator frequencies ω_θ and ω_- are defined as

$$
\omega_\theta = \sqrt{48\,cd\,(\lambda_\pi+1)(\lambda_\nu+1)} \qquad (5.30)
$$

$$
\omega_- = \sqrt{48\,cd\,(\mu_\pi+1)(\mu_\nu+1)}\,. \qquad (5.31)
$$

The general dependence of the oscillator frequencies on the proton and neutron SU(3) quantum numbers has a natural interpretation in terms of the geometrical picture associated with SU(3). Since a configuration with $\lambda \gg \mu$ corresponds to a shape which is almost axially deformed, a rotation around the z-axis - corresponding to the twist" mode - has a lower energy than a rotation around the y-axis - corresponding to the "scissors" mode. In the triaxial case when $\lambda = \mu$, both modes are equivalent and for $\lambda < \mu$ the roles of scissors and twist mode are interchanged.

Even though the above relation, Eq. (5.31), for the oscillator frequency ω_- might suggest that for the case of two axially deformed distributions - which in the SU(3) picture corresponds to $\mu_\pi = \mu_\nu = 0$ - a twist mode is possible since $\omega_- \neq 0$, only a scissors type excitation exists in this case. One reason the twist mode is ruled out can be found in the definition of the generalized momentum, $l_- = L_{x_\pi} - L_{x_\nu}$, of the oscillator that describes the twist mode. In the case of an axial symmetry $L_{x_\pi} = L_{x_\nu} = 0$ and the variable l_- disappears.

Another reason is related to the properties of SU(3) eigenstates that describe coupled proton and neutron systems. As it turns out, two proton and neutron irreps, (λ_π, μ_π) and (λ_ν, μ_ν) can only be coupled to a limited number of SU(3) irreps, corresponding to a quantization of the shapes possible in the (β, γ) plane. An analysis of the corresponding irreps in terms of eigenfunctions of the two-dimensional oscillator given in Eq. (5.28), also rules out a twist mode for the axial case, $\lambda_\pi = \lambda_\nu = 0$. It also gives further insight in the general structure of the scissors mode as will be discussed in the following section

For this discussion, the expectation values of θ and ϕ_- in terms of SU(3) quantum numbers are needed, which are given by the oscillator structure of the Hamiltonian (5.28) as:

$$\theta^2 = \frac{\hbar\omega_\theta}{12d(\lambda_\pi+1)(\lambda_\nu+1)}\left(n_\theta + \frac{1}{2}\right) \tag{5.32}$$

$$\phi_-^2 = \frac{\hbar\omega_-}{12d(\mu_\pi+1)(\mu_\nu+1)}\left(n_- + \frac{1}{2}\right) . \tag{5.33}$$

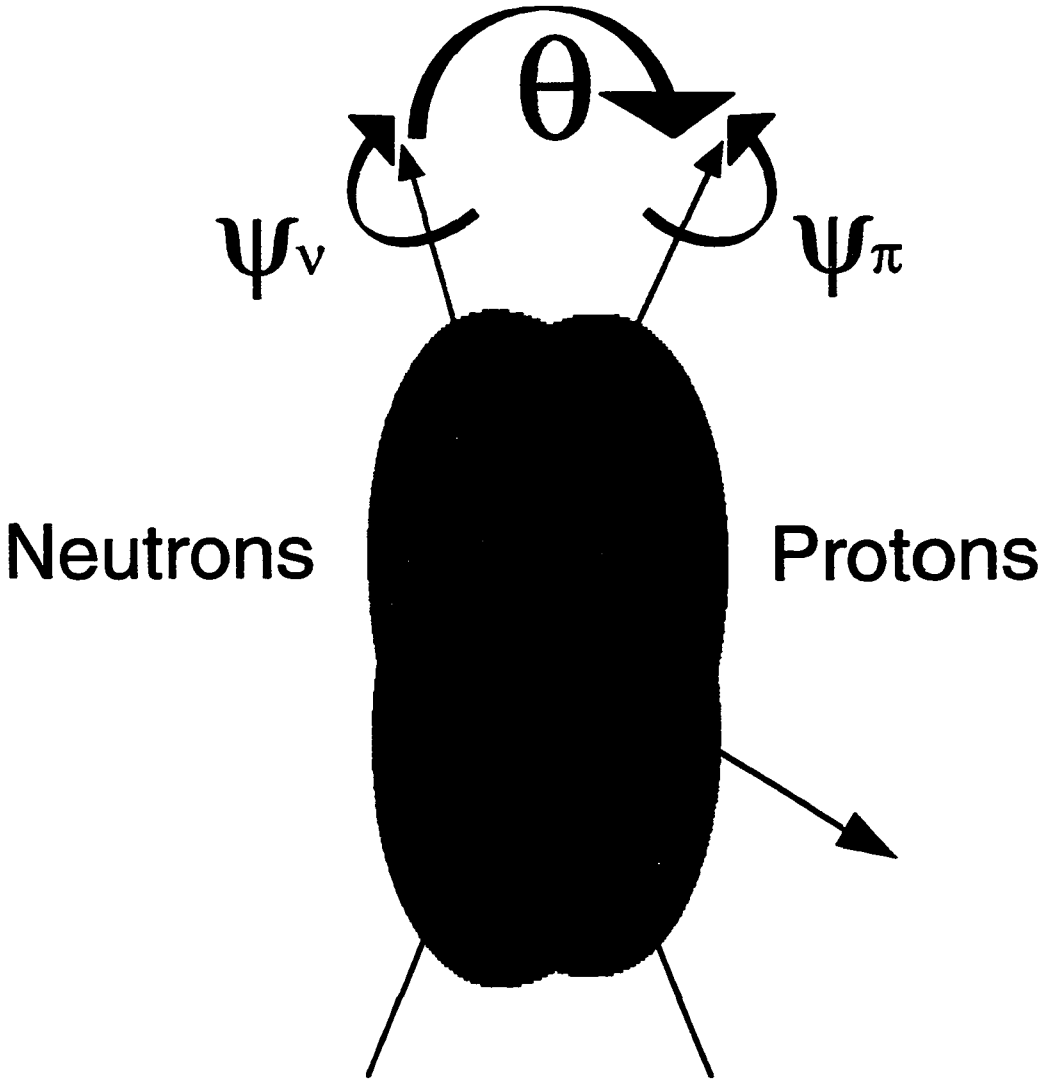

Figure 5.3: Geometric interpretation of "scissors and "twist" mode. In a geometric picture, the "scissors" mode corresponds to an oscillation in θ, the angle between the proton and neutron z-axes. For triaxial distributions, the difference in the angles that parameterize the rotation around the z-axis for protons and neutrons, $\phi_- = \frac{1}{2}(\psi_\pi - \psi_\nu)$, describes a twist-like oscillation.

5.3.2 Interpretion of the eigenstates

The structure of the intrinsic Hamiltonian also allows for an interpretation of the SU(3) irreps that are the basis states in the pseudo $SU(3)$ model in terms of oscillator eigenfunctions. The starting point for this is the decomposition of the coupled $SU(3)$ into the $SU(3)$ irreps (λ_π, μ_π) and (λ_ν, μ_ν) of protons and neutrons according to the Littelwood rules [30] for coupling Young diagrams. As was shown earlier, Eq. (2.69), three quantum numbers (m, l, k) [107] have to be introduced to express the allowed product configurations in mathematical terms,

$$\begin{aligned}(\lambda, \mu) &= (\lambda_\pi, \mu_\pi) \otimes (\lambda_\nu, \mu_\nu) \\ &= \bigoplus_{m,l,k} (\lambda_\pi + \lambda_\nu - 2m + l, \mu_\pi + \mu_\nu - 2l + m) \,, \end{aligned} \tag{5.34}$$

where the parameters k, l and m are defined in a fixed range given implicitly by the values of the initial $SU(3)$ representations.

In this formulation, the coupled SU(3) irrep (λ, μ) turns out to be independent of k. Hence, k serves to distinguish between multiple occurrences of the same (λ, μ) in the tensor product. The number of k values allowed corresponds to the maximum outer multiplicity index ρ_{max} ($\rho = 1, 2, \cdots, \rho_{max}$).

Assuming the nucleus consists of two overlapping ellipsoidal mass distributions, one for protons and one for neutrons, the geometrical counterpart of the $SU_\pi(3) \times SU_\nu(3) \supset SU(3)$ reduction above is given by an expansion of the product $(\beta_\pi, \gamma_\pi) \otimes (\beta_\nu, \gamma_\nu)$ in terms of quadrupole mass distributions (β, γ) of the system as a whole. To determine the (β, γ) value of the joint system, one can use the three parameters θ, ϕ_ν and ϕ_π in additional to the shape variables of the individual proton-neuron distributions. These extra parameters are required to specify the relative orientation of the proton and neutron principal axes sub-systems. Pictorially, changing the system's deformation can then be considered to correspond to a change in the relative angles of orientation of the principal axes of the proton and neutron sub-systems. While from a geometrical point of view the nuclear shape

is a function of the relative orientation angles of the protons and neutrons, the $(\lambda,\mu) \leftrightarrow (\beta,\gamma)$ correspondence implies the dependence of (β,γ) on the $SU(3)$ decomposition parameters, m and l, introduced above in Eq. (5.34). Due to this triangle-like relation, a mapping can be derived which associates the set of angles with the parameters m and l. This finding suggests a natural way to relate the coupled rotor to the harmonic oscillator in terms variables θ and $\phi_- = \frac{1}{2}(\phi_\pi - \phi_\nu)$ that has been introduced in Eq. (5.28) as an approximation for the proton-neutron interaction.

To find an interpretation of the coupled SU(3) eigenfunctions in terms of oscillator eigenfuctions, the above equation (5.34) can be used to express the $SU(3)$ operators C_2 and C_3,

$$\begin{aligned} \langle C_2 \rangle &= \lambda^2 + \lambda\mu + \mu^2 + 3(\lambda+\mu)\,, \\ \langle C_3 \rangle &= (\lambda-\mu)(\lambda+2\mu+3)(2\lambda+\mu+3)\,, \end{aligned}$$

using the proton and neutron $SU(3)$ labels so that $\langle C_2 \rangle$ takes on the form

$$\begin{aligned} &\langle C_2(m,l) \rangle = \\ &= (\lambda_\pi+\lambda_\nu)^2 + (\mu_\pi+\mu_\nu)(\lambda_\pi+\lambda_\nu) \\ &\quad +(\mu_\pi+\mu_\nu)^2 + 3(\lambda_\pi+\lambda_\nu+\mu_\pi+\mu_\nu) \\ &\quad 3\left[m(\lambda_\pi+\lambda_\nu+1-m) + l(\mu_\pi+\mu_\nu+1+m-l)\right]\,. \end{aligned} \tag{5.35}$$

Proceeding as above to determine the expectation value of the third order Casimir operator, C_3, in terms of the decomposition parameters, one finds its dependence on m and l to be

$$\begin{aligned} &\langle C_3(m,l) \rangle = \\ &= \frac{4}{27}(\lambda_\pi+\lambda_\nu-(\mu_\pi+\mu_\nu)+3(l-m)) \\ &\quad \times(2(\mu_\pi+\mu_\nu)+\lambda_\pi+\lambda_\nu-3(l-1)) \\ &\quad \times(2(\lambda_\pi+\lambda_\nu)+\mu_\pi+\mu_\nu-3(m-1))\,. \end{aligned} \tag{5.36}$$

On the other hand, expressions for C_2 and C_3 in terms of the geometric parameters θ and ϕ_- can be derived from Eqs. (5.25) and (5.26):

$$\begin{aligned}
&\langle C_2(\theta,\phi_-)\rangle = \\
&= (\lambda_\pi+\lambda_\nu+2)^2+(\mu_\pi+\mu_\nu+2)(\lambda_\pi+\lambda_\nu+2)+(\mu_\pi+\mu_\nu+2)^2 \\
&\quad -3\left(4(\lambda_\pi+1)(\lambda_\nu+1)\,\theta^2\right. \\
&\quad \left.+(\mu_\nu+1)(\mu_\pi+1)\phi_-^2+1\right)\,, \qquad (5.37)\\
&\langle C_3(\theta,\phi_-)\rangle = \\
&= \frac{4}{27}(\lambda_\pi+\lambda_\nu-(\mu_\pi+\mu_\nu))(2(\mu_\pi+\mu_\nu)+\lambda_\pi+\lambda_\nu+6) \\
&\quad \times(2(\lambda_\pi+\lambda_\nu)+\mu_\pi+\mu_\nu+6) \\
&\quad -\frac{16}{3}(\lambda_\pi+1)(\lambda_\nu+1)\,(\lambda_\pi+\lambda_\nu+2(\mu_\pi+\mu_\nu)+6)\,\theta^2 \\
&\quad +\frac{4}{3}(\mu_\pi+1)(\mu_\nu+1)\,(2(\lambda_\pi+\lambda_\nu)+\mu_\pi+\mu_\nu+6)\phi_-^2\,, \qquad (5.38)
\end{aligned}$$

which can be solved with repect to θ^2 and ϕ_-^2 to give

$$\begin{aligned}
\theta^2 &= \frac{4(2(\lambda_\pi+\lambda_\nu)+\mu_\pi+\mu_\nu)^3-27C_3-12(C_2+3)(2(\lambda_\pi+\lambda_\nu)+\mu_\pi+\mu_\nu)}{432(\lambda_\pi+1)(\lambda_\nu+1)\,(\lambda_\pi+\lambda_\nu+\mu_\pi+\mu_\nu+4)} \\
\phi_-^2 &= \frac{4(\lambda_\pi+\lambda_\nu+2(\mu_\pi+\mu_\nu))^3+27C_3-12(C_2+3)(\lambda_\pi+\lambda_\nu+2(\mu_\pi+\mu_\nu))}{432(\mu_\pi+1)(\mu_\nu+1)\,(\lambda_\pi+\lambda_\nu+\mu_\pi+\mu_\nu+4)}\,.
\end{aligned}$$

Using the expression of the eigenvalues of C_2 and C_3 in terms of the $SU(3)$ irrep labels given in Eqs. (5.35) and (5.36), one finally arrives at a solution for the expectation values as a function of the decomposition parameters m and l:

$$\begin{aligned}
\theta^2 &= \frac{(m+1)(\lambda_\pi+\lambda_\nu-m+1)}{(\lambda_\pi+1)(\lambda_\nu+1)} \qquad (5.39)\\
&\times \frac{(\lambda_\pi+\lambda_\nu+\mu_\pi+\mu_\nu+3-l)}{(\lambda_\pi+\lambda_\nu+\mu_\pi+\mu_\nu+4)} \\
\phi_-^2 &= \frac{(l+1)(\mu_\pi+\mu_\nu+2+m-l)}{(\mu_\pi+1)(\mu_\nu+1)} \qquad (5.40)
\end{aligned}$$

$$\times \quad \frac{(\lambda_\pi + \lambda_\nu + \mu_\pi + \mu_\nu + 3 - m)}{(\lambda_\pi + \lambda_\nu + \mu_\pi + \mu_\nu + 4)} ,$$

where certain restrictions apply to the parameters m and l that come from the application of the Littlewood rules [30].

Consistent with the derivation used to rewrite the internal Hamiltonian into an oscillator like expression, Eq. (5.28), an approximation of the above expression for small values of the decomposition labels ($m \ll \lambda_\pi + \lambda_\nu$ and $l \ll \mu_\pi + \mu_\nu$) can be derived, where θ^2 and ϕ^2_- behave as linear functions of only one of the parameters,

$$\theta^2 = \frac{m\,(\lambda_\pi + \lambda_\nu + 1)}{(\lambda_\pi + 1)\,(\lambda_\nu + 1)} + \theta_0^2 , \tag{5.41}$$

$$\phi^2_- = \frac{l\,(\mu_\pi + \mu_\nu + 1)}{(\mu_\pi + 1)\,(\mu_\nu + 1)} + \phi_0^2 , \tag{5.42}$$

with constants θ_0^2 and ϕ_0^2. By a comparison of the arguments of θ^2 in (5.32) and (5.41) as well as ϕ^2_- in (5.33) and (5.42), the associations

$$l = n_-, \quad m = n_\theta \tag{5.43}$$

that relate the oscillator quanta n_- and n_θ with the decomposition parameters l and m are suggested.

These results now allow for an interpretation of the different 1^+ states for which scissors modes are observed in terms of a scissors and twist mode within the framework of the pseudo SU(3) model.

5.3.3 Classification of coupled SU(3) eigenstates

With the interpretation of the coupling parameters l and m in terms of the oscillator quanta n_- and n_θ each SU(3) irrep, $(\lambda, \mu) = (\lambda_\pi + \lambda_\nu - 2m + l, \mu_\pi + \mu_\nu - 2l + m)$, can be interpreted as an excited state of a two-dimensional oscillator.

The leading irrep of the decomposed $SU(3)$ tensor product,

$$(\lambda, \mu) = (\lambda_\pi + \lambda_\nu, \mu_\pi + \mu_\nu) \tag{5.44}$$

which corresponds to $(m,l) = (0,0)$, is always associated with a minimum in the relative angular displacements. In the even-even case – to which we can restrict our discussion without loss of generality – this so-called "stretched" configuration contains the 0^+ ground state. For this coupling the proton and neutron distributions overlap maximally, generating maximum deformation of the system. Any other value for m and l corresponds to a specific expectation of the angular variables, θ and ϕ_- which, in turn, is related to a well-defined energy associated with the intrinsic motion.

The configuration

$$(\lambda,\, \mu) \,=\, (\lambda_\pi + \lambda_\nu - 2,\, \mu_\pi + \mu_\nu + 1) \tag{5.45}$$

is the first scissors-like configuration. In the prolate case, $\lambda_i > \mu_i$, it is always part of the tensor product decomposition and contains a $J^\pi = 1^+$ state which is the bandhead of a rotational band with $K = 1$. Its corresponding $SU(3)$ coupling parameters are $(m,l) = (1,0)$. Thus, it only excites the θ dependent motion by one quanta and thus corresponds to the scissors mode of the TRM.

A generalization of this picture is possible if one allows for triaxial proton or neutron distributions. In the $SU(3)$ model a triaxial deformation corresponds to an SU(3) irrep, (λ_i, μ_i), in which both quantum numbers are non-zero. In this case a second scissors state appears which is given by

$$(\lambda, \mu) = (\lambda_\pi + \lambda_\nu - 1, \mu_\pi + \mu_\nu - 1) \tag{5.46}$$

or $(1,1)$ in terms of (m,l). According to the underlying geometrical picture, this structure is produced by superimposing a ϕ_- twisting motion on top of the lowest scissors configuration. Since these modes are identical except for their total $SU(3)$ irrep, their energy difference is a result of different intrinsic motions.

The most general setting is given if all SU(3) quantum numbers are non-zero, i. e. if both the proton and neutron distributions are triaxial. Then a third 1^+ state can be identified that corresponds to $(m,l) = (0,1)$:

$$(\lambda,\, \mu) = (\lambda_\pi + \lambda_\nu + 1,\, \mu_\pi + \mu_\nu - 2)\,. \tag{5.47}$$

It differs from the first two not only in its intrinsic energy but also because it belongs to a $K = 0$ band.

In addition, in the triaxial-triaxial case one obtains a fourth scissors state which also is a scissors plus twist excitation, $(m, l) = (1, 1)$, and differs from the first combined scissors and twist mode, $(\lambda, \mu) = (\lambda_\pi + \lambda_\nu - 1, \mu_\pi + \mu_\nu - 1)$, solely in its value of the outer multiplicity parameter ρ. The interesting question if this outer multiplicity parameter that distinguishes the two states reflects some underlying physics will be discussed later in this chapter.

As has been shown earlier [24], the maximum number of SU(3) irreps that contain a $J^\pi = 1^+$ state and at the same time can be coupled to the ground state irrep $(\lambda, \mu) = (\lambda_\pi + \lambda_\nu, \mu_\pi + \mu_\nu)$ by the orbital part of M1 transition operator, which has a (1,1) tensor character, is four. Thus, all possible scissors mode can be classified according to the scheme given above.

5.3.4 M1 transitions in the pseudo SU(3) model

The transition operator

To determine the M1 transition strength between two specific eigenstates, the operator,

$$T^1_\mu = \sqrt{3/4\pi}\mu_N \sum_\sigma g^o_\sigma L^\sigma_\mu + g^s_\sigma S^\sigma_\mu \tag{5.48}$$

with the single particle terms,

$$\begin{aligned} L^\sigma &= \sum_i l^\sigma_\mu(i) \\ S^\sigma &= \sum_i s^\sigma_\mu(i) \end{aligned}$$

has to be evaluated.

Since other theories use effective g-factors, it has to be noted that in this work the "bare" orbital and spin g factors for protons and neutrons are used:

$$g^o_\pi = 1, \;\; g^o_\nu = 0 \quad \text{and} \quad g^s_\pi = 5.5857, \;\; g^s_\nu = -3.8263\,. \tag{5.49}$$

To evaluate the M1 transition operator for eigenstates given in a pseudo SU(3) basis, the pseudo SU(3) tensorial expansion of the expression given in Eq. (5.48) is needed. As is shown in Appendix A.5, this expansion has the form

$$T^1_M = \sqrt{3/4\pi} \sum_{\tilde{\eta}_\sigma} \sum_{\tilde{\lambda}_0,\tilde{\mu}_0} \sum_{\tilde{L}_0,\tilde{S}_0} \sum_{\tilde{\kappa}_0,\sigma} C_t(\tilde{\eta}_\sigma;(\tilde{\lambda}_0,\tilde{\mu}_0),\tilde{\kappa}_0,\tilde{L}_0,\tilde{S}_0) \tag{5.50}$$

$$\times \left[a^\dagger_{(\tilde{\eta}_\sigma,0);1/2} \otimes \tilde{a}_{(0,\tilde{\eta}_\sigma,0);1/2} \right]^{(\tilde{\lambda}_0,\tilde{\mu}_0);\tilde{S}_0,J_0=1}_{\tilde{\kappa}_0 \tilde{L}_0 M_0} , \tag{5.51}$$

where the tensor expansion coefficient C_t is the sum of C_l and C_s, the coefficients for the orbital and spin angular momentum, respectively. They are given as

$$C_l(\tilde{\eta};(\tilde{\lambda}_0,\tilde{\mu}_0),\tilde{\kappa}_0,\tilde{L}_0,\tilde{S}_0) =$$

$$= \sum_l \sum_{jj'} [2(2l+1)l(l+1)/(2j+1)]^{1/2} \begin{Bmatrix} l & \frac{1}{2} & j \\ l & \frac{1}{2} & j' \\ 1 & 0 & 1 \end{Bmatrix}$$

$$\times B(j,j',\tilde{l},\tilde{l};\tilde{\eta}_\sigma;\tilde{\lambda}_0,\tilde{\mu}_0,\tilde{\kappa}_0,\tilde{L}_0,\tilde{S}_0) \tag{5.52}$$

$$C_s(\tilde{\eta};(\tilde{\lambda}_0,\tilde{\mu}_0),\tilde{\kappa}_0,\tilde{L}_0,\tilde{S}_0) =$$

$$= \sum_l \sum_{jj'} [(3/2)(2l+1)/(2j+1)]^{1/2} \begin{Bmatrix} l & \frac{1}{2} & j \\ l & \frac{1}{2} & j' \\ 0 & 1 & 1 \end{Bmatrix}$$

$$\times B(j,j',\tilde{l},\tilde{l};\tilde{\eta}_\sigma;\tilde{\lambda}_0,\tilde{\mu}_0,\tilde{\kappa}_0,\tilde{L}_0,\tilde{S}_0) , \tag{5.53}$$

where the abbreviation

$$B(j,j',\tilde{l},\tilde{l};\tilde{\eta}_\sigma;\tilde{\lambda}_0,\tilde{\mu}_0,\tilde{\kappa}_0,\tilde{L}_0,\tilde{S}_0) =$$

$$= (-1)^{\eta}\sqrt{\frac{2j+1}{2j_0+1}}\begin{Bmatrix} \tilde{l} & \frac{1}{2} & j \\ \tilde{l}' & \frac{1}{2} & j' \\ \tilde{L}_0 & \tilde{S}_0 & 1 \end{Bmatrix}$$
$$\times\langle(\tilde{\eta},0)\tilde{l};(0,\tilde{\eta})\tilde{l}'||(\tilde{\lambda}_0,\tilde{\mu}_0)\tilde{\kappa}_0\tilde{L}_0\rangle \tag{5.54}$$

has been used.

If the spin of the initial and final wavefunction is 0, the pseudo expansion for T^1_M simplifies drastically. In this case the pseudo expansion reduces to just one coefficient which is a $(\tilde{\lambda}_0,\tilde{\mu}_0) = (1,1)$ pseudo SU(3) tensor,

$$C_l(\tilde{\eta};(\tilde{\lambda}_0,\tilde{\mu}_0),\tilde{\kappa}_0,\tilde{L}_0,\tilde{S}_0) = C(\tilde{\eta},(1,1)1,1,0)\,, \tag{5.55}$$

and comes from the proton orbital momentum. (Numerical values for this coefficient, depending on the pseudo shells $\tilde{\eta}$ can be found in [24]). In this case the action of the normal angular momentum operator L in the pseudo space is thus given by its pseudo counterpart $\tilde{L}$.

The reduced matrix element for the M1 transition operator in its pseudo expansion – the "tilde" for the pseudo space quantum numbers will be suppressed from now – between strong-coupled SU(3) wave function is given as

$$\langle\phi'||T^1(M)||\phi\rangle =$$
$$= \sqrt{3/4\pi}\sum_{\sigma,\eta_\sigma}\sum_{\lambda_0,\mu_0}\sum_{\tilde{L}_0,\tilde{S}_0}\sum_{\tilde{\kappa}_0} C_t(\eta_\sigma;(\lambda_0,\mu_0),\kappa_0,L_0,S_0)$$
$$\times\langle\phi'||\mathcal{U}^{(\lambda_0,\mu_0);S_0,J_0=1}_{\kappa_0 L_0}||\phi\rangle$$
$$= \sqrt{3/4\pi}\sum_{\sigma,\eta_\sigma}\sum_{\lambda_0,\mu_0}\sum_{\tilde{L}_0,\tilde{S}_0}\sum_{\tilde{\kappa}_0} C_t(\eta_\sigma;(\lambda_0,\mu_0),\kappa_0,L_0,S_0)$$
$$\times\sum_{\rho_f}\langle(\lambda,\mu)\kappa J;(\lambda_0,\mu_0)\kappa_0 J_0||(\lambda',\mu')\kappa' J'\rangle_{\rho_f}$$

$$\times \sum_{\rho_\pi \rho_\nu} \left\{ \begin{array}{cccc} (\lambda_\pi, \mu_\pi) & (\lambda_\tau, \mu_\tau) & (\lambda_\pi', \mu_\pi') & \rho_\pi \\ (\lambda_\nu, \mu_\nu) & (\lambda_s, \mu_s) & (\lambda_\nu', \mu_\nu') & \rho_\nu \\ (\lambda, \mu) & (\lambda_0 \mu_0) & (\lambda', \mu') & \rho_f \\ \rho & 1 & \rho' & \end{array} \right\}$$

$$\times \langle \{f_\sigma\}(\lambda_\sigma', \mu_\sigma') \| \| \mathcal{U}^{(\lambda_0, \mu_0)} \| \| \{f_\sigma\}(\lambda_\sigma, \mu_\sigma) \rangle \tag{5.56}$$

where the abbreviations

$$\begin{aligned} \mathcal{U}^{(\lambda_0,\mu_0);S_0,J_0=1}_{\kappa_0 L_0} &= \left[a^\dagger_{(\eta_\sigma,0);1/2} \otimes \tilde{a}_{(0,\eta_\sigma,0);1/2} \right]^{(\lambda_0,\mu_0);S_0,J_0=1}_{\kappa_0 L_0} \\ \langle \phi' | &= \langle \{f_\pi\}(\lambda_\pi', \mu_\pi'), \{f_\nu\}(\lambda_\nu', \mu_\nu'); \rho'(\lambda', \mu') \kappa' L' S' J' | \\ | \phi \rangle &= | \{f_\pi\}(\lambda_\pi, \mu_\pi), \{f_\nu\}(\lambda_\nu, \mu_\nu); \rho(\lambda, \mu) \kappa L S J \rangle \end{aligned}$$

for the one-body unit tensor and the initial and final wavefunctions have been used and the parameters (λ_τ, μ_τ) and (λ_s, μ_s) introduced in the 9-(λ, μ) symbol are $(\lambda_\tau, \mu_\tau) = (\lambda_0, \mu_0)$ $[(0,0)]$ and $(\lambda_s, \mu_s) = (0,0)$ $[(\lambda_0, \mu_0)]$ for $\sigma = \pi$ $[\nu]$. For the evaluation of the triple barred matrix elements and the SU(3) recoupling coefficients computer codes are available [6, 36].

Having given the expressions for the M1 transition operator in the pseudo SU(3) basis, a procedure to determine the pseudo SU(3) quantum numbers for a particular nucleus will be discussed next.

The pseudo SU(3) basis states

To select an appropriate set of SU(3) basis states for a specific nucleus, we first determine its deformation by finding the parameters β and γ for which the generalized Nilsson Hamiltonian [96],

$$h_0 = h_{osc} + C\, \mathbf{l} \cdot \mathbf{s} + D\, \mathbf{l}^2 - m\, \omega^2\, r^2\, \beta [Y^2_0 + \frac{\sin \gamma}{\sqrt{2}} (Y^2_2 + Y^2_{-2})], \tag{5.57}$$

with a β and γ dependent oscillator frequency ω,

$$\omega(\beta,\gamma) = \omega_0(1 + \frac{15}{4\pi}\beta^2 - \frac{1}{4}(\frac{5}{\pi})^{\frac{3}{2}}\cos^3 3\gamma)^{-\frac{1}{6}} , \tag{5.58}$$

gives the lowest total energy of the combined proton and neutron systems.

By filling the single particle levels for this deformation pair-wise from below, one then determines the number of valence-space nucleons in the normal and unique parity levels, the latter being intruder states that are pushed down into the valence space from the next higher shell by the strong spin-orbit interaction. In the rare earth region the normal parity spaces are built by single particle orbits of the pseudo harmonic oscillator shells $\tilde{N} = 3$ for protons and $\tilde{N} = 4$ for neutrons. The corresponding unique parity intruder levels are $h_{11/2}$ and $i_{13/2}$ states, respectively. The dimension of these spaces is thus given by:

$$\begin{aligned} &\text{Protons:} \quad \Omega_N^\pi = 20, \quad \Omega_A^\pi = 12, \quad \Omega_{tot}^\pi = 32 \\ &\text{Neutrons:} \quad \Omega_N^\nu = 30, \quad \Omega_A^\nu = 14, \quad \Omega_{tot}^\pi = 44 \end{aligned} \tag{5.59}$$

An overall simplifying assumption made in most pseudo SU(3) model calculations is that the relevant dynamics can be described by taking into account the nucleons in the normal parity sector only [45]; the nucleons in intruder states (unique-parity sector) are assumed to follow in an adiabatic manner the motion of the nucleons in normal-parity sector with their effect represented through a reparameterization of the theory.

In the SU(3) symmetry limit the quantum numbers for the ground state proton and neutron configurations are given by the so-called leading irrep for the given particle distribution. This leading irrep corresponds to a shape with maximum deformation and is characterized by the maximum number of quanta along the z-axis and the maximum of the maximum of the remaining quanta along the x-axis. The SU(3) quantum numbers are then given by

$$\lambda = \sum n_z - \sum n_x, \qquad \mu = \sum n_x - \sum n_y . \tag{5.60}$$

For the even-even rare earth nuclei discussed here, the particle distribution and the corresponding leading SU(3) irreps for protons and neutrons are given in Table 5.1.

A more complicated procedure is necessary if all possible SU(3) irreps for a certain particle configuration have to be determined. Computer codes that generate these basis states according to

Table 5.1: Deformation and occupation numbers for rare earth isotopes, which are used to determine the $SU(3)$ states basis for these nuclei.

Nucleus	β	γ	n_N^π	n_A^π	n_N^ν	n_A^ν	$SU_\pi(3)$	$SU_\nu(3)$
^{154}Sm	0.30	$0° \leq \gamma \leq 4°$	6	6	6	4	(12,0)	(18,0)
^{156}Gd	0.30	$0° \leq \gamma \leq 6°$	8	6	6	4	(10,4)	(18,0)
^{158}Gd	0.31	$0° \leq \gamma \leq 4°$	8	6	6	6	(10,4)	(18,0)
^{160}Gd	0.29	$0° \leq \gamma \leq 4°$	8	6	8	6	(10,4)	(18,4)
^{160}Dy	0.31	$0° \leq \gamma \leq 6°$	10	6	6	6	(10,4)	(18,0)
^{162}Dy	0.28	$0° \leq \gamma \leq 4°$	10	6	8	6	(10,4)	(18,4)
^{164}Dy	0.28	$0° \leq \gamma \leq 4°$	10	6	10	6	(10,4)	(20,4)
^{196}Pt	0.11	$0° \leq \gamma \leq 60°$	16	12	22	14	(2,8)	(4,18)

the reduction $U(\Omega) \supset SU(3)$ are publicly available [6] and can be used to select a larger basis. At this point of the discussion however, where the SU(3) symmetry limit is investigated, the leading irrep will be sufficient.

5.3.5 Algebraic results for M1 transition strength

The generalized picture for the "scissors" mode introduced above distinguishes three different cases for which examples can be found in Table 5.1. An example for the case of two coupled axial rotors is ^{154}Sm where the proton and neutron irreps are $(12,0)$ and $(18,0)$ respectively. The only possible $J^\pi = 1^+$ state with a non-zero M1 transition probability to the 0^+ ground state is given by the SU(3) irrep (28,1). In the SU(3) model interpretation discussed above, this irrep corresponds to a scissors mode with the excitation quanta in terms of an oscillator, Eq. (5.43), given as $(m,l) = (1,0)$.

As it turns out, a simple analytic expression for the M1 transition strength of a scissors state, $(\lambda_\nu + \lambda_\pi - 2, \mu_\nu + \mu_\pi + 1)$, can be given in terms of the proton and neutron SU(3) quantum numbers,

$$B(M1; 0^+ \rightarrow 1^+)_{sc} = \frac{3}{4\pi} \left[\frac{\lambda_\pi \lambda_\nu}{(\lambda_\pi + \lambda_\nu - 1)} \frac{\mu_\pi + \mu_\nu + 2}{(\mu_\pi + \mu_\nu + 1)} \right] \mu_N^2 \tag{5.61}$$

which in the case of two prolate deformations with $\mu_\pi = \mu_\nu = 0$ reduces to

$$B(M1;0^+ \rightarrow 1^+)_{sc} = \frac{3}{4\pi}\left[\frac{2\lambda_\pi\lambda_\nu}{(\lambda_\pi+\lambda_\nu-1)}\right]\mu_N^2 \,. \tag{5.62}$$

For ^{154}Sm the theory thus predicts one M1 transition, $B(M1;0^+ \rightarrow 1^+)$, with a strength of 3.56 μ_n^2.

An example for the axial-triaxial case is ^{156}Gd for which the proton SU(3) irrep is $(\lambda_\pi, \mu_\pi) = (10,4)$ - corresponding to a triaxial rotor - and the neutron SU(3) irrep is $(\lambda_\nu, \mu_\nu) = (18,0)$ - corresponding to an axial deformation. In addition to the scissors mode, a "scissors plus twist" excitation, $(m,l) = (1,1)$, with the SU(3) quantum numbers $(\lambda_\nu + \lambda_\pi - 1, \mu_\nu + \mu_\pi - 1)$ is possible if one of the nucleon distributions is triaxial. An analytic expression for the M1 transition strength of the "scissors plus twist" mode is given by

$$B(M1;0^+ \rightarrow 1^+)_{sc+tw} = \frac{3}{4\pi}\frac{1}{(\lambda_\pi+\lambda_\mu+\mu_\pi)}\left[\frac{\lambda_\pi\lambda_\nu\mu_\pi}{(\mu_\pi+1)} + \lambda_\nu\mu_\pi\right]\mu_N^2 \,. \tag{5.63}$$

Since the neutron distribution is axial symmetric, a pure twist mode that requires a rotation of the neutron distribution around the body fixed z-axis is not possible. In combination with a scissors mode, however, the rotational symmetry for the neutron is lifted and twist type motion becomes possible.

An example for the most general case of two coupled triaxial rotors is ^{160}Gd. For this configuration a pure "twist" mode is possible, which corresponds to a $(m,l) = (0,1)$ excitation with the SU(3) quantum numbers $(\lambda_\nu + \lambda_\pi + 1, \mu_\nu + \mu_\pi - 2)$. The analytic expression for the M1 transition strength of this "twist" mode is given by

$$B(M1;0^+ \rightarrow 1^+)_{tw} = \frac{3}{4\pi}\left[\frac{\mu_\pi\mu_\nu}{(\mu_\pi+\mu_\nu-1)}\frac{(\lambda_\pi+\lambda_\mu+2)}{(\lambda_\pi+\lambda_\nu+1)}\right]\mu_N^2 \,, \tag{5.64}$$

which is related to the corresponding expression for the scissors mode, Eq. (5.61), by an interchange of the λ and μ quantum numbers. For a prolate shape where $\lambda > \mu$, the M1 transition strength of

Table 5.2: Leading irreps of the pseudo $SU(3)$ scheme for three rare earth nuclei and the corresponding strong-coupled $SU(3)$ irreps associated with the ground-state band and the allowed 1^+ states that connect via the $M1$ operator to the ground state. Each transition is labeled as a scissors (s) or twist (t) or combination mode.

	(λ_π, μ_π)	(λ_ν, μ_ν)	$(\lambda, \mu)_{g.s}$	$(\lambda', \mu')_{1^+}$		$B(M1, 0^+ \rightarrow 1^+)$
^{154}Sm	(12,0)	(18,0)	(30,0)	(28,1)	s	$3.56\mu_N^2$
^{156}Gd	(10,4)	(18,0)	(28,4)	(26,5)	s	$1.91\mu_N^2$
				(27,3)	s+t	$1.61\mu_N^2$
^{160}Gd	(10,4)	(18,4)	(28,8)	(29,6)	t	$0.56\mu_N^2$
				(26,9)	s	$1.77\mu_N^2$
				$(27,7)_1$	s+t	$1.82\mu_N^2$
				$(27,7)_2$	s+t	$0.083\mu_N^2$

the "scissors" state is thus larger than the one of a "twist" state which is in agreement with the geometric picture for these modes given above.

In addition to the pure scissors and twist excitations two "scissors plus twist" modes, $(m, l) = (1, 1)$, are associated with the case of triaxial proton and neutron deformations. An analytic expression for the total M1 transition strength of the two "scissors plus twist" modes, $(\lambda_\nu + \lambda_\pi - 1, \mu_\nu + \mu_\pi - 1)$, that differ only by the outer multiplicity label ρ, is given by

$$\sum B(M1; 0^+ \rightarrow 1_i^+)_{sc+tw} = \\ = \frac{3}{4\pi} \frac{1}{\lambda + \mu} \left[\frac{\mu_\pi \mu_\nu \lambda}{\lambda + 1} + \frac{\lambda_\pi \lambda_\nu \mu}{\mu + 1} + \lambda_\nu \mu_\pi + \lambda_\pi \mu_\nu \right] \mu_N^2 \,, \tag{5.65}$$

where the abbreviations $\lambda = \lambda_\pi + \lambda_\nu$ and $\mu = \mu_\pi + \mu_\nu$ have been used.

The question of weather an analytical result exists for the individual "scissors plus twist" M1 transition strengths remains open and is closely related to the important question about the physical significance of the outer multiplicity label ρ.

Using the expression given in Eq. (5.56) to compute the M1 transition strength, it can be shown that the results for the two "scissors plus twist" states are very different. In the case of ^{156}Gd for

example, these values are

$$B(M1;0^+ \rightarrow 1^+)_{sc+tw_1} = 1.82\mu_N^2$$

$$B(M1;0^+ \rightarrow 1^+)_{sc+tw_2} = 0.0083\mu_N^2 \, .$$

Other calculations for triaxial-triaxial isotopes [24] also show M1 transition strengths for these two states that are either large – slightly larger or slightly smaller than the M1 transition of a "scissors" mode – or very small.

As can be seen in Eq. (5.56), the only difference in the reduced matrix elements for the M1 strength of the two "scissors plus twist" modes is a change in the multiplicity label ρ that enters the SU(3) 9-(λ, μ) symbol. Since a 9-(λ, μ) recoupling coefficient can be rewritten as a sum of Clebsch-Gordan coefficients, the difference in transition strength reflects the dependence of the Clebsch-Gordan coefficient on the outer multiplicity label ρ – a parameter that has no counterpart in angular momentum theory where the coupling of to angular momenta is unique. The ρ dependence reflects a phase convention made by Draayer and Akiyama [36] in their definition of Wigner and Racah coefficients for SU(3).

Other phase conventions are possible, however, and recent results by Filippov and and Lisetskyi [51, 50] suggest the following two expressions for the individual M1 transition strengths of the two "scissors plus twist" modes that give the same total strength as the expression in Eq. (5.65) but differ from the computational results that are based on the phase convention introduced by Draayer and Akiyama

$$B(M1;0^+ \rightarrow 1^+))_{sc+tw_1} = \frac{3}{4\pi}\frac{1}{\lambda+\mu}\left[\lambda_\nu\mu_\pi + \frac{\lambda_\pi\lambda_\nu\mu_\pi}{\mu+1} + \frac{\mu_\pi\mu_\nu\lambda_\nu}{\lambda+1}\right]\mu_N^2 \tag{5.66}$$

$$B(M1;0^+ \rightarrow 1^+)_{sc+tw_2} = \frac{3}{4\pi}\frac{1}{\lambda+\mu}\left[\lambda_\pi\mu_\nu + \frac{\lambda_\pi\lambda_\nu\mu_\nu}{\mu+1} + \frac{\mu_\pi\mu_\nu\lambda_\pi}{\lambda+1}\right]\mu_N^2 \, . \tag{5.67}$$

Table 5.3: Total B(M1) transition strengths $[\mu_N^2]$ as given by experiment [77] and pseudo SU(3) model calculations without symmetry breaking terms.

Nucleus	$\sum$ B(M1) $[\mu_N^2]$	
	Exp.	Theo.
^{156}Gd	3.40	3.52
^{158}Gd	4.32	3.52
^{160}Gd	4.21	4.23
^{160}Dy	2.48	3.52
^{162}Dy	3.29	4.23
^{164}Dy	5.63	4.36

The physics related to these different results has to be explored in future work.

5.3.6 The pseudo SU(3) symmetry limit and experiment

The analytic expressions for the M1 transition strength given above can be used to determine the total M1 transition strength in the pseudo SU(3) symmetry limit. For some well-deformed isotopes for which the SU(3) model is expected to work well, these results for the total M1 strength together with experimental results are given in Table 5.3.

A comparison of the experimental and theoretical results shows, in general, good agreement, thus giving evidence for the underlying collective nature of the "scissors" mode, since the pseudo SU(3) model is closely related to the rotor model.

The underlying collective nature of the scissors mode is also reflected in the structure of the experimentally observed M1 transition spectrum. Even though the number of experimental observed states is larger than the maximum of three states with strong transitions predicted by a model that preserves SU(3) symmetry, each clusters of states can be associated with a "scissors", "twist" or "scissors plus twist" state as is illustrated in Fig. 5.4.

How a more realistic description of the experimental observed spectrum is possible within the framework of the pseudo SU(3) model is the topic of the next section.

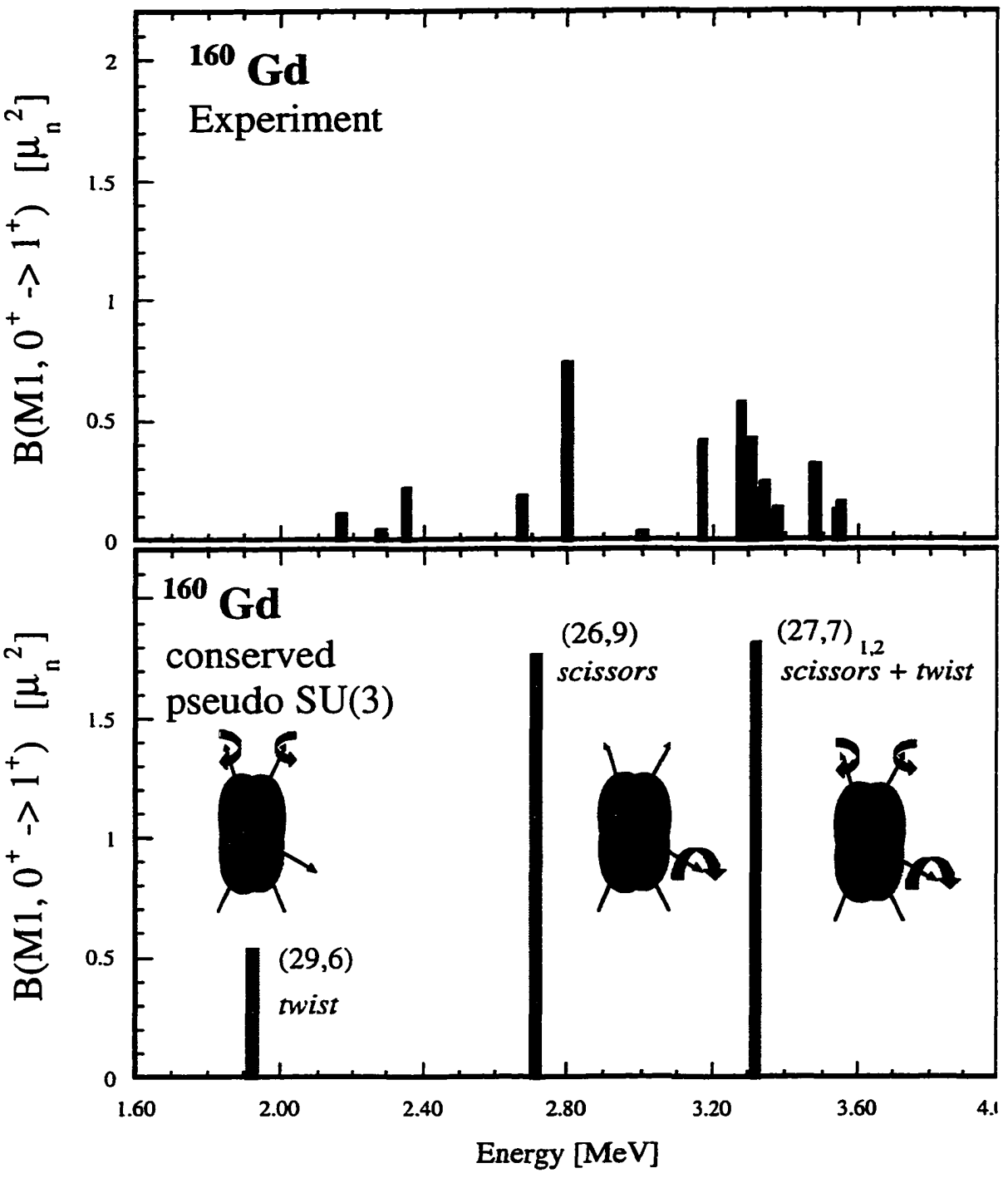

Figure 5.4: Interpretation of M1 transition spectrum in terms of "scissor" and "twist" modes. For comparison the experimental M1 transition spectrum for ^{160}Gd is given with the one given by a pseudo SU(3) Hamiltonian without any SU(3) symmetry breaking terms. As can be seen, the clusters observed in the experimental spectrum can be associated with the "scissors", "twist" and "scissors + tiwst" modes predicted by the SU(3) theory.

5.4 Calculations with a realistic Hamiltonian

To describe the experimentally observed fragmentation of the M1 transition spectrum, that is, the breakup of a strong transition among a cluster of closely packed states, SU(3) symmetry breaking terms have to be added to the Hamiltonian.

An obvious choice for those terms are the proton and neutron pairing which describe the short range part of the nuclear interaction and are known to play an important role in a realistic nuclear model. The importance of the single particle spin-orbit and orbit-orbit terms in the single particle model also suggests one should include these one-body operators. Since the spin-orbit term doesn't contribute in the S = 0 case, however, it will not be used in the investigation of even-even nuclei.

Thus, the following generalization of the SU(3) conserving Hamiltonian was used to investigate the effect of the symmetry breaking interaction terms

$$\begin{aligned} H_{PSU(3)} &= -(a_2 + a_{sym})C_2 + a_3 C_3 + bK_L^2 + cL^2 \\ &\quad + D_\pi \sum_{i_\pi} l_{i_\pi}^2 + D_\nu \sum_{i_\nu} l_{i_\nu}^2 \\ &\quad - G_\pi H_P^\pi - G_\nu H_P^\nu \, . \end{aligned} \tag{5.68}$$

Here C_2 and C_3 are the second and third order invariants of SU(3), which are related to the axial and triaxial deformation of the nucleus, and L^2 and K_L^2 are the square of the angular momentum and its projection on the intrinsic body-fixed symmetry axis, which generate rotational bands and K_L-band splitting, respectively. The parameter a_{sym} is introduced to shift SU(3) irreps with either λ or μ odd relative to those with λ and μ both even, for which a_{sym} is zero, as the former belongs to different symmetry types (B_α, $\alpha = 1, 2, 3$, rather than A) of the intrinsic Vierergruppe (D_2) [78]. The one-body proton and neutron angular momentum terms, together with the two-body pairing terms, H_P^π and H_P^ν, are SU(3) symmetry breaking interactions.

Since the quadrupole-quadrupole interaction, $Q \cdot Q = 4C_2 - 3L^2$, dominates for deformed nuclei, only basis states with C_2 larger than a certain value are expected give a significant contribution

in the low-energy region. In the present application, for both proton and neutron distributions, all SU(3) basis states with $C_2 \geq C_{2_{min}}$ were selected with $C_{2_{min}}$ set so that all irreps lying below approximately 6 MeV were included in the analysis. Then all possible couplings of these, typically three or four, proton and neutron SU(3) irreps were taken to give coupled SU(3) irreps that form basis states of the model space. Also, only states with $J \leq 8$ and $S = 0$ were considered for the investigation of the even-even case. Since experimental results show the mainly orbital character of the $J^\pi = 1^+$ states in the energy region between 2 and 4 MeV and $\mathbf{S} = 1$ states only for energies above 6 MeV, these restrictions seem to be justified.

The parameters for the Hamiltonian given in Eq. (5.68) and the effective charges $e_\pi = 1 + q_{eff}$ and $e_\nu = q_{eff}$ used in the E2 transition operator

$$T^2_M(E2) = A^{1/3} \sum_{\sigma=\pi,\nu} \sum_i e_\sigma r^2_\sigma(i) Y_{2M}(\hat{r}_\sigma(i)) \tag{5.69}$$

were determined through a fitting procedure that included as input all known levels with $J \leq 8$ up through 2 MeV in energy and selected B(E2) transition strengths. This procedure gave, in general, very good agreement between the experimental and theoretical numbers (Figures 5.5, 5.6 and 5.8), which gives an indication of the goodness of the pseudo SU(3) model in this mass and energy region.

5.4.1 Results for even-even Gd and Dy isotopes

A first test for the generalized Hamiltonian introduced in Eq. 5.68 were calculations for the even-even $^{156-160}$Gd and $^{160-164}$Dy isotopes for which the experimental data are well established [77]. As deformed nuclei in the mid-shell region they are expected to be well suited for a description by the pseudo SU(3) model.

Results from the fitting of the low energy spectrum in the energy region up to 2 MeV, Figs. 5.5 and 5.6, confirm this assumption and give, in general, a good description for the different bands. The experimental and theoretical results for the E(2) transition strength that were used in the fitting

Table 5.4: Hamiltonian parameters. The parameters for the even-even $^{156-160}$Gd and $^{160-164}$Dy isotopes and ^{163}Dy derived from the fitting procedure. An effective charge was used in the calculation of the B(E2) transition strength.

Nucl.	a_2	a_{sym}	a_3	b	c	D_π	D_ν	$G_{\pi,\nu}$	q_{eff}
^{156}Gd	0.0230	0.0008	$77.2*10^{-6}$	0.0121	0.1435	0.0756	-0.0724	0.1052	1.3119
^{158}Gd	0.0245	0.0006	$80.4*10^{-6}$	0.0080	0.2259	-0.0738	0.0478	0.0685	1.3634
^{160}Gd	0.0224	0.0004	$39.4*10^{-6}$	0.0085	0.1871	0.0271	-0.0817	0.1096	1.2361
^{160}Dy	0.0212	0.0008	$9.1*10^{-6}$	0.0127	0.0517	0.0798	-0.1134	0.1386	1.2000
^{162}Dy	0.0218	0.0005	$36.3*10^{-6}$	0.0070	0.1421	-0.0835	-0.0470	0.1245	1.2486
^{163}Dy	0.0103	0.0000	$13.7*10^{-6}$	0.0091	-0.0121	0.0000	-0.0267	0.0004	1.203
^{164}Dy	0.0233	0.0001	$46.2*10^{-6}$	0.0083	0.1005	-0.1116	-0.1309	0.0879	1.2053

Table 5.5: Total B(M1) transition strength $[\mu_N^2]$ as given by experiment [77] and calculation. Experimental and theoretical values $[e^2b^2]$ for the ground band B(E2,$0_1^+ \rightarrow 2_1^+$) transition strengths are also given.

Nucleus	$\sum$ B(M1) $[\mu_N^2]$		B(E2,$0_1^+ \rightarrow 2_1^+$) $[e^2b^2]$	
	Exp.	Theo.	Exp.	Theo.
^{156}Gd	3.40	2.91	4.66	4.79
^{158}Gd	4.32	3.02	5.02	5.23
^{160}Gd	4.21	3.29	5.19	5.00
^{160}Dy	2.48	3.20	4.98	4.87
^{162}Dy	3.29	3.19	5.22	5.14
^{164}Dy	5.63	3.38	5.57	5.37
^{196}Pt	0.69	1.27	1.40	1.56

routine can be found in Table 5.5. The eigenvectors given by this fitting procedure were then used to determine the structure of the M1 transition spectrum.

As expected, the SU(3) symmetry breaking terms in the Hamiltonian lead to a break-up of the M1 transition spectra into relatively closely packed levels centered around the sharp peaks of the pure SU(3) limit of the theory. In particular, it seems that pairing is essential for a proper description of the fragmentation of the M1 strength. A noteworthy feature is that the rotational structure of the low-energy spectrum given by the pure-SU(3) model survives the mixing induced by the pairing.

More specifically, one finds a number of transitions that, in general, are very close to the experimentally observed ones, varying from five for ^{162}Dy to eleven for ^{156}Gd, which turns out to be

in good agreement with the experimental result for these cases. Also, for most of the nuclei, the centroid of the experimental and theoretical M1 transition strength distribution lie at about the same energy, so that good overall agreement is obtained. The total M1 strength, which for the full Hamiltonian is a bit lower then for its pure SU(3) limit due to destructive interference associated with the mixing (see Table 5.5), also shows reasonable agreement with the experimental results, in most cases slightly underestimating them. One possible reason for this discrepancy is the missing spin 1 admixture in our wave functions.

A plot of the total M1 strength versus $B(E2,0_1^+ \rightarrow 2_1^+)/Z^2$, Figure 5.7, shows that the theoretical results found for the even-even Gd and Dy isotopes are in agreement with the empirically found linear relationship between these two observables.

In summary, the pseudo SU(3) results give a very reasonable description of the fragmentation observed in even-even Gd and Dy isotopes, which show at least the same quality as the corresponding QRPA calculations by Zawicha and Speth [125].

5.4.2 Results for the γ-soft ^{196}Pt

As was mentioned in the introduction for this chapter, very recent experimental results [22] have also confirmed the existence of the scissors mode for the γ-soft rotor ^{196}Pt. In order to explore the limits of the pseudo SU(3) model, this nucleus has also been included into our investigation.

Following the same procedure as used above for the even-even Gd and Dy isotopes, as the first step a fitting procedure was used to obtain the Hamilonian parameters and eigenstates while reproducing the low-energy spectrum for energies to about 2 MeV.

The results (see Fig. 5.8) show that the pseudo SU(3) model indeed is able to give a reasonable description of the ^{196}Pt spectrum which does not show rotor but rather vibrator characteristics. Also, a relatively small value for the $B(E2,0_1^+ \rightarrow 2_1^+)$ transition strength was obtained which is about a factor three smaller than the corresponding results for Gd and Dy isotopes but still overestimates the experimental value by a factor of two (see Table 5.5).

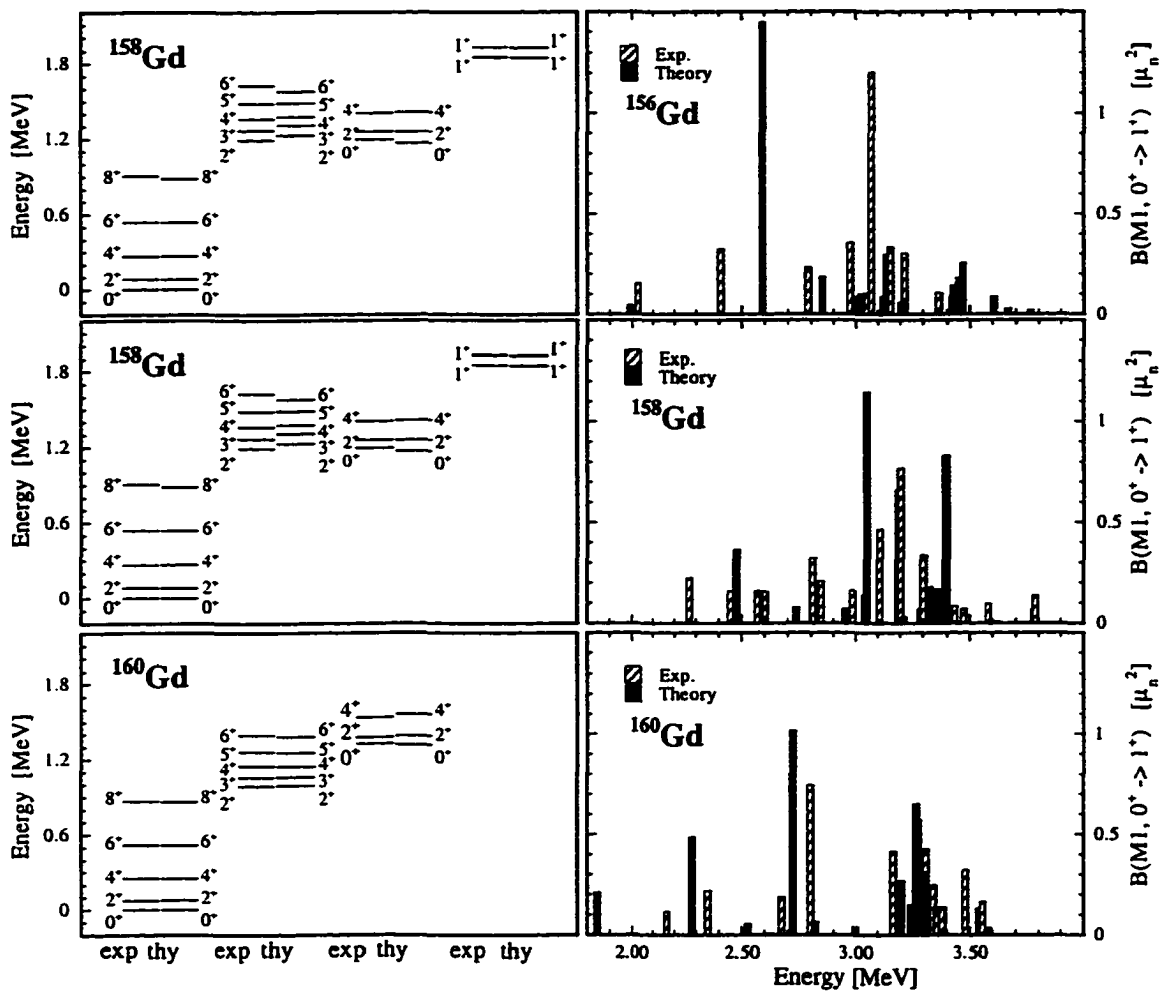

Figure 5.5: Low-energy and M1 transition spectra for the even-even $^{156-160}$Gd isotopes. Experimental excitation energies and E2 transition strengths were used as input in a fitting routine to determine parameters of the Hamiltonian for each system. These were then used to calculate the theoretical spectrum and corresponding M1 transition strengths.

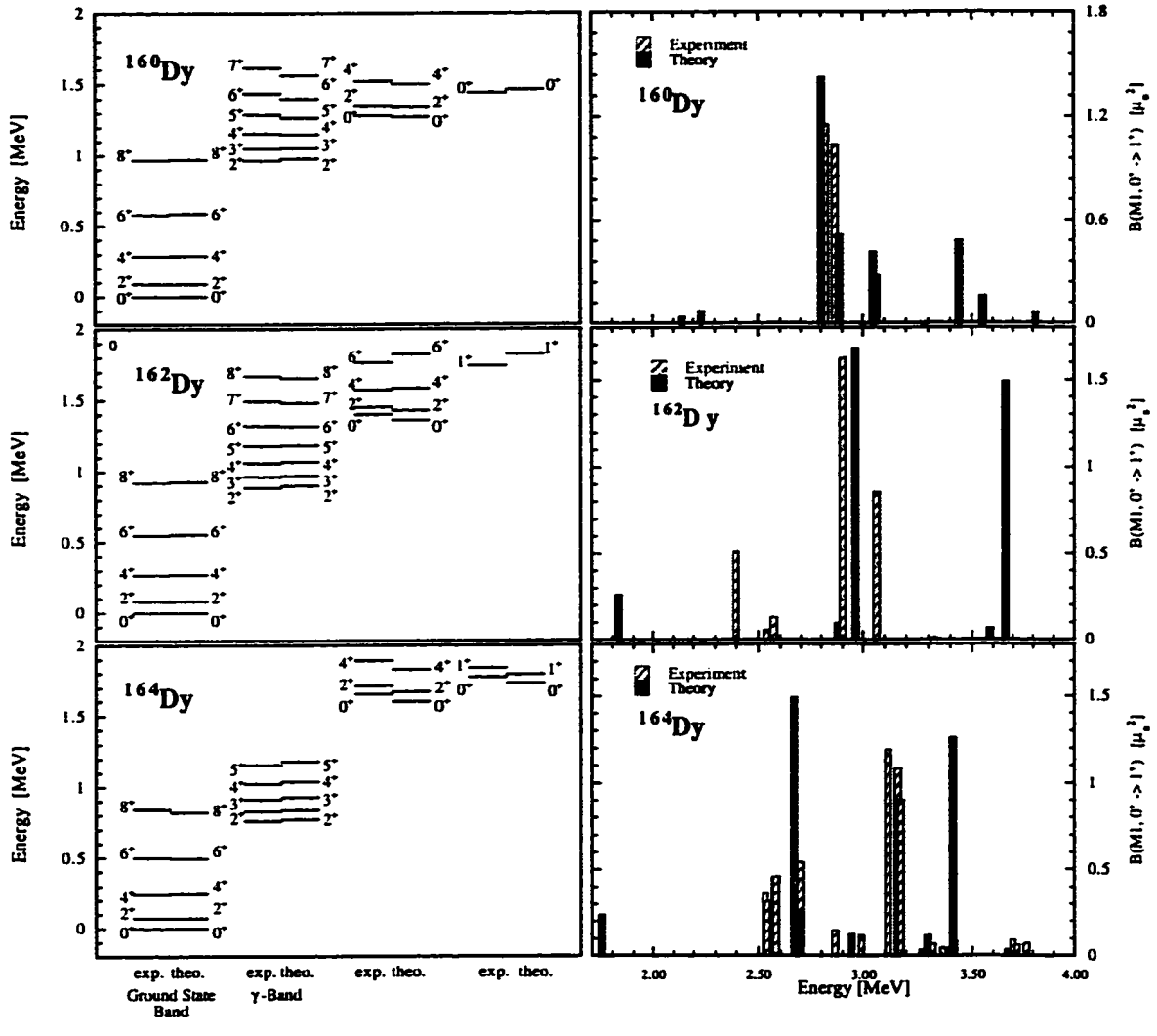

Figure 5.6: Low-energy and M1 transition spectra for the even-even $^{160-164}$Dy isotopes. Experimental excitation energies and E2 transition strengths were used as input in a fitting routine to determine parameters of the Hamiltonian for each system. These were then used to calculate the theoretical spectrum and corresponding M1 transition strengths.

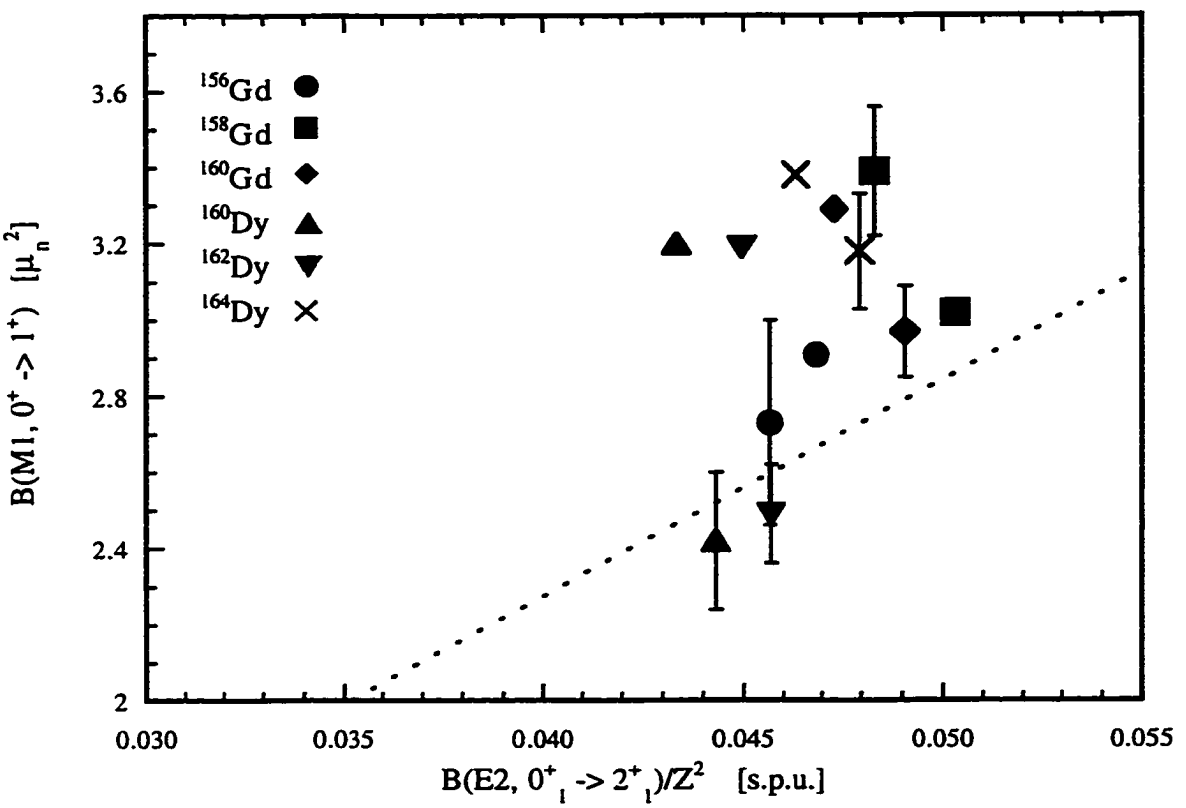

Figure 5.7: Relation between B(M1) and B(E2) values. The results for B(M1) and B(E2) values for $^{156-160}$Gd and $^{160-164}$Dy (without error bars) as given by our calculation are plotted together with the experimental values. The dashed line indicates the linear realtionship prediced by IBM sum rules.

In this case a relatively strong pairing interaction with $G_{\pi,\nu} = 0.23$ MeV was found to mix different SU(3) irreps and produce the required soft rotor results with its weaker E2 transition strengths. An analysis of the 0^+ ground state shows that it is a mix of three SU(3) irreps that are coupled from the proton irrep $(\lambda_\pi, \mu_\pi) = (2, 8)$ and the neutron irrep $(\lambda_\nu, \mu_\nu) = (4, 18)$:

$$40.5\% \text{ of } |\,(6,26)\,\rangle, \quad 9.5\% \text{ of } |\,(2,28)\,\rangle, \quad 49.8\% \text{ of } |\,(8,22)\,\rangle, \tag{5.70}$$

so that the "stretched" representation (6, 26) is not the dominate one. This result is in agreement with the analysis of Bahri [4, 46] who found that the pairing interaction drives the nucleus to a more triaxial shape, thus softening it.

In contrast, for a well-deformed nucleus like ^{156}Gd the pairing interaction is smaller by about a factor of two, $G_{\pi,\nu} = 0.105$ MeV, and the contribution of the leading irrep to the 0^+ ground state is 85 % with the next largest contribution being 4 % .

The structure of the theoretical M1 transition spectrum compares favorably with the experimental results, giving a relatively large transition strength in the energy region around 2.5 MeV and two smaller transitions at 3.1 and 3.6 MeV. The total M1 strength of 1.27 μ^2, however, is almost a factor of two too large (see Table 5.5). Keeping in mind that for this case the total M1 strength is only about one sixth of that for good rotors like the Gd isotopes, this is not unreasonable because the starting point of the theory is the assumption of a reasonably well-deformed system which ^{196}Pt is not. Nevertheless, it is important to emphasize that in this case the theory predicts a significant reduction (by a factor of 1/3 from the value of 3.55 μ^2 predicted in the SU(3) limit of the theory) in the M1 strength, in agreement with what is observed experimentally.

To summarize, the description of the γ-soft rotor shows some of the limits of the pseudo SU(3) model but still gives a reasonable description of the experimentally observed low-energy features and the M1 transition spectra, thus being the first nuclear model to address the scissors mode in the transition region.

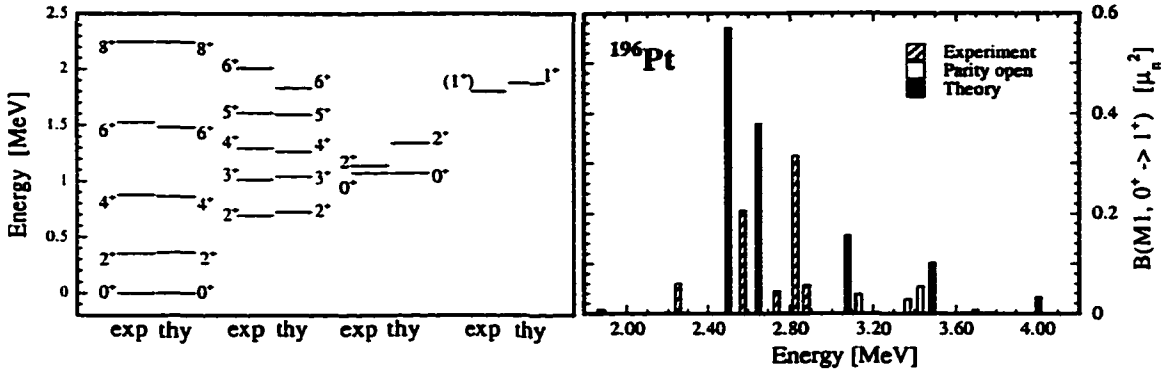

Figure 5.8: Low-energy and M1 transition spectrum for ^{194}Pt. The experimentally oberved low-enery energy spectrum for ^{196}Pt does not show typical rotor characteristics. As for the Gd isotopes, the experimentally determined energy spectrum and known E2 values were used in a fitting routine to determine the parameters of the Hamiltonian. The M1 transition spectrum that was derived using these results is in reasonable agreement with the experiment.

5.4.3 Results for odd-even nuclei

As a many particle theory, the pseudo SU(3) model is also able to describe the much more complex case of odd-even nuclei. The single unpaired nucleon introduces strong single particle features which pose a strong challenge to the ability of the pseudo SU(3) model to incorporate collective and non-collective aspects of the nuclear interaction at the same time.

To investigate the scissors mode in the odd-even case, the following generalization of the SU(3) Hamiltonian introduced in the even-even case (see Eq. (5.68)) is used

$$\begin{aligned} H_{PSU(3)} &= -(a_2 + a_{sym})C_2 + a_3 C_3 + bK_J^2 + cJ^2 \\ &\quad + C_\pi \sum_{i_\pi} \vec{l}_{i_\pi} \vec{s}_{i_\pi} + C_\nu \sum_{i_\nu} \vec{l}_{i_\nu} \vec{s}_{i_\pi} \\ &\quad + D_\pi \sum_{i_\pi} l_{i_\pi}^2 + D_\nu \sum_{i_\nu} l_{i_\nu}^2 \\ &\quad - G_\pi H_P^\pi - G_\nu H_P^\nu. \end{aligned} \tag{5.71}$$

Here J^2 and K_J^2, the square of the total angular momentum and its projection on the intrinsic body-fixed symmetry axis, have been introduced as a generalization of L^2 and K_L^2 and the single

particle spin-orbit terms, $\vec{l}_{i_\sigma}\vec{s}_{i_\sigma}$, have been added to the Hamiltonian. To reduce the number of fitting parameters, we decided to take the well-established values for the single particle spin-orbit and orbit-orbit coefficients that are given for example in [106].

A restriction for our investigation is the fact that we cannot describe a nucleus where the unpaired nucleus is from an intruder level, i. e. has a unique parity, and is thus not included in the pseudo SU(3) basis space. This is the case for ^{157}Gd which might be a reason for the different M1 transitions spectrum which shows an even distribution of about 80 states with similar small transition strengths.

The nucleus we picked for a first test of the pseudo SU(3) model for odd-even nuclei in the actinide region was ^{163}Dy, where the unpaired nucleon is a neutron from the $N = 5$ ($\tilde{N} = 4$) shell with $J^+ = \frac{5}{2}^-$. To reproduce the correct low-energy spectrum, the single particle spin-orbit interaction turns out to be essential. In a simple SU(3) model with only a quadrupole-quadrupole interaction, the lowest state would be a $J^+ = \frac{1}{2}^-$ state. In principle, an additional K_J^2 term with a negative sign should be able to lower the energy [92] of a state with larger J enough to make it the ground state. As it turns out, however, in order to get the correct $J^+ = \frac{5}{2}^-$ ground state from K_J^2 alone it would have to be so large that the rotational structure of low-energy spectrum would be destroyed.

By adding the single particle spin-orbit terms to the SU(3) Hamiltonian, with the parameters given as in the literature [106], the low-energy spectrum almost automatically has the correct structure and a very good fit can be achieved (see Fig.5.9).

As it turns out (see Table 5.4), the strength of the pairing interaction resulting from this fit is almost zero, a result that could not be changed with different starting parameters.

Results for the M1 transition spectrum also look very promising. The general structure of the spectrum is reproduced, where the maximum strength is much smaller than for the neighboring ^{162}Dy and ^{164}Dy isotopes. Also, the total M1 strength of 1.45 μ_N^2 given by our calculation is close to the experimental value of 1.77 μ_N^2 for ^{163}Dy. The corresponding theoretical and experimental

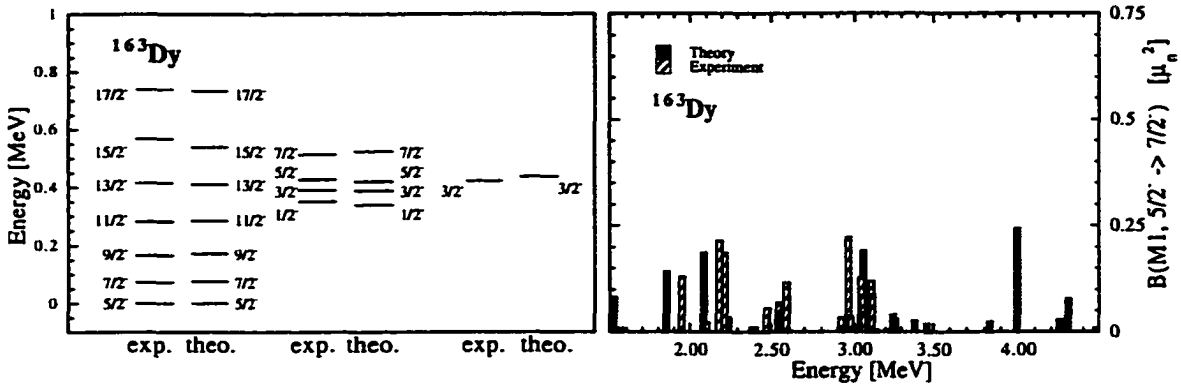

Figure 5.9: Low-energy and M1 transition spectrum for ^{163}Dy. The experimentally observed low-energy spectrum for odd-even ^{163}Dy is characterized by a combination of single particle and rotor features. As for the even-even examples studied, the experimentally determined energy spectrum and known E2 values were used to determine the parameters of the Hamiltonian. The calculated M1 transition spectrum is in reasonable agreement with the relatively large number of experimentally observed low-lying transitions.

results for the neighboring ^{162}Dy were 3.19 μ_N^2 and 3.29 μ_N^2, respectively, demonstrating the ability of the model to describe the different features of each nucleus.

The experimentally observed reduction in total transition strength by a factor of two or three for the odd-even case as compared to the even-even case [44] can not be reproduced by other microscopic [113] or core-coupling model calculations [99, 100]. These models predict that the scissors mode strength should be nearly equal to that of the even-mass neighbors as is also predicted by a sum rule approach by Ginocchio and Leviatan [54].

Whether the pseudo SU(3) model can give a more realistic description for other odd-even nuclei will be explored in future work.

Chapter 6

Conclusion

The goal of this work was to explore the collective and non-collective features of the so-called scissors mode within the framework of the pseudo SU(3) model.

On the basis of a linear connection between the invariants operators of the rotor group and SU(3), it was possible to generalize the original geometrical picture of the Two Rotor Model that assumes axial deformations by adding an additional "twist" mode for triaxial proton or neutron distributions. In the most general case, i. e. for triaxial proton and neutron distributions, four modes are realized: In addition to the "scissors mode" – the only one possible in the axial-axial case – a "twist" mode and two combined "scissors plus twist" modes. Each of these modes corresponds to a well-defined $SU(3)$ irrep that includes a $J^\pi = 1^+$ state with non-zero M1 transition strength to the $J^\pi = 0^+$ ground state. These irreps then define the basic structure of the transition spectrum. This feature and the ability of the pure pseudo SU(3) model to reproduce the total M1 strength in good agreement with the experimental results (less than 3% difference for ^{156}Gd and ^{160}Gd), are strong indications for the underlying collective structure of the scissors mode.

As has been noted, no fitting parameters like effective g factors were used to compute the results for the M1 transition strengths. It was shown that a simple analytic expression gives the M1 transition strength for the each of the different modes in terms of the SU(3) parameters (λ_π, μ_π) and (λ_ν, μ_ν), respectively, for proton and neutron distributions.

As a many particle theory, the pseudo-SU(3) model can be modified by adding non-collective one-body and two-body residual interactions to the Hamiltonian. This allows one to describe the

experimentally observed fragmentation of the M1 strength, thus giving a natural explanation for the observed breakup of the transition strength into clusters of closely packed transitions. While the underlying collective structure of the pseudo SU(3) Hamiltonian dictates the general structure of the M1 transition spectrum, the additional pairing interaction appears to be essential for a realistic description of the experimentally observed fragmentation [14].

A first test for a realistic Hamiltonian with collective and non-collective features were calculations for the well-deformed even-even $^{156-160}$Gd and $^{160-164}$Dy isotopes, for which the pseudo SU(3) model is supposed to work well. It has to be emphasized, however, that the description of the M1 transition spectrum which requires the correct M1 transition strength in a small energy region, poses a much larger challenge for a microscopic theory than the rotational structure and E2 transitions of the low-energy spectrum. The results found in our investigation showed good agreement with the experimentally observed values and appear to be of better quality than comparable calculations using the QRPA model [125].

To demonstrate the ability of the pseudo SU(3) model to address a large variety of cases, we also investigated the nature of the scissors mode for ^{196}Pt [37]. Experimental results for the M1 strength distribution of this γ-soft rotor have been obtained only very recently and have not yet been addressed by other nuclear models.

Our results show some of the limits of the pseudo SU(3) model that starts with the assumption of a well-deformed rotor. However, the configuration mixing introduced by the pairing interaction "softens" the rotor enough to give a reasonable description of the low-energy spectrum as well as of the M1 transition spectrum. These results are another example for how the interplay of collective and non-collective features in the nuclear interaction is reflected in the nuclear structure. This application of the pseudo SU(3) model for a triaxial deformed nuclei is based on results of an earlier project that used a statistical measure to show the goodness of the pseudo-spin symmetry for all deformations [13].

In the odd-even case, the unpaired nucleon introduces additional non-collective features in the low-energy spectrum as well as in the M1 transition spectrum. Here it was shown for ^{163}Dy that the single particle spin-orbit interaction is crucial for a realistic description for both the energy structure and the scissors mode. In contrast with other theories that predict the same total M1 transition strength for odd-even nuclei and their even-even neighbors, our results could reproduce the drop by a factor of one half that was oberved in different experiments [77].

To summarize, the results presented here demonstrate the ability of the pseudo SU(3) model to describe the complex interplay of collective and single particle features in atomic nuclei.

Bibliography

[1] Y. Akiyama and J. P. Draayer, Comp. Phys. Commun. **5**, p. 405 (1973).

[2] A. Arima and F. Iachello, Ann. Phys. **99**, p. 253 (1976).

[3] A. Arima and F. Iachello, Ann. Phys. **111**, p. 201 (1978)

[4] C. Bahri. Ph. D. thesis, Louisiana State University, Baton Rouge (1994).

[5] C. Bahri, J. P. Draayer. and S.A. Moszkowski, Phys. Rev. Lett. **68**, p. 2133 (1992).

[6] C. Bahri and J. P. Draayer, Comp. Phys. Comm. **83**, p. 59 (1994).

[7] C. Bahri, J. Escher, and J. P. Draayer, Nucl. Phys. **A 592**, p. 171 (1995).

[8] C. Bahri, J. Escher, and J. P. Draayer, Nucl. Phys. **A 594**, p. 485 (1995).

[9] S. T. Belyaev, Dan. Mat. Fys. Medd. **31**, p. 11 (1959).

[10] R. Bengtson, J. Dudek, W. Nasarewicz, and P. Olanders, Phys. Scr. **39**, p. 196 (1989).

[11] U. E. P. Berg, C. Bläsing, J. Drexler, R. D. Heil, U. Kneisl, W. Naatz, R. Ratzek, S. Schennach, R, Stock, T. Weber, B. Fischer, H. Hollick, and D. Kollewe, Phys. Lett. **149 B**, pp. 59–63 (1984).

[12] D. R. Bes and R. A. Sorensen, Advances in Nuclear Physics **2**, p. 129 (1969).

[13] T. Beuschel, A. L. Blokhin, and J. P. Draayer, Nucl. Phys. **A 619**, pp. 119–128 (1997).

[14] T. Beuschel, J. P. Draayer, D. Rompf, and J. Hirsch, Phys. Rev. C **57**, p. 1233 (1998).

[15] A. L. Blokhin, C. Bahri, and J. P. Draayer, Phys. Rev. Lett. **74**, p. 4149 (1995).

[16] A. L. Blokhin, T. Beuschel, and J. P. Draayer, Revista Mexicana de Física **42**, p. 21 (1996).

[17] A. L. Blokhin, T. Beuschel, J. P. Draayer, and C. Bahri, Nucl. Phys. **A 612**, p. 163 (1997).

[18] A. Bohr, I. Hamamoto, and B. R. Mottelson, Physica Scripta **26**, p. 267 (1982).

[19] A. Bohr and B. Mottelson, Mat. Fys. Medd. Dan. Vid. Selsk. **27**, p. 1 (1953).

[20] A. Bohr and B. Mottelson, *Nuclear Structure, Vol. 1,* Benjamin, Reading, (1969).

[21] P. von Brentano, A. Zilges, R.-D. Herzberg, U. Kneissl, J. Margraf, and H. H. Pitz, Nucl. Phys. **A 577**, pp. 191c–196c (1994).

[22] P. von Brentano, J. Eberth, J. Enders, L. Esser, R.-D. Herzberg, N. Huxel, H. Meise, P. von Neumann-Cosel, N. Nicolay, N. Pietralla H. Prade, J. Reif, A. Richter, C. Schlegel, R. Schwengner, S. Skoda, H. G. Thomas, I. Widenhöver, G. Winter, and A. Zilges, Phys. Rev. Lett. **76**, p. 2029 (1996).

[23] H. B. G. Casimir, *Rotataions of a Rigid Body in Quantum Mechanics*, J. B. Wolters, La Hague, (1931).

[24] O. Castaños, J. P. Draayer, and Y. Leschber, Ann. Phys. **180**, p. 290 (1987).

[25] O. Castaños, J. P. Draayer, and Y. Leschber, Z. Phys. **A 329**, p. 33 (1988).

[26] O. Castaños, J. G. Hirsch, O. Civitarese, and P. O. Hess, Nuc. Phys. **A 571**, p. 276–300 (1994).

[27] O. Castaños, M. Moshinsky and C. Quesne, Phys. Lett. **227 B**, p. 238 (1992).

[28] O. Castaños, V. Velázques A., P. O. Hess, and J. G. Hirsch, Phys. Lett. **B321**, p. 303 (1994).

[29] R. F. Casten, J. P. Draayer, K. Heyde, P. Lipas, T. Otsuka, and D. Warner, *Algebraic Approaches to Nuclear Structure: Interacting Boson and Fermion Models*, Harcourt, Brace, and Jovanovich, New York, p. 436 (1993).

[30] J. F. Cornwell, *Technics in Physics 7: Group Theory in Physics, Vol. 2*, Academic Press, Orlando, (1985).

[31] C. de Coster and K. Heyde, Nucl. Phys. **A 529**, p. 507 (1991).

[32] A. Degener, C. Blässing, R. D. Heil, A. Jung, U. Kneissl, H. H. Pitz, H. Schacht, S. Schennach, R. Stock, and W. Wesselborg, Nucl. Phys. **A 513**, pp. 29–42 (1990).

[33] A. E. L. Dieperink, Prog. Part. Nucl. Phys. **9**, pp. 121–146 (1983).

[34] A. E. L. Dieperink and G. Wenes, Ann. Rev. Nucl. Part. Sci. **35**, pp. 77–105 (1985).

[35] C. Djalali, N. Marty, M. Morlet, A. Willis, J. C. Jourdain, D. Bohle, U. Hartmann, G. Küchler, A. Richter, G. Caskey, G. M. Craley, and A Galonsky, Phys. Lett. **164 B**, pp. 269–273 (1985).

[36] J. P. Draayer and Akiyama, J. Math. Phys. **14**, p. 1904 (1973).

[37] J. P. Draayer, T. Beuschel, D. Rompf, and J. G. Hirsch, in: *Proceedings of the International Conference "Nuclear Structure and related Topics"*, edited by: S. N. Ershov, R. V. Jolos, and V. V. Voronov, Dubna, Russia, p. 65 (1997).

[38] J. Eisenberg and W. Greiner, *Nuclear Theory, Vol. 1, Nuclear Models* North-Holland, Amsterdam, p. 540 (1970).

[39] J. P. Elliott, Proc. Roy. Soc. A **245**, pp. 128–154 (1958).

[40] J. P. Elliott, Proc. Roy. Soc. A **245**, pp. 562–581 (1958).

[41] J. P. Elliott and M. Harvey, Proc. Roy. Soc. A **272**, pp. 557-577 (1963).

[42] J. P. Elliott and C. E. Wilsdon, Proc. Roy. Soc. A **302**, pp. 509-528 (1968).

[43] J. P. Elliott, *Proceedings of the international school of physics "Enrico Fermi"*, Academic Press, New York (1966).

[44] J. Enders, N. Huxel, P. von Neumann-Cosel, and A Richter, Phys. Rev. Lett. **79**, pp. 2010–2013 (1997).

[45] J. Escher, J. P. Draayer, and A. Faessler, Nucl. Phys. **A 586**, p. 73 (1995).

[46] J. Escher, C. Bahri, D. Troltenier, and J. P. Draayer, Nucl. Phys. **A 633** , pp. 662–680 (1998).

[47] J. Escher, Ph. D. thesis, Louisiana State University, Baton Rouge (1997).

[48] A. Faessler and R. Nojarov, Prog. Part. Nucl. Phys. bf 19, pp. 167–195 (1987).

[49] A. Faessler, R. Nojarov, and F. G. Scholz, Nucl. Phys. **A 515**, pp. 237–272 (1990).

[50] G. F. Filippov and A. F. Lisetskyi, private communications (1998).

[51] G. F. Filippov, A. F. Lisetskyi, and J. P. Draayer, J. Math. Phys. **39**, pp. 1350–1365 (1998).

[52] D. Frekers, D. Bohle, A. Richter, R. Abegg, R. E. Azuma, A. Celler, C. Chan, T. E. Drake, K. P. Jackson, J. D King, C. A Miller, R. Schubank, J. Watson, and S. Yen, Phys. Rev. Lett. **58**, p. 658 (1989).

[53] I. M. Gel'fand and M. L. Zetlin, Dokl. Akad. Nauk SSSR **71**, 824 (1950).

[54] J. N. Ginocchio and A. Leviatan, Phys. Rev. Lett. **79**, p. 813 (1997).

[55] M. Goeppert Mayer, Phys. Rev. **75**, pp. 1969–1970 (1949).

[56] M. Goeppert Mayer, Phys. Rev. **78**, pp. 16–21 (1950).

[57] M. Goeppert Mayer, Phys. Rev. **78**, pp. 22–23 (1950).

[58] O. W. Greenberg and A. M. L. Messiah, Phys. Rev. **138**, p. B1155 (1965).

[59] C. Gustafsson, I. L. Lamm, B. Nilsson, and S. G. Nilsson, Ark. Fys. **36** p. 613 (1967).

[60] I. Hamamoto, and C. Rönström, Phys. Lett. **194B**, p. 6 (1987).

[61] M. Y. Han and Y. Nambu, Phys. Rev. **139**, B1006 (1965).

[62] O. Haxel, J. H. D. Jensen, and H. E. Suess, Phys. Rev. **75**, p. 1766 (1949).

[63] A. Hayashi, K. Hara, and P. Ring, Phys. Rev. Lett. **53**, p. 337 (1984).

[64] K. T. Hecht, Nucl. Phys. **A 62**, pp. 1–36 (1965).

[65] K. T. Hecht and A. Adler, Nucl. Phys. **A 137**, p. 129 (1969).

[66] R. D. Heil, H. H. Pitz, U. E. P. Berg. U. Kneissl, K. D. Hummel G. Kilus, D. Bohle, A. Richter, C. Wesselborg, and P. von Brentano, Nucl. Phys. **A 476**, pp. 39–47 (1988).

[67] K. Heyde and C. De Coster, Phys. Rev. **C 44**, pp. R2262–R2266 (1991).

[68] K. Heyde, C. De Coster, D. Ooms, and A. Richter, Phys. Lett. **B 312** pp. 267–271 (1993).

[69] K. Heyde, C. De Coster, S. Rombouts, and S. J. Freeman, Nucl. Phys. **A 569** pp. 30–52 (1996).

[70] J. Hirsch, O. Castaños, P. O. Hess, and O. Civitarese, Nuc. Phys. **A 589**, p. 445 (1995).

[71] J. Hirsch, O. Castaños, P. O. Hess, and O. Civitarese, Phys. Rev. C **51**, p. 2252 (1995).

[72] F. Iachello, Nucl. Phys. **A 358**, pp. 89c–112c (1981).

[73] F. Iachello, Phys. Rev. Lett. **53**, pp. 1427–1429 (1983).

[74] B. R. Judd, W. Miller Jr, J. Patera, and P. Winternitz, J. Math. Phys. **15**, pp. 1787–1799 (1974).

[75] O. Klein, Zeit. Phys. **29**, p. 60 (1929).

[76] U. Kneissl, J. Margraf, H. H. Pitz, P. von Brentano, R.-D. Herzberg, and A. Zilges, Prog. Part. Nucl. Phys. **34**, pp. 285–294 (1995).

[77] U. Kneissl, H. H Pitz, and A. Zilges, Prog. Part. Nucl. Phys. **37**, p. 349 (1996).

[78] Y. Leschber, Hadronic Journal Supplement **3**, p. 1 (1987).

[79] N. Lo Iudice and F. Palumbo, Phys. Rev. Lett. **41**, p. 1532 (1978).

[80] N. Lo Iudice and P. Palumbo, Nuc. Phys. **A 326**, pp. 193–208 (1979).

[81] N. Lo Iudice, P. Palumbo, A. Richter, and H. J. Wörtche, Phys. Rev. **42**, pp. 241–246 (1990).

[82] J. Margraf, A. Degener, H. Friedrichs, R. D. Heil, A. Jung, U. Kneissl, S. Lindenstruth, H. H. Pitz, H. Schacht, U. Seemann, R. Stock, C. Wesselborg, A. Zilges, and P. von Brentano, Phys. Rev. **C 42**, pp. 771–773, (1990).

[83] R. Machleid, Adv. Nucl. Phys. **19** p. 189 (1989).

[84] J. Margraf, C. Wesselborg, R. D. Heil. U. Kneissl, H. H. Pitz, C. Rangacharyulu, A. Richter, H. J. Wörtche, and W. Ziegler, Phys. Rev. **C 45**,pp. R521–524 (1992).

[85] J. Margraf, R. T. Eckert, M. Rittner, I. Bauske, O. Beck, U. Kneissl, H. Maser, H. H. Pitz, A. Schiller, P. von Brentano, R. Fischer, R.-D. Herzberg, N. Pietralla, A. Zilges, and H. Friedrichs, Phys. Rev. C **52**, pp. 2429–2443 (1995).

[86] H. Maser, N. Pietrella, P. von Brentano, R.-D. Herzberg, U. Kneissl, J. Margraf, H. H. Pitz, and A. Zilges, Phys. Rev. C **54**, pp. 2129–2133 (1996).

[87] A. Messiah, *Quantum Mechanics*, North Holland: Wiley and Sons (1958).

[88] D. J. Millener, J. Math. Phys. **19**, pp. 1513–1514 (1978).

[89] M. Moshinsky *Group Theory and the Many-Body Problem*, Gordon and Breach, Science Publishers, New York, (1968).

[90] Y. Nambu and G. Jona-Lasinio, Phys. Rev. **124**, p. 246 (1961).

[91] H. A. Naqvi and J. P. Draayer, Nuc. Phys. **A 516**, pp. 351–364 (1990).

[92] H. A. Naqvi and J. P. Draayer, Nucl. Phys. **A 536**, pp. 297–308 (1992).

[93] W. Nazarewicz, M. A. Riley, and J. D. Garrett, Nucl. Phys. **A 512**, p. 61 (1990).

[94] R. Nojarov, Prog. Part. Nucl. Phys. **34**, pp. 297–307 (1995).

[95] P. von Neumann-Cosel, J. N. Ginocchio, H. Bauer, and A. Richter, Phys. Rev. Lett., **75**, p. 4178 (1995).

[96] S. G. Nilsson, Dan. Videns. Selsk. Mat. Fys. Medd. **29**, No.16 (1955).

[97] N. Pietralla, P. von Brentano, R.-D. Herzberg, U. Kneissl, J. Margraf, H. Maser, H. H. Pitz, and A. Zilges, Phys. Rev. C. **52**, p. R2317 (1995).

[98] N. Pietrella, Ph. D. thesis, Inst. für Kernphysik, Universität zu Köln, Germany (1996).

[99] A. A. Raduta, and N. Lo Iudice, Z. Phys. A **334**, p. 403 (1989).

[100] A. A. Raduta, and D. S. Delion, Nucl. Phys. **A 513**, p. 11 (1990).

[101] R. D. Ratna Raju, J. P. Draayer, and K. T. Hecht, Nucl. Phys. **A 202**, p. 433 (1973).

[102] A. Richter, in:*Proc. of the Int. Conf. on Nuclear Physisc, Florence (Italy) 1983*, edited by P. Blasi and R. A. Ricci, Tipografica Compositori, Bologna, pp. 189–217 (1983).

[103] A. Richter, Prog. Part. Nucl. Phys. **13**, pp. 1–62 (1985).

[104] A. Richter, Nucl. Phys. **A 507**, pp. 99c–128c (1990).

[105] A. Richter, Prog. Part. Nucl. Phys. **34**, pp. 261–284 (1995).

[106] P. Ring and P. Schuck *Nuclear many body problem*, Springer, Berlin (1979).

[107] D. Rompf, J. P. Draayer, D. Troltenier, and W. Scheid, Z. Phys. **A 354**, p. 359 (1996).

[108] D. Rompf, Ph. D. thesis, Inst. für Theoretische Physik der Justus-Liebig-Universität, Gießen, Germany (1997).

[109] D. Rompf, T. Beuschel, J. P. Draayer, and W. Scheid, Phys. Rev. C **57**, p. 1703, (1998).

[110] A. Schiller, Diploma thesis, Universität Stuttgart, Stuttgart, Germany (1995).

[111] B. D. Serot and J. D. Walecka, in: *Advances in Nuclear Physics*, edited by J. W. Negele and E. Vogt, Plenum, New York, (1986)

[112] V. G. Soloviev, A. V. Sushkov, N. Yu. Shirikova, and N. Lo Iudice, Nucl. Phys. **A 600**, p. 155 (1996).

[113] V. G. Soloviev, et al. , Nucl. Phys. **A 613**, p. 47 (1996).

[114] J. Speth and D. Zawischia, Phys. Lett. **211 B**, pp. 247–251 (1988).

[115] D. Troltenier, C. Bahri, and J. P. Draayer, Nuc. Phys. **A 586**, p. 53 (1995).

[116] D. Troltenier, A. L. Blokhin, J. P. Draayer, D. Rompf, and J. Hirsch, in: *Latin-American school of physics XXX Elaf*, edited by O. Castaños, R. Lòpez-Peña, J. Hirsch and, K. B. Wolf, AIP Conference proceedings 365, Woodbury, New York (1996).

[117] D. Troltenier, J. P. Draayer, P. O. Hess, and O. Castaños, Nucl. Phys. **A 576**, p. 351 (1994).

[118] D. Troltenier, W. Nazarewicz, Z. Szymański, and J. P. Draayer, Nucl. Phys. **A 567**, p. 591 (1994).

[119] H. Ui, Prog. Theor. Phys. **44**, p. 153 (1970).

[120] P. Van Isaker, and D. D. Warner, J. Phys. G. **20**, pp. 853-890 (1995).

[121] D.A. Varshalovich, A.N. Moskalev, and V.K. Khersonskii *Quantum Theory of Angular Momentum*, World Scientific, Singapore (1988).

[122] C. Wesselborg, K. Schiffer, K. O. Zell, P. von Brentano, D. Bohle, A. Richter, G. P. A. Berg, B. Brinkmöller, J. G. M. Römer, F. Osterfeld, and M. Yabe, Z. Phys. **323 A**, pp. 485–486 (1986)

[123] W. Ziegler, N. Huxel, P. von Neumann-Cosel, C. Rangacharyulu, A. Richter, and C. Spieler, Nucl. Phys.**A 564** pp. 366–382 (1993).

[124] D. Zawischia, M. Macfarlane, and J. Speth, Phys. Rev. C **44**, p. 1461 (1990).

[125] D. Zawischia and J. Speth, Z. Phys. **339 A** pp. 97–109 (1991).

[126] D. Zawischia and J. Speth, Nuc. Phys. **A 569** pp. 343c–1352 (1994).

[127] J. Zimanyi and S. A. Moszkowski, Phys. Rev. C **42**, p. 1416 (1990).

Appendix A

SU(3) group theoretical tools

Among the most appealing features of the SU(3) model are the powerful group theoretical tools that make calculations more efficient and transparent. Definitions and notation for these tools that are used throughout this work are summarized in this appendix.

In earlier versions of the SU(3) shell model, when some of these techniques and especially the corresponding computer code were not yet developed, it was only possible to investigate operators that could be written in terms of SU(3) generators. Using the second-quantization formalism in its tensorial form and the SU(3) generalization of the Wigner-Eckhart theorem, however, it is now possible to efficiently evaluate matrix elements of the one- and two-body operators that are part of a more general shell model Hamiltonian.

As will be shown in this appendix, these operators can be expanded using only two kinds of SU(3) unit tensors constructed from fermion annihilation and creation operators for either the one- or two-body case. Since the operator dependent coefficients for these expansions can be derived relatively easily and are known for the operators used here, only the reduced matrix elements of these unit tensors have to be evaluated for a particular nucleus and basis selection. This is done by a computer code developed by Bahri and Draayer [4, 6] which uses sophisticated logical operations and bit manipulation procedures to save disk storage and computing time.

Also discussed is the transformation of an operator given in real space into the pseudo SU(3) space, such that the advantages of a expansion in unit tensors can also be used in this case. A basic ingredient for these calculations are the SU(3) equivalents of the 3J, 6J and 9J recoupling

coefficients known from angular momentum theory. Their definitions and some basic properties will be presented next.

A.1 SU(3) Wigner coefficients

Different from the SU(2) case where the coupling of the angular momenta $\vec{l}_1$ and $\vec{l}_2$ to $\vec{l}$ is unique, the situation in the SU(3) case is more complicated and an outer multiplicity label ρ is needed to distinguish multiple occurrences of a given total irrep, (λ,μ), in the direct product $(\lambda_1,\mu_1)\otimes(\lambda_1,\mu_1)$. This outer multiplicity label also enters the SU(3) Wigner coefficients, $\langle\,(\lambda_1,\mu_1)\alpha_1;(\lambda_2,\mu_2)\alpha_2\,|\,(\lambda,\mu)\alpha\,\rangle_\rho$, for the coupling of two SU(3) irreps, $(\lambda_1\mu_1)$ and $(\lambda_2\mu_2)$, to a total SU(3) irrep (λ,μ). Using this notation for the coupling coefficients, the unitary transformation from an uncoupled to a coupled SU(3) basis can be written as

$$|(\lambda,\mu)\alpha\,\rangle_\rho = \sum_{\alpha_1\alpha_2} \langle\,(\lambda_1,\mu_1)\alpha_1;(\lambda_2,\mu_2)\alpha_2\,|\,(\lambda,\mu)\alpha\,\rangle_\rho\;|(\lambda_1,\mu_1)\alpha_1\,\rangle|(\lambda_2,\mu_2)\alpha_2\,\rangle, \tag{A.1}$$

and the inverse transformation is given as

$$|\,(\lambda_1,\mu_1)\alpha_1\rangle|\,(\lambda_2,\mu_2)\alpha_2\,\rangle = \sum_{\alpha}\langle\,(\lambda_1,\mu_1)\alpha_1;(\lambda_2,\mu_2)\alpha_2\,|\,(\lambda,\mu)\alpha\,\rangle_\rho\;|(\lambda,\mu)\alpha\,\rangle_\rho\,. \tag{A.2}$$

With the phase conventions chosen by Draayer and Akiyama [36], the orthonormality relations for these Wigner SU(3) coefficients are

$$\begin{aligned}\sum_{\alpha_1\alpha_2} &\langle\,(\lambda_1,\mu_1)\kappa_1 l_1 m_1;\,(\lambda_2,\mu_2)\kappa_2 l_2 m_2\,|\,(\lambda,\mu)\kappa l m\,\rangle_\rho \\ &\times\langle\,(\lambda_1,\mu_1)\kappa_1' l_1' m_1';\,(\lambda_2,\mu_2)\kappa_2' l_2' m_2'\,|\,(\lambda,\mu)\kappa l m\,\rangle_\rho \\ &= \delta_{\lambda'\lambda}\delta_{\mu'\mu}\delta_{\rho'\rho}\,,\end{aligned} \tag{A.3}$$

and

$$\sum_{\{-\}} \langle (\lambda_1,\mu_1)\kappa_1 l_1 m_1;\ (\lambda_2,\mu_2)\kappa_2 l_2 m_2 \,|\, (\lambda,\mu)\kappa l m \rangle_\rho \times \langle (\lambda_1,\mu_1)\kappa_1' l_1' m_1';\ (\lambda_2,\mu_2)\kappa_2' l_2' m_2' \,|\, (\lambda,\mu)\kappa l m \rangle_\rho = \delta_{l_1 l_1'} \delta_{l_2 l_2'} \delta_{m_1 m_1'} \delta_{m_2 m_2'} \delta_{\kappa_1 \kappa_1'} \delta_{\kappa_2 \kappa_2'} , \tag{A.4}$$

with the summation $\{-\}$ running over all possible ρ, λ, μ and κ, l, m combinations. For the SU(3) $\supset$ SU(2)$\otimes$U(1) group chain the sublabels in equation (A.4) have to be replaced by the corresponding quantum numbers ϵ, λ and μ.

By defining so-called double-barred or "reduced" SU(3) coupling coefficients, it is possible to factor out the dependence of the SU(3) Wigner coefficients on the m or M_Λ subgroup labels into a "geometric" part that is simply a SO(3) Clebsch-Gordan coefficient. For the $SU(3) \supset SO(3)$ group chain with the sublabel $\alpha = \kappa l m$, the relation between the "full" and "reduced" Wigner coefficients is:

$$\langle (\lambda_1,\mu_1)\kappa_1 l_1 m_1;\ (\lambda_2,\mu_2)\kappa_2 l_2 m_2 \,|\, (\lambda,\mu)\kappa l m \rangle_\rho = \underbrace{\langle (\lambda_1,\mu_1)\kappa_1 l_1;\ (\lambda_2,\mu_2)\kappa_2 l_2 \,||\, (\lambda,\mu)\kappa l \rangle_\rho}_{\text{reduced Wigner coefficient}} \underbrace{\langle l_1 m_1,\ l_2 m_2 \,|\, l m \rangle}_{\text{geometric part}} . \tag{A.5}$$

and the equivalent relation for the reduction SU(3) $\supset$ SU(2)$\otimes$U(1) is:

$$\langle (\lambda_1,\mu_1)\epsilon_1 \Lambda_1 M_{\Lambda_1};\ (\lambda_2,\mu_2)\epsilon_2 \Lambda_2 M_{\Lambda_2} \,|\, (\lambda,\mu)\epsilon \Lambda M_\Lambda \rangle_\rho = \underbrace{\langle (\lambda_1,\mu_1)\epsilon_1 \Lambda_1;\ (\lambda_2,\mu_2)\epsilon_2 \Lambda_2 \,||\, (\lambda_3,\mu_3)\epsilon \Lambda \rangle_\rho}_{\text{reduced Wigner coefficient}} \underbrace{\langle \Lambda_1 M_{\Lambda_1},\ \Lambda_2 M_{\Lambda_2} \,|\, \Lambda M_\Lambda \rangle}_{\text{geometric part}} \tag{A.6}$$

Like the "full" SU(3) and SO(3) Wigner coefficients, the double-bar coefficients are unitary and real.

A.1.1 Symmetry properties

Related to the extra multiplicity ρ are more complicated symmetry properties than for the $SU(2)$ case where the Clebsch-Gordan coefficients transform simply with a phase factor under particle interchange. Following the convention introduced by Draayer and Akiyama [36] for the SU(3) case, the $1 \leftrightarrow 2$ interchange of quantum labels requires a summation over the multiplicity ρ' of the final coupling and a "geometrical" phase matrix $\Phi_{\rho\rho'}[(\lambda_1,\mu_1),(\lambda_2,\mu_2),(\lambda_3,\mu_3)]$

$$\begin{aligned}&\langle\,(\lambda_1,\mu_1)\alpha_1;\,(\lambda_2,\mu_2)\alpha_2\,|\,(\lambda_3,\mu_3)\alpha_3\,\rangle_\rho = \\ &\quad = \sum_{\rho'} \Phi_{\rho\rho'}[(\lambda_1,\mu_1),(\lambda_2,\mu_2),(\lambda_3,\mu_3)]\,\langle\,(\lambda_2,\mu_2)\alpha_2;\,(\lambda_1,\mu_1)\alpha_1\,|\,(\lambda_3,\mu_3)\alpha_3\,\rangle_{\rho'}\,, \qquad \text{(A.7)}\end{aligned}$$

where Φ is a special case of the recoupling coefficient Z that will be introduced in the following section (A.2.1) on SU(3) recoupling coefficients,

$$\Phi_{\rho\rho'}[(\lambda_1,\mu_1),(\lambda_2,\mu_2);(\lambda_3,\mu_3)] = Z[(\lambda_1,\mu_1)(00)(\lambda_3,\mu_3)(\lambda_2,\mu_2);(\lambda_1,\mu_1)1\rho(\lambda_2,\mu_2)1\rho')\,. \qquad \text{(A.8)}$$

For the special case where the coupling $(\lambda_1,\mu_1)\times(\lambda_2,\mu_2) \rightarrow (\lambda_3,\mu_3)$ is unique, Φ reduces to a simple phase factor

$$\Phi_{11}[(\lambda_1,\mu_1),(\lambda_2,\mu_2),(\lambda_3,\mu_3)] = (-1)^{\varphi} = (-1)^{(\lambda_1+\mu_1)+(\lambda_2+\mu_2)-(\lambda_3+\mu_3)}\,. \qquad \text{(A.9)}$$

The situation is simpler for the $1 \leftrightarrow 3$ interchange where the multiplicity index ρ is conserved and the Wigner coefficients are related by a simple factor,

$$\begin{aligned}&\langle\,(\lambda_1,\mu_1)\alpha_1;\,(\lambda_2,\mu_2)\alpha_2\,|\,(\lambda_3,\mu_3)\alpha_3\,\rangle_\rho = \\ &\quad = (-1)^{\varphi+\chi_2}\sqrt{\frac{\dim(\lambda_3,\mu_3)}{\dim(\lambda_1,\mu_1)}}\,\langle\,(\lambda_3,\mu_3)\alpha_3;\,(\mu_2\lambda_2)\bar{\alpha}_2\,|\,(\lambda_1,\mu_1)\alpha_1\,\rangle_\rho\,, \qquad \text{(A.10)}\end{aligned}$$

with the dimension of a SU(3) irrep (λ_i, μ_i) and the phase factor φ given by

$$\begin{aligned} \dim(\lambda_i\mu_i) &= \frac{1}{2}(\lambda_i+1)(\mu_i+1)(\lambda_i+\mu_i+2) \\ \varphi &= (\lambda_1+\mu_1)+(\lambda_2+\mu_2)-(\lambda_3+\mu_3)\,, \end{aligned} \tag{A.11}$$

and the conjugate quantum number $\bar{\alpha}$ and the phase factor χ_i for the SU(3) $\supset$ SO(3) or SU(3) $\supset$ SU(2) $\otimes$ SU(1) reduction are given as follows:

$$\begin{aligned} \bar{\alpha} &= \kappa l - m = -\epsilon\Lambda - M_\Lambda \\ \chi_i &= (\lambda_i-\mu_i)+l_i-m_i = \frac{1}{3}(\lambda_i-\mu_i)-\frac{1}{6}\epsilon_i - M_{\Lambda_i}\,. \end{aligned} \tag{A.12}$$

A.2 SU(3) recoupling coefficients

A.2.1 Recoupling of two states

Because of the symmetry properties of the Wigner SU(3) coefficients which transform differently under the $1 \leftrightarrow 2$ and $1 \leftrightarrow 3$ interchange (see Eqs. (A.7) and (A.10)), the SU(3)-Racah coefficients for the recoupling of three SU(3) irreps depend on the order of the couplings. If the initial coupling is:

$$i.)\quad \Big[[(\lambda_1,\mu_1)\otimes(\lambda_2,\mu_2)]^{(\lambda_{12}\mu_{12})\rho_{12}}\otimes(\lambda_3,\mu_3)\Big]^{(\lambda,\mu)\rho_{12,3}}\,, \tag{A.13}$$

possible final couplings are either

$$ii.)\quad [(\lambda_1,\mu_1)\otimes[(\lambda_2,\mu_2)\otimes(\lambda_3,\mu_3)]^{(\lambda_{23}\mu_{23})\rho_{23}}]^{(\lambda,\mu)\rho_{1,23}}\,, \tag{A.14}$$

or

$$iii.)\quad \Big[[(\lambda_1,\mu_1)\otimes(\lambda_3,\mu_3)]^{(\lambda_{13}\mu_{13})\rho_{13}}\otimes(\lambda_2,\mu_2)\Big]^{(\lambda,\mu)\rho_{13,2}}\,. \tag{A.15}$$

Using a similar notation as for the SU(2) case, the recoupling from case *i.*) to case *ii.*) is expressed using U-Racah coefficients

$$\begin{aligned}
&\Big|[[(\lambda_1,\mu_1)\otimes(\lambda_2,\mu_2)]^{(\lambda_{12}\,\mu_{12})\rho_{12}}\otimes(\lambda_3,\mu_3)]^{(\lambda,\mu)\rho_{12,3}}\Big\rangle = \\
&= \sum_{\{-\}} U((\lambda_1,\mu_1)(\lambda_2,\mu_2)(\lambda,\mu)(\lambda_3,\mu_3);(\lambda_{12}\,\mu_{12})\rho_{12}\rho_{12,3}(\lambda_{23}\,\mu_{23})\rho_{23}\rho_{1,23}) \\
&\quad\times\Big|[(\lambda_1,\mu_1)\otimes[(\lambda_2,\mu_2)\otimes(\lambda_3,\mu_3)]^{(\lambda_{23}\mu_{23})\rho_{23}}]^{(\lambda,\mu)\rho_{1,23}}\Big\rangle\ , \qquad \text{(A.16)}
\end{aligned}$$

with the summation $\{-\}$ over all possible intermediate states $(\lambda_{23}\,\mu_{23})\rho_{23}$ and muliplicities $\rho_{1,23}$.

For the recoupling from case *i.*) to case *iii.*), Z-Racah coefficients have been introduced [88]

$$\begin{aligned}
&\Big|[[(\lambda_1,\mu_1)\otimes(\lambda_2,\mu_2)]^{(\lambda_{12}\,\mu_{12})\rho_{12}}\otimes(\lambda_3,\mu_3)]^{(\lambda,\mu)\rho_{12,3}}\Big\rangle = \\
&= \sum_{\{-\}} Z((\lambda_2,\mu_2)(\lambda_1,\mu_1)(\lambda,\mu)(\lambda_3,\mu_3);(\lambda_{12}\,\mu_{12})\rho_{12}\rho_{12,3}(\lambda_{13}\,\mu_{13})\rho_{13}\rho_{13,2}) \\
&\quad\times\Big|[[(\lambda_1,\mu_1)\otimes(\lambda_3,\mu_3)]^{(\lambda_{13}\,\mu_{13})\rho_{13}}\otimes(\lambda_2,\mu_2)]^{(\lambda,\mu)\rho_{13,2}}\Big\rangle\ , \qquad \text{(A.17)}
\end{aligned}$$

where again the summation is over the intermediate states $(\lambda_{13}\,\mu_{13})_{\rho_{13}}$ and multiplicities $\rho_{13,2}$. U and Z-Racah coefficients are related in a nontrivial way [4] and do not depend on the specific subgroup chosen to specify the SU(3) states.

Similar to the SU(2) case where a 6J coefficient can be written as a sum of Clebsch-Gordan coefficients, the SU(3) U-coefficients can be expressed in terms of SU(3) Wigner coefficients [64]. For the reduction SU(3) $\supset$ SO(3) this relation between SU(3) Racah and Wigner coefficients is:

$$\begin{aligned}
&U[(\lambda_1,\mu_1)(\lambda_2,\mu_2)(\lambda,\mu)(\lambda_3,\mu_3);\,(\lambda_{12}\,\mu_{12})\rho_{12}\,\rho_{12,3}\,(\lambda_3\,\mu_3)\rho_{23}\,\rho_{1,23}] = \\
&= \sum_{\{-\}} U(l_1l_2ll_3;\,l_{12}l_{23})\,\langle(\lambda_1,\mu_1)\kappa_1l_1;\,(\lambda_2,\mu_2)\kappa_2l_2||(\lambda_{12}\mu_{12})\kappa_{12}l_{12})_{\rho_{12}} \\
&\quad\times\langle(\lambda_{12}\mu_{12})\kappa_{12}l_{12};\,(\lambda_3,\mu_3)\kappa_3l_3||(\lambda\mu)\kappa l\rangle_{\rho_{12,3}} \\
&\quad\times\langle(\lambda_2,\mu_2)\kappa_2l_2;\,(\lambda_3,\mu_3)\kappa_3l_3||(\lambda_{23}\mu_{23})\kappa_{23}l_{23})_{\rho_{23}} \\
&\quad\times\langle(\lambda_1,\mu_1)\kappa_1l_1;\,(\lambda_{23}\mu_{23})\kappa_{23}l_{23}||(\lambda\mu)\kappa l\rangle_{\rho_{1,23}}\ , \qquad \text{(A.18)}
\end{aligned}$$

with the summation going over the sublabels $\{-\} = \{l_1, l_2, l_3, l_{12}, l_{23}, \kappa_1, \kappa_2, \kappa_3, \kappa_{12}, \kappa_{23}\}$.

A.2.2 Recoupling of four states

For a recoupling of four SU(3) irreps with the initial coupling

$$i.)\quad \Big[[(\lambda_1,\mu_1)\otimes(\lambda_2,\mu_2)]^{(\lambda_{12}\mu_{12})\rho_{12}}\otimes[(\lambda_3,\mu_3)\otimes(\lambda_4,\mu_4)]^{(\lambda_{34}\mu_{34})\rho_{34}}\Big]^{(\lambda,\mu)\rho_{12,34}}\ , \tag{A.19}$$

possible final couplings are

$$ii.)\quad \Big[[(\lambda_1,\mu_1)\otimes(\lambda_3,\mu_3)]^{(\lambda_{13}\mu_{13})\rho_{13}}\otimes[(\lambda_2,\mu_2)\otimes(\lambda_4,\mu_4)]^{(\lambda_{24}\mu_{24})\rho_{24}}\Big]^{(\lambda,\mu)\rho_{13,24}}\ , \tag{A.20}$$

or:

$$iii.)\quad \Big[[(\lambda_1,\mu_1)\otimes(\lambda_4,\mu_4)]^{(\lambda_{14}\mu_{14})\rho_{14}}\otimes[(\lambda_2,\mu_2)\otimes(\lambda_3,\mu_3)]^{(\lambda_{23}\mu_{23})\rho_{23}}\Big]^{(\lambda,\mu)\rho_{14,24}}\ . \tag{A.21}$$

Again using a similar notation as in the SU(2) case, the 9-(λ,μ) recoupling coefficient for the transformation from case *i.*) to case *ii.*) is defined as:

$$\Big|\Big[[(\lambda_1,\mu_1)\otimes(\lambda_2,\mu_2)]^{\rho_{12}(\lambda_{12}\mu_{12})}\otimes[(\lambda_3,\mu_3)\otimes(\lambda_4,\mu_4)]^{\rho_{34}(\lambda_{34}\mu_{34})}\Big]^{\rho_{12,34}((\lambda,\mu))\alpha}\Big\rangle =$$

$$= \sum_{\{-\}} \begin{Bmatrix} (\lambda_1,\mu_1) & (\lambda_2,\mu_2) & (\lambda_{12}\mu_{12}) & \rho_{12} \\ (\lambda_3,\mu_3) & (\lambda_4,\mu_4) & (\lambda_{34}\mu_{34}) & \rho_{34} \\ (\lambda_{13}\mu_{13}) & (\lambda_{24}\mu_{24}) & (\lambda,\mu) & \rho_{13,24} \\ \rho_{13} & \rho_{24} & \rho_{12,34} & \end{Bmatrix}$$

$$\times\Big|\Big[[(\lambda_1,\mu_1)\otimes(\lambda_3\mu_3)]^{\rho_{13}(\lambda_{13}\mu_{13})}\otimes[(\lambda_2\ \mu_2)\otimes(\lambda_4,\mu_4)]^{\rho_{24}(\lambda_{24}\mu_{24})}\Big]^{\rho_{13,24}((\lambda,\mu))\alpha}\Big\rangle \tag{A.22}$$

with $\{-\} = \{\rho_{13}(\lambda_{13}\mu_{13}), \rho_{24}(\lambda_{24}\mu_{24})\rho_{13,24}\}$.

The transformation from case *i.*) to *iii.*) can be written as a combination of a 9-(λ,μ) and Racah SU(3) coefficients:

$$\left|\left[[(\lambda_1,\mu_1)\otimes(\lambda_2,\mu_2)]^{\rho_{12}(\lambda_{12}\mu_{12})}\otimes[(\lambda_3,\mu_3)\otimes(\lambda_4,\mu_4)]^{\rho_{34}(\lambda_{34}\mu_{34})}\right]^{\rho_{12,34}((\lambda,\mu))\alpha}\right\rangle =$$

$$= \sum_{\{-\}} \left\{ \begin{array}{cccc} (\lambda_1,\mu_1) & (\lambda_2,\mu_2) & (\lambda_{12}\mu_{12}) & \rho_{12} \\ (\lambda_4,\mu_4) & (\lambda_3,\mu_3) & (\lambda_{34}\mu_{34}) & \rho_{34} \\ (\lambda_{14}\mu_{14}) & (\lambda_{23}\mu_{23}) & (\lambda,\mu) & \rho_{14,23} \\ \rho_{14} & \rho_{23} & \rho_{12,34} & \end{array} \right\}$$

$$\times \sum_{\rho'_{34}} \Phi_{\rho_{34}\rho'_{34}}((\lambda_3,\mu_3),(\lambda_4\mu_4);(\lambda_{34}\mu_{34}))$$

$$\times \left|\left[[(\lambda_1,\mu_1)\otimes(\lambda_4,\mu_4)]^{\rho_{14}(\lambda_{14}\mu_{14})}\otimes[(\lambda_2,\mu_2)\otimes(\lambda_3,\mu_3)]^{\rho_{23}(\lambda_{23}\mu_{23})}\right]^{\rho_{14,23}((\lambda,\mu))\alpha}\right\rangle \quad \text{(A.23)}$$

where $\{-\} = \{\rho_{14}(\lambda_{14}\mu_{14}), \rho_{23}(\lambda_{23}\mu_{23})\rho_{14,23}\}$.

A.3 Second quantization

The techniques of second quantization provide a common formalism for the construction of many particle states and operators. The major application of this formalism used in this work is to express one- and two-body operators in second quantization that are part of a Hamiltonian operator and thus preserve the particle number. In addition, the second quantization formalism allows one to describe operators that change particle numbers by either a stripping or pick-up process.

Since the creation operator and, after adding a phase, the annihilation operator have a well-known SU(3) tensor structure, the second quantized from of a many-body operator is directly related to its tensor expansion. This SU(3) tensor expansion together with the many particle wave functions expressed in a SU(3) basis, allows us to use powerful group theoretical methods for the evaluation of matrix elements.

The starting point is the introduction of a fermion creation operator $a^\dagger_\gamma$ which creates a single particle state $|\gamma\rangle$ by acting on a vacuum state $|0\rangle$:

$$a^\dagger_\gamma|0\rangle = |\gamma\rangle \ , \tag{A.24}$$

where γ is an abbreviation for the quantum numbers necessary to describe this state. In a SU(3) shell model these are irrep and intra-irrep labels of SU(3) and the spin quantum numbers, specifically, $(\eta, 0)\, l m_l \frac{1}{2} m_s$ for a particle in the η shell using the SU(3) $\supset$ SO(3) scheme.

The conjugate operator a_γ can be interpreted as the annihilator of a state $|\gamma\rangle$:

$$a_\gamma|\gamma\rangle = |0\rangle \ . \tag{A.25}$$

Acting on a vacuum state, a annihilation operator gives zero,

$$a_\gamma|0\rangle = 0 \tag{A.26}$$

which in turn can be used as a definition of an abstract vacuum state. The interpretation for shell model calculations identify an empty shell with $|0\rangle$.

The fundamental symmetry properties that distinguish fermions from bosons can be expressed by a set of anticommutation relations for the creation and annihilation operators so that the requirement of a antisymmetric wavefunction under particle exchange is equivalent to:

$$\begin{aligned} \{a^\dagger_\gamma, a_{\gamma'}\} = a^\dagger_\gamma a_{\gamma'} + a_{\gamma'} a^\dagger_\gamma &= \delta_{\gamma,\gamma'} \\ \{a^\dagger_\gamma, a^\dagger_{\gamma'}\} = \{a_\gamma, a_{\gamma'}\} &= 0 \ , \end{aligned} \tag{A.27}$$

In comparison, the requirement of a totally symmetric wave function for the boson case where creation and annihilation operators are denoted, respectively, as $b^\dagger_\gamma$ and b_γ, is equivalent to the

following commutation relations:

$$\begin{aligned} \left[b_\gamma^\dagger,\, b_{\gamma'}\right] = b_\gamma^\dagger\, b_{\gamma'} - b_{\gamma'}\, b_\gamma^\dagger &= \delta_{\gamma\gamma'} \\ \left[b_\gamma^\dagger,\, b_{\gamma'}^\dagger\right] = \left[b_\gamma,\, b_{\gamma'}\right] &= 0\,. \end{aligned}$$

A.3.1 Many particle wavefunctions in second quantization

A many particle state representing N fermions can be generated from a vacuum state $|0\rangle$ by the successive action of N creation operators:

$$|\gamma_1\,\gamma_2,..,\gamma_N\rangle^F = a_{\gamma_1}^\dagger\, a_{\gamma_2}^\dagger ... a_{\gamma_N}^\dagger |0\rangle\,, \tag{A.28}$$

which is equivalent to a representation using a Slater determinant

$$|\gamma_1\,\gamma_2,..,\gamma_N\rangle^F = (N!)^{-\frac{1}{2}} \sum_P (-1)^{\sigma_P} P\left(\phi_{\gamma_1}(x_1)\phi_{\gamma_2}(x_2)...\phi_{\gamma_N}(x_N)\right)\,, \tag{A.29}$$

with the summation over all possible permutations P and the phase factor $(-1)^{\sigma_P}$ is $+1$ for an even or -1 for an odd permutation.

To show that the two wavefunctions constructed in Eqs. (A.28) and (A.29) are equal, the scalar product of two states of the form (A.28) can be expressed as:

$$\langle 0\,|\, a_{\gamma'_N} ... a_{\gamma'_1}^\dagger a_{\gamma_1}^\dagger ... a_{\gamma_N}^\dagger |0\rangle = \det ||\delta_{\gamma_j',\gamma_i}||\,, \tag{A.30}$$

using the anti-commutation relations for the fermion creation and annihilation operators given in Eq. (A.27). This is the same result that holds for two Slater determinants of the form given in Eq. (A.29).

A.3.2 Many body operators in second quantization

The next step is to express symmetric one- and two-body operators in second quantization. A one-particle operator of a system of N identical particles is defined as

$$F = \sum_{i=1}^{N} f(x_i) \tag{A.31}$$

where $f(x_i)$ acts on a particle with coordinates x_i. It is called symmetric if it acts in the same way on every particle, i. e. commutes with the permutation operator, P. This operator can be expressed in second quantization as

$$F = \sum_{\beta,\gamma} \langle \beta | f | \gamma \rangle \, a^{\dagger}_{\beta} a_{\gamma} \, , \tag{A.32}$$

so that its matrix elements with respect to a wavefunction in second quantization (A.28) are the same as the one of F in first quantization (A.31) with repect to a Slater determinant (A.29). Similary a two-body operator,

$$G = \sum_{i<j=1}^{N} g(x_i, x_j) \, , \tag{A.33}$$

can be expressed in second quantization as

$$G = \frac{1}{4} \sum_{\beta,\gamma,\delta,\epsilon} \langle \beta\, \gamma \,|\, f \,|\, \delta\, \epsilon \rangle a^{\dagger}_{\beta} \, a^{\dagger}_{\gamma} \, a_{\delta} a_{\epsilon} \, , \tag{A.34}$$

where $\langle \beta\, \gamma |$ and $| \delta\, \epsilon \rangle$ are normalized antisymmetric two-particle states.

This formalism can be generalized for an operator O that creates m and annihilates n particles:

$$O = \frac{1}{m!\, n!} \sum_{\alpha_i\, \beta_j} \langle \alpha_1 \alpha_2 ... \alpha_m | \, 0 \, | \, \beta_1 \beta_2 ... \beta_n \rangle a^{\dagger}_{\alpha_1} \, a^{\dagger}_{\alpha_2} ... a^{\dagger}_{\alpha_m} \, a_{\beta_n} ... a_{\beta_2} \, a_{\beta_1} \, . \tag{A.35}$$

For the $n \neq m$ case this generalization allows one to describe particle transfer, where $m > n$ corresponds to a pick-up and $m < n$ to a stripping process. Since a Hamiltonian conserves particle numbers, they must be $m = n$ objects and only the cases $n = 1$ and $n = 2$ are used in this work. The

next step is to expand these operators in terms of irreducible SU(3) tensors so that group theoretical methods can be used for their evaluation.

A.4 SU(3) Tensors

Tensor operators are characterized by their especially easy transformation behavior with respect to a certain group. Specifically, operators $T(\Lambda)$ are called tensor operators with respect to a group G if they transform among themselves like a representation Λ of G:

$$\mathcal{R}\,T(\Lambda_\lambda)\,\mathcal{R}^{-1} = \sum_{\lambda'} \langle \Lambda_{\lambda'} |\, \mathcal{R} \,| \Lambda_\lambda \rangle\, T(\Lambda_{\lambda'}) \,. \tag{A.36}$$

If $\mathcal{R}$ is replaced by the infinitesimal transformation

$$\mathcal{R} = 1 + \epsilon_\sigma X_\sigma \,, \tag{A.37}$$

relation (A.36) can be also expressed by:

$$[X_\sigma, T(\Lambda_\lambda)] = \sum_{\lambda'} \langle \Lambda_{\lambda'} |\, \mathcal{R} \,| \Lambda_\lambda \rangle\, T(\Lambda_{\lambda'}) \,. \tag{A.38}$$

Specifically, in the SU(3) case where the generators are denoted as C^{11}_α this means that a set of operators T form irreducible tensors $T^{(\lambda,\mu)}$ with respect to SU(3) if the elements of T transform under SU(3) as

$$[C^{11}_\alpha, T^{(\lambda,\mu)}_\beta] = \sum_\gamma \langle (\lambda,\mu)\gamma | C^{11}_\alpha | (\lambda,\mu)\beta \rangle T^{(\lambda,\mu)}_\gamma \,, \tag{A.39}$$

where α, β and γ are, respectively, the irrep and intra-irrep labels of SU(3). With the SU(3) coupling coefficients introduced above (see section A.1), irreducible tensors may be coupled according to the rules for coupling SU(3) irreps to give a new tensor:

$$[T^{(\lambda_1,\mu_1)} \otimes U^{(\lambda_2,\mu_2)}]^{(\lambda_3,\mu_3)_\rho}_{\alpha_3} = \sum_{\alpha_1,\alpha_2} \langle (\lambda_1,\mu_1)\alpha_1; (\lambda_2,\mu_2)\alpha_2 | (\lambda_3,\mu_3)\alpha_3 \rangle_\rho \, T^{(\lambda_1,\mu_1)}_{\alpha_1} U^{(\lambda_2,\mu_2)}_{\alpha_2} \,. \tag{A.40}$$

A.4.1 Wigner-Eckart theorem

The Wigner-Eckart Theorem, known from angular momentum theory allows one to express the matrix element of a tensor operator in terms of the product of a reduced matrix element that is only a function of the angular momenta and a Clebsch-Gordan coefficient that contains the projection quantum numbers [87]:

$$\langle l_3 m_3 | T^{l_2}_{m_2} | l_1 m_1 \rangle = \frac{(-1)^{l_2}}{\sqrt{2l_3+1}} \langle l_1 m_1 \, l_2 m_2 | l_3 m_3 \rangle \langle l_3 || T^{l_2} || l_1 \rangle \, . \tag{A.41}$$

This factorization into a geometric part and a reduced matrix element allows one to calculate and store relatively few reduced matrix elements before running a computer code to evaluate the full set of matrix elements which can then be easily generated by just multiplying these reduced matrix elements with a Clebsch-Gordan coefficient.

This procedure can be generalized for the SU(3) case where the matrix element of a SU(3) irreducible tensor operator can be written as the product of a SU(3) Clebsch-Gordan coefficient and a so-called triple barred reduced matrix element [36]. For the the SU(3) $\supset$ SU(2) $\times$ U(1) subgroup chain, this generalized SU(3) Wigner-Eckart Theorem has the form

$$\begin{aligned}
&\langle (\lambda_3,\mu_3)\epsilon_3\Lambda_3 M_{\Lambda_3} | T^{(\lambda_2,\mu_2)\epsilon_2\Lambda_2 M_{\Lambda_2}} | (\lambda_1,\mu_1)\epsilon_1\Lambda_1 M_{\Lambda_1} \rangle = \\
&\quad = \sum_{\rho} \langle (\lambda_1,\mu_1)\epsilon_1\Lambda_1 M_{\Lambda_1}; (\lambda_2,\mu_2)\epsilon_2\Lambda_2 M_{\Lambda_2} | ((\lambda,\mu)\epsilon_3\Lambda_3 M_{\Lambda_3}\rangle_\rho \\
&\qquad \times \langle (\lambda_3,\mu_3) ||| T^{(\lambda_2,\mu_2)} ||| (\lambda_1,\mu_1) \rangle_\rho \; = \\
&\quad = \sum_{\rho} \langle \Lambda_1 M_{\Lambda_1}, \Lambda_2 M_{\Lambda_2} | \Lambda_3 M_{\Lambda_3} \rangle \langle (\lambda_1,\mu_1)\epsilon_1\Lambda_1; (\lambda_2,\mu_2)\epsilon_2\Lambda_2 || (\lambda_3,\mu_3)\epsilon_3\Lambda_3 \rangle_\rho \\
&\qquad \times \langle (\lambda_3,\mu_3) ||| T^{(\lambda_2,\mu_2)} ||| (\lambda_1,\mu_1) \rangle_\rho \, ,
\end{aligned} \tag{A.42}$$

and for the SU(3) $\supset$ SU(2) chain, the Wigner-Eckart theorem takes the form

$$\langle (\lambda_3,\mu_3)\kappa_3 l_3 m_3 | T^{(\lambda_2,\mu_2)\kappa_2 l_2 m_2} | (\lambda_1,\mu_1)\kappa_1 l_1 m_1 \rangle =$$

$$
\begin{aligned}
=&\sum_{\rho} \langle ((\lambda_1,\mu_1)\,\kappa_1 l_1 m_1;(\lambda_2,\mu_2)\,\kappa_2 l_2 m_2|\,((\lambda,\mu)\kappa_3 l_3 m_3\rangle_\rho \\
&\times \langle (\lambda_3,\mu_3)\,|||\,T^{(\lambda_2,\mu_2)}\,|||\,(\lambda_1,\mu_1)\rangle_\rho \;= \\
=&\sum_{\rho} \langle l_1 m_1,\; l_2 m_2\,|\,l_3 m_3\rangle\,\langle (\lambda_1,\mu_1)\,\kappa_0 l_1;\;(\lambda_2,\mu_2)\,\kappa_2 l_2||\,(\lambda_3,\mu_3)\,\kappa l_3\rangle_\rho \\
&\times \langle (\lambda_3,\mu_3)\,|||\,T^{(\lambda_2,\mu_2)}\,|||\,(\lambda_1,\mu_1)\rangle_\rho\,, \qquad \text{(A.43)}
\end{aligned}
$$

where the triple barred reduced matrix elements are of course independent from the subgroup chain chosen.

A useful expression is the relation between the tripple barred reduced matrix elements of two irreducible tensor operators $T^{(\lambda_t\mu_t)}$ and $U^{(\lambda_u\mu_u)}$ and the reduced matrix element of the coupled operator $[T^{(\lambda_t\mu_t)}\otimes U^{(\lambda_u\mu_u)}]^{\rho_0(\lambda_0\mu_0)}$:

$$
\langle [(\lambda_1,\mu_1)\otimes(\lambda_2,\mu_2)]^{\rho(\lambda,\mu)}|||[T^{(\lambda_t\mu_t)}\otimes U^{(\lambda_u\mu_u)}]^{\rho_0(\lambda_0\mu_0)}|||[(\lambda_1'\mu_1')\otimes(\lambda_2'\mu_2')]^{\rho'(\lambda',\mu')}\rangle_{\tilde{\rho}}
$$

$$
= \sum_{\rho_1\rho_2} \left\{ \begin{array}{cccc}
(\lambda_1'\mu_1') & (\lambda_t\mu_t) & (\lambda_1,\mu_1) & \rho_1 \\
(\lambda_2'\mu_2') & (\lambda_u\mu_u) & (\lambda_2,\mu_2) & \rho_2 \\
(\lambda',\mu') & (\lambda_0\mu_0) & (\lambda',\mu') & \tilde{\rho} \\
\rho' & \rho_0 & \rho &
\end{array} \right\}
$$

$$
\langle (\lambda_1,\mu_1)|||T^{(\lambda_t\mu_t)}|||(\lambda_1'\mu_1')\rangle_{\rho_1}\;\langle (\lambda_2,\mu_2)|||U^{(\lambda_u\mu_u)}|||(\lambda_2'\mu_2')\rangle_{\rho_2}\,. \qquad \text{(A.44)}
$$

A.4.2 Tensorial second quantization

The SU(3) Wigner-Eckart theorem can now be used to simplify the evaluation of many-body operators with SU(3) tensor character. Following the notation introduced in section A.3.2, a one-body tensor operator $\mathcal{F}^{(\lambda_0\mu_0);s_0}_{\kappa_0 l_0 m_{l_0};m_{s_0}}$ of rank $(\lambda_0\mu_0)$ and spin s_0 can be expressed in second quantization as

$$
\mathcal{F}^{(\lambda_0,\mu_0);s_0}_{\kappa_0 l_0 m_{l_0};m_{s_0}} \;=\; \sum_{\{-\}} \langle (\eta,0)\,l'm';\,\frac{1}{2}m'_s\,|\,f^{(\lambda_0,\mu_0);s_0}_{\kappa_0 l_0 m_{l_0};m_{s_0}}\,|\,(\eta,0)lm;\,\frac{1}{2}m_s\rangle\;\times
$$

$$\times\ a^{\dagger}_{(\eta,0)l'm';\frac{1}{2}m'_s}\, a_{(\eta,0)lm;\frac{1}{2}m_s}\ . \tag{A.45}$$

In general, the SU(3) irreps of the initial and final single particle state could be different, corresponding to an "excitation" operator that shifts a particle from shell η to shell η'. In this work, however, the so called symplectic extension of the SU(3) model which describes such shell mixing effects [47] are not used and only operators that act within a single shell are considered.

By applying the Wigner-Eckart theorem and the symmetry properties of the SU(3) and SU(2) coupling coefficients, the above expression for a second quantized operator can be rewritten in terms of a triple barred reduced matrix element:

$$\begin{aligned}
\mathcal{F}^{(\lambda_0,\mu_0);s_0}_{\kappa_0 l_0 m_{l_0};m_{s_0}} &= \langle(\eta 0);\tfrac{1}{2}|||f^{(\lambda_0,\mu_0);s_0}|||(\eta 0);\tfrac{1}{2}\rangle \\
&\times \left[\frac{2\dim(\eta,0)}{(2s_0+1)\dim(\lambda_0,\mu_0)}\right]^{\frac{1}{2}} \{\sum_{ll'}\sum_{mm'm_sm'_s}(-1)^{\eta+l-m+\frac{1}{2}-m_s} \\
&\times \langle\tfrac{1}{2}m'_s,\tfrac{1}{2}-m_s|s_0m_{s_0}\rangle\langle l'm',l-m|l_0m_{l_0}\rangle \\
&\times \langle(\eta,0)l',(0,\eta)l|||(\lambda_0,\eta_0)\kappa_0 l_0\rangle\ a^{\dagger}_{(\eta,0)l'm';\frac{1}{2}m'_s}\, a_{(\eta,0)lm;\frac{1}{2}m_s}\}\ .
\end{aligned} \tag{A.46}$$

The expression for an operator in second quantized form can be simplified if we use the fact that the creation operator for a spin $\frac{1}{2}$ particle in shell η is a proper SU(3) tensor of rank $(\eta,0)$,

$$a^{\dagger\,(\eta,0),\frac{1}{2}}_{lm_l,m_s}|0\rangle = |(\eta,0)lm_l,\tfrac{1}{2}m_s\rangle\ , \tag{A.47}$$

and determine that the corresponding annihilation tensor $\tilde{a}^{(0,\eta),\frac{1}{2}}$ is related to the annihilation operator by

$$\tilde{a}^{(0,\eta),\frac{1}{2}}_{lm_l;m_s} \equiv (-)^{\eta+l+m_l+\frac{1}{2}+m_s} a^{(0,\eta),\frac{1}{2}}_{l-m_l;-m_s}\ . \tag{A.48}$$

By coupling the single particle creation and annihilation operators to a tensor of rank (λ_0,μ_0) and

spin s_0,

$$
\begin{aligned}
[a^{\dagger\,(\eta,0);\frac{1}{2}} \otimes \tilde{a}^{(0,\eta);\frac{1}{2}}]^{(\lambda_0,\mu_0);s_0}_{\kappa_0 l_0 m_{l_0};m_{s_0}} &= \\
&= \sum_{ll'} \langle (\eta,0)l', (0,\eta)l || (\lambda_0,\eta_0)\kappa_0 l_0 \rangle \\
&\times \sum_{mm'm_s m'_s} \langle \frac{1}{2}m'_s, \frac{1}{2} - m_s | s_0 m_{s_0} \rangle \langle l'm', l-m | l_0 m_{l_0} \rangle \\
&\times a^{\dagger}_{(\eta,0)l'm';\frac{1}{2}m'_s} a_{(\eta,0)lm;\frac{1}{2}m_s} \,, \qquad \text{(A.49)}
\end{aligned}
$$

Eq. (A.46) can be simplified to

$$
\begin{aligned}
\mathcal{F}^{(\lambda_0,\mu_0);s_0,J}_{\kappa_0 l_0 m_{l_0}\,M} &= \left[\frac{(\eta+1)(\eta+2)}{(2s_0+1)\dim(\lambda_0,\mu_0)}\right]^{\frac{1}{2}} \\
&\times \langle (\eta,0); \frac{1}{2} ||| f^{(\lambda_0,\mu_0);s_0} ||| (\eta,0); \frac{1}{2} \rangle \\
&\times [a^{\dagger\,(\eta,0);\frac{1}{2}} \otimes \tilde{a}^{(0,\eta);\frac{1}{2}}]^{(\lambda_0,\mu_0);s_0,J}_{\kappa_0 l_0 m_{l_0}\,M} \,, \qquad \text{(A.50)}
\end{aligned}
$$

where the tensors have been coupled to conserved angular momentum J,

$$
\mathcal{F}^{(\lambda_0,\mu_0);s_0,J}_{\kappa_0 l_0 m_{l_0}\,M} = \sum_{m_{l_0} m_{s_0}} \langle l_0 m_{l_0}, s_0 m_{s_0} | JM \rangle \mathcal{F}^{(\lambda_0,\mu_0);s_0}_{\kappa_0 l_0 m_{l_0};m_{s_0}} \,, \qquad \text{(A.51)}
$$

and

$$
\begin{aligned}
[a^{\dagger\,(\eta,0);\frac{1}{2}} \otimes \tilde{a}^{(0,\eta);\frac{1}{2}}]^{(\lambda_0,\mu_0);s_0,J}_{\kappa_0 l_0 m_{l_0}\,M} &= \\
&= \sum_{m_{l_0} m_{s_0}} \langle l_0 m_{l_0}, s_0 m_{s_0} | JM \rangle \, [a^{\dagger\,(\eta,0);\frac{1}{2}} \otimes \tilde{a}^{(0,\eta);\frac{1}{2}}]^{(\lambda_0,\mu_0);s_0}_{\kappa_0 l_0 m_{l_0};m_{s_0}} \,. \qquad \text{(A.52)}
\end{aligned}
$$

A two-body tensor operator $\mathcal{G}^{(\lambda_0,\mu_0);s_0}$ in second quantized form can be written as

$$
\begin{aligned}
\mathcal{G}^{(\lambda_0\mu_0);s_0} &= -\frac{1}{2} \sum_{\{-\}} \langle (\lambda_1,\mu_1); s_1 ||| g^{(\lambda_0\mu_0);s_0} ||| (\lambda_2,\mu_2); s_2 \rangle_{\rho_0} \\
&\times \sqrt{\frac{\dim(\lambda_1,\mu_1)(2s_1+1)}{\dim(\lambda_0\mu_0)(2s_0+1)}} (-1)^{\varphi} \sum_{\rho'_0} \phi_{\rho\rho'_0}((\lambda_0\mu_0)(\lambda_2,\mu_2);(\lambda_1,\mu_1))
\end{aligned}
$$

$$\times \quad [[a^{\dagger\,(\eta 0);\frac{1}{2}} \otimes a^{\dagger\,(\eta 0);\frac{1}{2}}]^{(\lambda_1,\mu_1);s_1} \otimes [\tilde{a}^{(0\eta);\frac{1}{2}} \otimes \tilde{a}^{(0\eta);\frac{1}{2}}]^{(\lambda_2,\mu_2);s_2}]^{(\lambda_0\mu_0)}{}_{\rho_0';s_0} \,. \qquad \text{(A.53)}$$

A.5 Tensor expansion of pseudo SU(3) operators

If a one-body SU(3) tensor operator has to be evaluated in a pseudo SU(3) basis, it is necessary to rewrite it using pseudo quantum numbers. For this relabeling it is convenient to express the operator in a J coupled scheme since this quantum number is invariant under the transformation from the real to the pseudo space:

$$\begin{aligned}
\mathcal{F}^{j_0}_m &= \sum_{ll'} \sum_{jj' m_j m_{j'}} \langle (\eta,0)l;\frac{1}{2},jm_j|g^{j_0}|(\eta,0)l';\frac{1}{2},j'm_{j'}\rangle \\
&\quad \times a^{\dagger\,(\eta,0)l;\frac{1}{2},j}_{m_j} a^{(0,\eta)l';\frac{1}{2},j'}_{m_{j'}} \\
&= \sum_{ll'}\sum_{jj'} \langle (\eta,0)l;\frac{1}{2},j||g^{j_0}||(\eta,0)l';\frac{1}{2},j'\rangle \\
&\quad \times \{(-1)^{\eta}\sqrt{\frac{2j+1}{2j_0+1}}[a^{\dagger\,(\eta,0)l;\frac{1}{2},j} \otimes \tilde{a}^{(0,\eta)l';\frac{1}{2},j'}]^{j_0}_{m_{j_0}}\} \,. \qquad \text{(A.54)}
\end{aligned}$$

Discarding the terms with $j = \eta + \frac{1}{2}$, the tensor product of creation and annihilation operator can be relabeled using pesudo SU(3) quantum numbers,

$$(-1)^{\eta}[a^{\dagger\,(\eta,0)l;\frac{1}{2},j} \otimes \tilde{a}^{(0,\eta)l';\frac{1}{2},j'}]^{j_0}_{m_{j_0}} = (-1)^{\bar{\eta}}[a^{\dagger\,(\bar{\eta},0)\bar{l};\frac{1}{2},j} \otimes \tilde{a}^{(0,\bar{\eta})\bar{l}';\frac{1}{2},j'}]^{j_0}_{m_{j_0}} \qquad \text{(A.55)}$$

and recoupled into unit tensors

$$\begin{aligned}
&[a^{\dagger\,(\bar{\eta},0)\bar{l};\frac{1}{2},j} \otimes \tilde{a}^{(0,\bar{\eta})\bar{l}';\frac{1}{2},j'}]^{j_0}_{m_{j_0}} = \\
&= \sum_{l_0 s_0} \begin{Bmatrix} \bar{l} & \frac{1}{2} & j \\ \bar{l}' & \frac{1}{2} & j' \\ \bar{l}_0 & \bar{s}_0 & j_0 \end{Bmatrix} [a^{\dagger\,(\bar{\eta},0)\bar{l};\frac{1}{2}} \otimes \tilde{a}^{(0,\bar{\eta})\bar{l}';\frac{1}{2}}]^{\bar{l}_0;\bar{s}_0,j_0}_{m_{j_0}}
\end{aligned}$$

$$= \sum_{\tilde{\lambda}_0,\tilde{\mu}_0} \sum_{l_0 s_0} \begin{Bmatrix} \tilde{l} & \frac{1}{2} & j \\ \tilde{l}' & \frac{1}{2} & j' \\ \tilde{l}_0 & \tilde{s}_0 & j_0 \end{Bmatrix} \langle (\tilde{\eta},0)\tilde{l};(0,\tilde{\eta})\tilde{l}' || (\tilde{\lambda}_0,\tilde{\mu}_0)\tilde{\kappa}_0 \tilde{l}_0 \rangle$$

$$\times \quad [a^{\dagger\,(\tilde{\eta},0)\tilde{l};\frac{1}{2}} \otimes \tilde{a}^{(0,\tilde{\eta})\tilde{l}';\frac{1}{2}}]^{(\tilde{\lambda}_0,\tilde{\mu}_0)\tilde{l}_0;\tilde{s}_0,j_0}_{m_{j_0}} . \qquad \text{(A.56)}$$

Substituting this result into Eq. (A.54), the matrix element for one-body operator becomes

$$\mathcal{F}^{j_0}_{m_0} = \sum_{\tilde{\lambda}_0\tilde{\mu}_0} \sum_{l_0 s_0} C^{j_0}(\tilde{\eta},\tilde{\lambda}_0,\tilde{\eta}_0,\tilde{\kappa}_0,\tilde{l}_0,\tilde{s}_0) \times [a^{\dagger\,(\tilde{\eta},0)\tilde{l};\frac{1}{2}} \otimes \tilde{a}^{(0,\tilde{\eta})\tilde{l}';\frac{1}{2}}]^{(\tilde{\lambda}_0,\tilde{\mu}_0)\tilde{l}_0;\tilde{s}_0,j_0}_{m_{j_0}} \qquad \text{(A.57)}$$

where a coefficient C^{j_0} has been introduced,

$$C^{j_0}(\tilde{\eta},\tilde{\lambda}_0,\tilde{\mu}_0,\tilde{\kappa}_0,\tilde{l}_0,\tilde{s}_0) =$$

$$= \sum_{ll'} \sum_{jj'} \begin{Bmatrix} \tilde{l} & \frac{1}{2} & j \\ \tilde{l}' & \frac{1}{2} & j' \\ \tilde{l}_0 & \tilde{s}_0 & j_0 \end{Bmatrix} \langle (\tilde{\eta},0)\tilde{l};(0,\tilde{\eta})\tilde{l}' || (\tilde{\lambda}_0,\tilde{\mu}_0)\tilde{\kappa}_0 \tilde{l}_0 \rangle$$

$$\times \{(-1)^{\eta} \sqrt{\frac{2j+1}{2j_0+1}} \langle (\eta,0)l;\frac{1}{2},j || g^{j_0} || (\eta,0)l';\frac{1}{2},j' \rangle . \qquad \text{(A.58)}$$

Vita

Thomas Beuschel was born on February 25, 1965, in Köln, Germany. He attended high school (Gymnasium) in Köln, and studied physics at the University of Bonn, where he received his Diplom degree in 1991. His degree of Doctor of Philosophy in physics will be awarded in December of 1998.

DOCTORAL EXAMINATION AND DISSERTATION REPORT

Candidate: Thomas Beuschel

Major Field: Physics

Title of Dissertation: M1 Strength Distributions in Deformed Nuclei

Approved:

Major Professor and Chairman

Dean of the Graduate School

EXAMINING COMMITTEE:

Date of Examination:

October 16, 1998

IMAGE EVALUATION
TEST TARGET (QA-3)

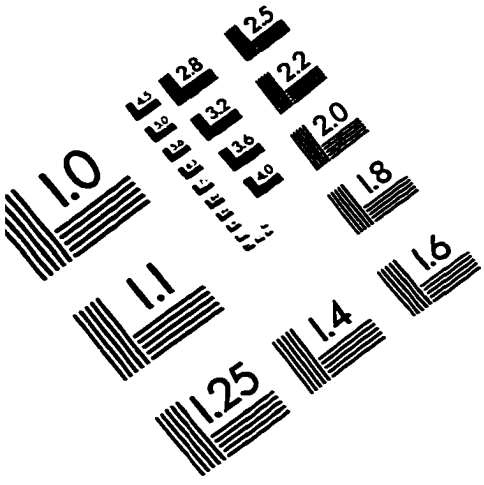

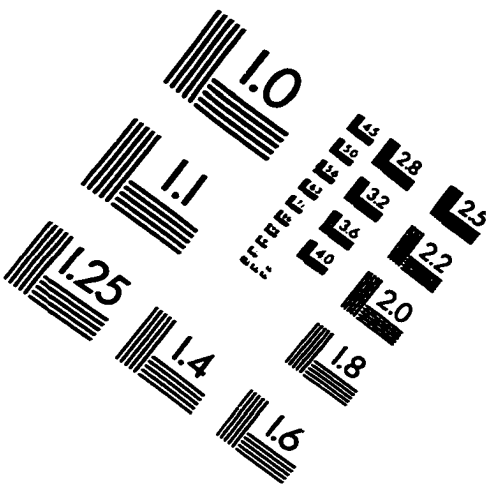

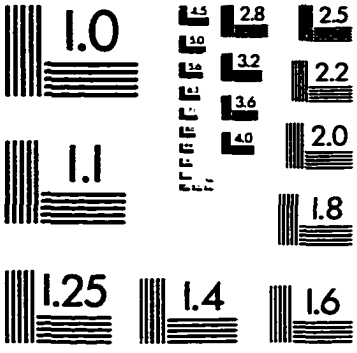

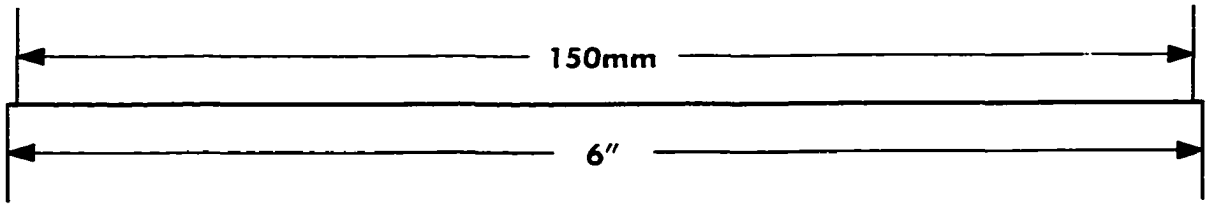

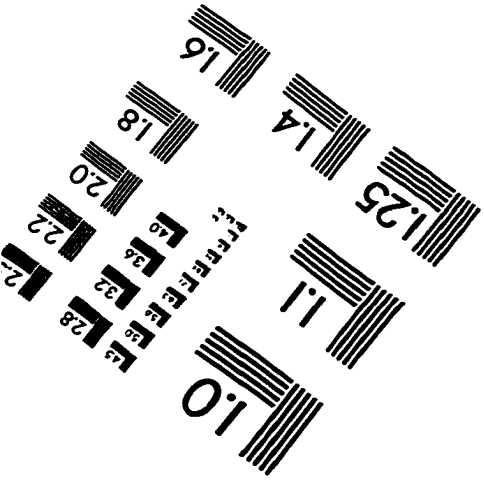

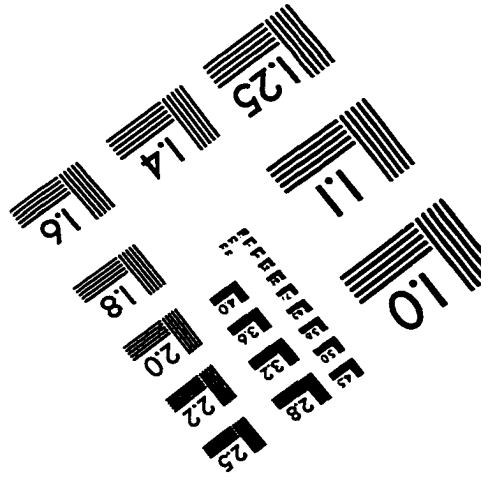

APPLIED IMAGE, Inc
1653 East Main Street
Rochester, NY 14609 USA
Phone: 716/482-0300
Fax: 716/288-5989